Dynamic interactions between skeletal muscle and breast cancer cells following chemotherapeutic treatment

by

Daleen Conradie

Thesis presented in partial fulfillment of the requirements for the degree of Master of Science (Physiological Sciences) in the Faculty of Science at Stellenbosch University

Supervisor: Prof. Anna-Mart Engelbrecht

Co-Supervisor: Dr. Ashwin Isaacs

Co-Supervisor: Dr. Tanja Davis

April 2019

Plagiarism Declaration Form

Name: Daleen Conradie

Module: Masters in Physiological Sciences

1. I know that plagiarism is wrong. Plagiarism is to use another's work and to pretend that it is one's own.

2. I have used a recognized convention for citation and referencing. Each significant contribution to and quotation in this thesis, from the work, or works, of other people has been acknowledged through citation and reference.

3. This thesis is my own work. I have not used the material in this thesis in any other thesis or project.

Signature: D.Conradie Date: April 2019

Abstract

Background: Breast cancer is the most common cancer found among women of South Africa with the prominent effective form of treatment being chemotherapy. Many cancer patients receiving chemotherapeutic treatment experience skeletal muscle wasting, however, the contribution of muscle wasting to the metastatic properties of breast cancer and response to current treatment strategies has not yet been fully investigated. The aims of this study were to investigate the reciprocal interactions between mouse breast cancer cells (E0771) and mouse myotubes (C2C12) as well as the effects of doxorubicin (DXR) on these interactions.

Methods: Conditioned media was collected from two separate cycles. The initial cycle of conditioned media was collected from E0771 breast cancer cells after treatment with/without 1.6 μM of DXR. Myotubes were then treated with/without DXR as well as conditioned media collected during the initial cycle from the E0771 cells. A new series of E0771 cells were then treated with/without DXR as well as with the second cycle of conditioned media collected from the myotubes. Mitochondrial integrity of myotubes was investigated using MitoSOX™ stain analysis while myotube cell viability and integrity was assessed using a Cell Tracker™ stain analysis. Cell viability of E0771 cells was assessed with an MTT assay and the migratory properties (wound closure) using a migration scratch assay. Western blot analyses were used to determined alterations in proliferation, apoptotic, and epithelial-mesenchymal transition (EMT) signaling pathways.

Results: Treatment of myotubes with 1.6 μM of DXR significantly induced mitochondrial ROS production (5.580 ± 0.4, $p<0.001$) when compared to Control but myotube integrity was maintained. Treatment of E0771 cells with 1.6 μM of DXR compared to Control significantly decreased cell viability (60.354% ± 1.237, $p<0.001$), significantly increased the phosphor/total ERK expression ratio (3.946 ± 0.520, $p<0.001$), and significantly decreased the cleaved/total PARP expression ratio (0.651 ± 0.027, $p<0.001$). Additionally, a significant increase in the percentage of wound closure was also observed in the DXR group (16.049% ± 1.11, $p<0.01$) compared to Control after 24-hours. E0771 cells treated with myotube conditioned media after treatment of DXR (C.DXR), induced a significant decrease in expression of the cleaved/total PARP ratio (0.662 ± 0.097, $p<0.01$) as well as a significant difference in percentage of wound closure (17.19 ± 0.758, $p<0.001$) compared to C.Control. Following treatment of the E0771 cells with myotube conditioned media, harvested after the

treatment of conditioned media from DXR treated E0771 cells (C.C.DXR), a significant increase in cell viability (121.743% ± 3.442, $p<0.05$) when compared to C.C.Control. Additionally, comparison of C.C.DXR to C.C.Control observed a significant decrease in expression of total Akt (65.554% ± 17.55, $p<0.05$), MCM2 (55.167% ± 14.64, $p<0.05$), and the cleaved/total PARP ratio (0.456 ± 0.111, $p<0.001$) was observed.

Conclusion: Investigation of the dynamic interactions between myotubes and breast cancer cells revealed novel evidence of the influence of the myotube environments on cancer progression. Our study also revealed novel evidence that this myotube environment significantly affected the response of breast cancer cells to the chemotherapeutic treatment of DXR. These findings identified new mechanisms that may promote breast cancer metastasis, which can be utilized to improve chemotherapy in cancer patients.

Opsomming

Agtergrond: Borskanker is die mees algemene kanker wat onder die vroue van Suid-Afrika voorkom, met chemoterapie wat tans die mees effektiewe vorm van behandeling is. Baie kankerpasiënte wat chemoterapeutiese behandeling ontvang, ervaar skeletspieratrofie, maar die bydrae van spierverlies tot metastatiese eienskappe van borskanker asook die reaksie op huidige behandeling is nog nie volledig ondersoek nie. Die doel van die studie was om ondersoek in te stel na die wederkerige interaksies tussen muis borskankerselle (E0771) en muis spiervesels (C2C12) asook die effekte van doxorubicin (DXR) op hierdie interaksies.

Metodes: Voorgeskrewe media is versamel uit twee afsonderlike siklusse. Die aanvanklike siklus van gekondisioneerde media is uit E0771 borskanker selle versamel na behandeling met/sonder 1.6 µM van DXR. Spiervesels is dan behandel met/sonder DXR sowel as met gekondisioneerde media wat tydens die aanvanklike siklus van die E0771-selle versamel is. ‘n nuwe reeks van E0771-selle is behandel met/sonder DXR en met die tweede siklus gekondisioneerde media wat van die spiervesels versamel is. Mitokondriale integriteit van die spiervesels is ondersoek deur van MitoSOX™ kleuring met fluoresensie mikroskopie te gebruik terwyl die lewensvatbaarheid en integriteit van spiervesels bepaal is met behulp van 'n Cell Tracker ™ kleuring. Die lewensvatbaarheid van E0771-selle is geassesseer met 'n MTT-toets en die migrerende eienskappe (wond sluiting) met behulp van ‘n migrasiekrapassessering. Westerse kladanalise is gebruik om veranderinge in proliferasie-, apoptotiese- en epiteel-mesenkiemale oorgang (EMT) seinweë te bepaal.

Resultate Behandeling van spiervesels met 1.6 µM van DXR het 'n aansienlike induksie van mitochondriale ROS-produksie (5.580 ± 0.4, p <0.001) gelewer n vergelyking met die konrole groep (Control), maar die integriteit van spiervesels het behoue gebly. Behandeling van E0771-selle met 1,6 µM DXR in vergelyking met die konrole groep (Control) het die lewensvatbaarheid van die selle aansienlik verminder (60.354% ± 1.237, p <0.001), die fosfo/totale ERK-uitdrukkingsverhouding (3.946 ± 0.520, p <0.001) laat toeneem en die gesplete/totale PARP-uitdrukkingsverhouding (0.651 ± 0,027, p <0,001). Daarbenewens is 'n beduidende verskil in die persentasie wondsluiting ook waargeneem (16.049% ± 1.11, p <0.01) in vergelyking met die konrole groep na 24 uur. E0771 selle behandel met DXR behandelde spiervesel gekondisioneerde media (C.DXR) het 'n beduidende afname in die uitdrukking van die gesplete/totale PARP-verhouding (0.662 ± 0.097, p <0.01) sowel as 'n beduidende verskil in persentasie wondsluiting veroorsaak (17.19 ± 0,758, p <0.001) n vergelyking met die konrole groep (C.Control). Die behandeling van E0771-selle met

spiervesel-gekondisioneerde media, na behandeling met gekondisioneerde media van DXR behandeled E0771-selle (C.C.DXR), 'n beduidende toename in die lewensvatbaarheid van die selle (121.743% ± 3.442, $p < 0.05$) in vergelyking met die konrole groep (C.C.Control). Daarbenewens het die vergelyking van C.CDXR tot C.C.Control 'n beduidende afname in die uitdrukking van totale Akt (65.554% ± 17.55, $p < 0.05$), MCM2 (55.167% ± 14.64, $p < 0.05$), en die gesplete/totale PARP verhouding (0.456 ± 0.111, $p < 0.001$) waargeneem.

Gevolgtrekking: Ondersoek na die dinamiese interaksies tussen skeletspiervesels en borskankerselle het nuwe bewyse getoon van die invloed van die spiervesel-omgewings op die verloop van kanker. Ons studie het ook nuwe bewyse getoon dat hierdie spiervesel-omgewing die reaksie van borskankerselle op die chemoterapeutiese behandeling met DXR aansienlik beïnvloed het. Hierdie bevindings het nuwe meganismes geïdentifiseer wat metastase van borskanker beïnvloed en nuwe teikens uitgewys wat moontlik chemoterapie in kankerpasiënte kan verbeter.

Acknowledgements

Thank you to my parents Max and Deon Conradie for your unconditional love and support throughout my MSc but more importantly my life. I appreciate all the opportunities you have given me and for working hard in order for me to achieve my dreams. I love you.

Prof. Anna-Mart Engelbrecht, thank you for never giving up on me even after so much has gone wrong throughout this whole process. I have never had someone believe I can do anything the way you have over the last three years. I am grateful for all the confidence you have helped me to gain in my work and myself.

Dr. Tanja Davis, I will never be able to thank you enough for everything you have done for me. A mentor is someone who is a brain to pick, an ear to listen, and a push in the right direction. You are more than just a mentor to me, you are one of the most valuable friends I have the honour to have.

Dr. Ashwin Isaacs, when my confidence was at the lowest you trusted me with a very expensive microscope. Thank you for teaching me so much in a matter of months, pushing me to keep going, and for giving me this amazing project. Your “never give up” attitude pushed me to finish.

Soon to be Dr. Jurgen Kriel, in the final stretch of this MSc you have helped to keep me going with enormous quantities of caffeine. Thank you for assisting me when I truly needed a helping hand.

DSG and CRG, thank you for all the help and advice throughout this project. I know we all had our own things to do but I appreciate all the friendly hellos at two in the morning. A special thank you to MRG for all the assistance and answering the multiple questions I had.

Taryn Tibble-Vega, Kirsty Wandrag and Danielle Millar, thank you for all the meals, support, laughs, and help throughout this degree. I appreciate having you both motivating me to keep going and picking me up whenever I got knocked down.

The Sequel and Royal Imperium, while it is not conventional to thank animals, I say thank you. Getting out the laboratory and into nature helped me to keep a clear head throughout this thesis.

Finally, I would like to thank the NRF for giving me the remarkable opportunity of completing this thesis with their financial support.

Table of Contents

Plagiarism Declaration Form ii

Abstract iii

Opsomming v

Acknowledgements vii

Table of Contents viii

List of Figures xii

List of Abbreviations xiv

Chapter 1 – Literature Review 1

Introduction 1

1.1. Mammary Gland 1

1.1.1. Embryonic development 2

1.1.2. Pubertal development 3

1.1.3. Pregnancy development 4

1.1.4. Mammary gland microenvironment 4

1.2. Breast Cancer 5

1.2.1. The structure of breast tumours 6

1.2.2. Classification 7

1.2.3. Treatments 7

1.2.3. Metastasis 8

1.3. Doxorubicin 8

1.3.1. Structure and metabolism 9

1.3.2. Mechanisms of action 10

1.3.3. Negative side effects of chemotherapy 11

1.3.4. Resistance to chemotherapy 12

1.4. Proliferation Signaling 13
1.4.1. The cell cycle *13*
1.4.2. PI3K/Akt pathway *14*
1.4.3. ERK pathway *16*
1.4.4. Mini-chromosome maintenance proteins *18*
1.5. Evasion of Apoptosis 19
1.5.1. Extrinsic death receptor pathway *20*
1.5.2. Intrinsic mitochondrial pathway *20*
1.5.3. Execution pathway *21*
1.5.4. Cancer and apoptosis *22*
1.6. Invasion and Metastasis 22
1.6.1. Epithelial-Mesenchymal Transition *23*
1.6.2. α-Smooth muscle actin *25*
1.6.3. Vimentin *26*
1.6.4. SNAIL *26*
1.6.5. E-cadherin *27*
1.6.6. Hybrid phenotypes *27*
1.7. Skeletal Muscle 28
1.7.1. Cancer Cachexia *28*
1.8. Problem Statement 30
1.9. Hypothesis 30
1.10. Aims 30
1.11. Objectives 31
Chapter 2: Materials and Methods 32
2.1. Cell Culture 32
2.2. Conditioned Media 32
2.3. Treatments 32

2.4. Assessment of Mitochondrial ROS Production (MitoSOX™) 34
2.5. Assessment of myotube width (Cell Tracker™) 34
2.6. Cell Viability Assessment 35
2.7. Migration Scratch Assay 35
2.8. Protein Extraction 37
2.9. Protein Determination & Sample Preparation 37
2.10. SDS-PAGE & Western blot 38
2.11. Statistical analyses 39
Chapter 3 – Results I 40
Introduction 40
3.1. Induction of oxidative stress in myotubes 40
3.1.1. Assessment of Mitochondrial ROS Production (MitoSOX™) 40
3.2. Maintenance of myotube integrity 42
3.2.1. Assessment of myotube width (Cell Tracker™) 43
Chapter 4 – Results II 45
Introduction 45
4.1. Conditioned media induce resistance in E0771 cells 45
4.1.1. Cell Viability Assessment 45
4.2. The effect of conditioned media on markers of cell proliferation 47
4.2.1. PI3K/Akt Pathway 47
4.2.2. ERK pathway 48
4.2.3. Mini-chromosome maintenance (MCM) proteins 49
4.3. The effect of conditioned media on apoptosis 50
4.3.1. Caspase 3 51
4.3.2. Poly ADP ribose polymerase (PARP) 52
4.4. The effect of conditioned media on cell migration 53
4.4.1. Percentage (%) of wound closure 55

4.4.2. Rate of wound closure *57*

4.5. The effect of conditioned media on markers of Epithelial-Mesenchymal Transition (EMT) 59

4.5.1. α-Smooth muscle actin *59*

4.5.2. Vimentin *60*

4.5.3. SNAIL *61*

4.5.4. E-cadherin *62*

Chapter 5 – Discussion **64**

Introduction 64

5.1. Myotube Mitochondrial Oxidative Stress 64

5.2. Myotubes Integrity 65

5.3. Resistance 66

5.4. Proliferation 67

5.5. Apoptosis 69

5.6. Invasion and Metastasis 71

Chapter 6 – Conclusion **76**

Chapter 7 – Limitations and Future Studies **78**

References **79**

Appendix A – Supplementary Data **88**

Appendix B - Reagents **92**

Appendix C – Reagent Protocols **96**

Appendix D – Protocols **100**

List of Figures

Chapter 1

Figure 1.1: Structure of epithelial terminal end bud in mammary gland during branching morphogenesis at puberty development phase.

Figure 1.2: Anatomical structure of mammary gland and surrounding microenvironment.

Figure 1.3: The chemical structure of the chemotherapeutic agent doxorubicin.

Figure 1.4: Basic mechanisms of action induced by doxorubicin.

Figure 1.5: Activation of PI3K/Akt pathway and downstream effects.

Figure 1.6: Activation of ERK pathway and downstream effects.

Figure 1.7: Regulation of apoptosis: extrinsic, intrinsic, and execution pathways.

Figure 1.8: Markers of the Epithelial- Mesenchymal Transition (EMT) and Mesenchymal-Epithelial Transition (MET) dynamic processes.

Figure 1.9: Scheme representing the reciprocal workflow for study.

Chapter 2

Figure 2.1: A visual representation of 24-hour treatments for the production of conditioned media and experiments on E0771 cells and myotubes.

Figure 2.2: Equations used for analyses of wound closure in migration scratch assay.

Chapter 3

Figure 3.1: Representative images of MitoSOX™ assay after 24-hour treatment of myotubes.

Figure 3.2: Mitochondrial ROS analysis from MitoSOX™ assay after 24-hour treatment of myotubes.

Figure 3.3: Representative images of Cell Tracker™ assay after 24-hour treatment of myotubes.

Figure 3.4: Myotube width (μm^2) analysis from Cell Tracker™ assay after 24-hour treatment of myotubes.

Chapter 4

Figure 4.1: Mitochondrial reductive capacity assessed from MTT assay after 24-hour treatment of E0771 cells as an indicator of cell viability.

Figure 4.2: Protein expression of total Akt from western blot analysis after 24-hour treatment of E0771 cells.

Figure 4.3: Ratio of protein expression of phospho-ERK2 / total ERK2 from western blot analysis after 24-hour treatment of E0771 cells.

Figure 4.4: Protein expression of MCM2 from western blot analysis after 24-hour treatment of E0771 cells.

Figure 4.5: Ratio of protein expression of cleaved Caspase 3 / total Caspase 3 from western blot analysis after 24-hour treatment of E0771 cells.

Figure 4.6: Ratio of protein expression of cleaved PARP / total PARP from western blot analysis after 24-hour treatment of E0771 cells.

Figure 4.7: Representative images of migration scratch assay over 24-hours of treatment of E0771 cells.

Figure 4.8: Percentage wound closure from migration scratch assay analysis over 24-hours of treatment of E0771 cells.

Figure 4.9: Rate wound closure (%.hr^{-1}) from migration scratch assay analysis over 24-hours of treatment of E0771 cells.

Figure 4.10: Protein expression of α-Smooth Muscle Actin from western blot analysis after 24-hour treatment of E0771 cells.

Figure 4.11: Protein expression of Vimentin from western blot analysis after 24-hour treatment of E0771 cells.

Figure 4.12: Protein expression of SNAIL from western blot analysis after 24-hour treatment of E0771 cells.

Figure 4.13: Protein expression of E-cadherin from western blot analysis after 24-hour treatment of E0771 cells.

Chapter 5

Figure 5.1: Interactions between PI3K/Akt pathway, ERK pathway, Apoptosis, and EMT.

Chapter 6

Figure 6.1: Proposed alterations in signaling pathways due to the dynamic relationships between E0771 cells, myotubes and DXR treatment.

List of Abbreviations

Symbol	
α-SMA	α-smooth muscle actin
κβ	kappa-light-chain-enhancer of activated β cells
kDa	Kilo-Dalton

A

Apaf-1	Apoptotic peptide activating factor-1
ALK-5	Activin receptor-like kinase-5
ANP	Atrial natriuretic peptide
ATM	Ataxia telangiectasia
ATP	Adenosine-5'-triphosphate
ATR	ATM-and-RAD3-related

B

Bcl-2	B-cell lymphoma 2
BNP	Brain natriuretic peptide
BRCA 1/2	Breast cancer 1 and 2 genes
BSA	Bovine serum albumin

C

CARD	Caspase activation and recruitment domains
Cdc	Cell division cycle
CDK	Cyclin-dependent kinases
c-FLIP	Cellular FLICE (FADD-like IL-1β-converting enzyme)-inhibitory protein
CMFDA	5-chloromethylfluorescein diacetate
CMG	Cdc45-MCMs-Gins
CREB	cAMP response element-binding protein

D

DD	Death domain
DDK	Dbf4-dependent kinase
DED	Death effector domain
DISC	Death-inducing signaling complex
DMEM	Dulbecco's Modified Eagle's Medium

DMSO	Dimethyl sulfoxide
DNA	Deoxyribonucleic acid
DXR	Doxorubicin

E

ECL	Enhanced chemiluminescence
ECM	Extracellular matrix
EDTA	Ethylenediamine tetraacetic acid
EGTA	Ethylene glycol-bis (β-aminoethyl ether)-N,N,N',N'-tetraacetic acid
EMT	Epithelial-mesenchymal transition
ERK	Extracellular signal-regulated kinase
ETC	Electron transport chain
EtOH	Ethanol

F

FBS	Fetal bovine serum
FDA	Food and Drug Administration

G

GDP	Guanine diphosphate
GINS	Go, Ichi, Ni, and San
Grb2	Growth factor receptor-bound protein 2
GTP	Guanosine triphosphate

H

H3K9me3	H3 lysine 9 methylation
HER2	Human epidermal growth factor receptor type 2
HGF	Hepatocyte growth factor

I

I-κβ	Inhibitor of κβ
IF	Intermediate filament
IKK	Inhibitor κβ kinase
IR	Ionizing radiation

J

K

L

LSD	Least significant difference

M

MAPK	Mitogen-activated protein kinase
MAP2K2	Mitogen-activated protein kinase kinase 2
MCM	Mini-chromosome maintenance proteins
MEK	Mitogen-activated protein kinase/ERK kinase
MET	Mesenchymal-epithelial-transition
MMC	Mitomycin C
MMP	Matrix metalloproteinase
MPT	Mitochondrial permeability transition
mTORC2	Mammalian target of rapamycin complex 2
MTT	3-(4,5-Dimethylthiazol-2-yl)-2,5 diphenyltetrazolium bromide

N

NaCl	Sodium chloride
NaF	Sodium fluoride
NF-κβ	Nuclear factor κβ
NP-40	Nonyl phenoxypolyethoxylethanol-40

O

P

PARP	Poly (ADP-ribose) polymerase
PBS	Phosphate-buffered saline
PDK1	Phosphoinositol-dependent kinase-1
PDVF	Polyvinylidene fluoride
PDGF	Platelet-derived growth factor
PI3K	Phosphoinositide 3-kinase
PIP_2	Phosphatidylinositol 4,5 bisphosphate
PIP_3	Phosphatidylinositol 3, 4, 5 trisphosphate
PKB	Protein Kinase B
PMSF	Phenylmethanesulfonylfluoride
PPAR	Proliferator-activated receptor
PTEN	Phosphatase and tensin homologue deleted on chromosome 10

Q

R

RB	Retinoblastoma
RIPA	Radioimmunoprecipitation
RNA	Ribonucleic acid
ROS	Reactive oxygen species
RT	Room temperature
RTK	Receptors tyrosine kinases

S

SDS	Sodium dodecyl sulphate
SDS-PAGE	Sodium dodecyl sulphate – polyacrylamide gel electrophoresis
SHIP-1/2	Src homology 2 (SH2) containing phosphatases 1 and 2
SIP1	Survival of motor neuron protein interacting protein 1
SOS	Son of sevenless

T

TBS-T	Tris-Buffered Saline – Tween 20
TCE	Trichloroethylene
TGF-β	Transforming growth factor beta
TNBC	Triple Negative Breast Cancer

U

UV	Ultraviolet

V

VEGF	Vascular endothelial growth factor

W

X

Y

Z

Chapter 1 – Literature Review

Introduction

Cancer is defined as abnormal and excessive cell growth within tissues or organs (Cheung-Ong, Giaever & Nislow, 2013). Each year a reported 14 million people worldwide are diagnosed with cancer and this number is predicted to increase over time (CANSA, 2018). Breast cancer is the most common cancer found among the women of South Africa with ±19.4 million women at risk (National Cancer Institute, 2015). The hallmarks of cancer include: 1) cell proliferation and growth that do not adhere to proper signaling, 2), evasion of growth suppression signaling, 3) cell death avoidance, 4) immune destruction avoidance, 5) infinite replication, 6) promoting inflammation that benefits tumour, 7) cellular energetics dysregulation, 8) instability and mutations in genome, 9) promotion of angiogenesis in tumour, and 10) invasion and metastasis activation (Hanahan & Weinberg, 2011). Doxorubicin is currently one of the most effective chemotherapeutic agents to treat cancer, including breast cancer, and is used for the treatment of cancer in South Africa (Hudis & Gianni, 2011). Unfortunately, chemotherapeutic drugs are not specialized agents that only target cancer cells. The systemic induction results in a systemic response in all tissues including healthy cells. This results in loss of healthy cells and tissues as well the development of drug resistance in patients. Skeletal muscle comprises 50% of the total human body and has been observed to undergo wasting, known as cachexia, as a response to cancer and chemotherapeutic treatment (Surov *et al.,* 2009; Hardee, Montalvo & Carson, 2017). The contribution of cachexia to the response of breast cancer to current chemotherapeutic treatment and metastatic properties has not yet been fully investigated. Due to the complex composition and regulation of cancer, research into systemic interactions focuses on mechanisms that could be targeted for more effective treatments. Investigation into the mammary gland, its cancer, skeletal muscle, and the interactions will be discussed in the following review.

1.1. Mammary Gland

The mammary gland is a glandular organ that consists of a variety of cell types that undergoes remodeling due to various stages of cell proliferation, differentiation, and apoptosis throughout the lifespan of a female. These alterations are in response to stimuli from menstrual cycles, pregnancy, lactation and involution (Inman *et al.*, 2015). The

mechanisms and pathways present in normal mammary gland development and remodeling are observed to be dysfunctional in the progression of breast cancer.

Normal mammary glands consist of epithelial and non-epithelial compartments. The epithelial compartments are heterogeneous as they originate from stem cells. These stem cells undergo heterotypic signaling into multiple subpopulations that are able to dynamically interrelate (Mareel & Constantino, 2011). The non-epithelial compartments are referred to as the stroma, which comprises of resident as well as recruited cells that mainly consists of a mesenchymal phenotype. Adipocytes are mesenchymal cells that form the stromal compartment that is also known as the mammary fat pad (Mareel & Constantino, 2011). An intact basement membrane separates the stroma from the epithelium. Clear separation of the epithelial and stromal compartment however, is doubtful due to the ability of epithelial cells to express phenotypes similar to stromal cells (Monks *et al.*, 2008). These compartments interact in order to regulate embryonic organogenesis, adult maintenance of homeostasis in organs as well as cancer development or suppression (Mareel & Constantino, 2011; Bissell and Hines, 2011). The mammary gland development involves epithelial structures and therefore molecules involved in epithelial cell-cell adhesion, such as the E-cadherin/β-catenin complex, have a significant influence in its development (Mareel & Constantino, 2011). Endocrine gland interactions also modulate the normal development of the mammary gland (Mareel & Constantino, 2011).

1.1.1. Embryonic development

During the embryonic development phase, a single ectoderm layer expands to form mammary lines. These ectoderm cells migrate and form multilayered lens-shaped arrangements called placeodes (Sakakura, Nishizuka & Dawe, 1976; Hens & Wysolmerski, 2005). The placodes develop into bulbs of epithelial cells that are distinct from the surrounding dermis. A mammary mesenchyme forms from the condensation of mesenchymal cells around the epithelial buds. Subsequently, mammary fat pad precursors differentiate on the outside of the first mammary mesenchyme surrounding the epithelial compartment (Sakakura, Nishizuka & Dawe, 1976). Epithelium-induced expression of hormone receptors found on the mesenchyme modulates organogenesis (Heuberger *et a*l., 1982.). In male embryos, the activation of androgen receptors within the mesenchyme, initiates the degradation of mammary buds while female embryos continue the development of the mammary buds with epithelial cell proliferation. This proliferation induces elongation of the mammary bud to form a sprout, which enters into the fat pad precursor (Sakakura, Nishizuka & Dawe, 1976; Inman *et al.*, 2015). The epidermal cells covering the bud forms

the nipple while a lumen develops within the sprout (Inman *et al.*, 2015). A rudimentary ductal tree is form from the branching of the sprout into the fat pad (Sakakura, Nishizuka & Dawe, 1976). The mammary epithelium at the nipple remains quiescent until the female reaches puberty.

1.1.2. Pubertal development

Hormones and additional factors expressed during puberty induce branching morphogenesis, which is the enlargement of the terminal end bud of the epithelial duct invading into the mammary fat pad (Lyons, 1958; Williams & Daniel, 1983). These epithelial terminal end buds contain multilayered epithelial body cells and epithelial luminal cells surrounded by a layer of epithelial cap cells and myoepithelial cells as seen in **Figure 1.1** (Silberstein & Daniel, 1982; Williams & Daniel, 1983; Sternlicht, 2006; Inman *et al.*, 2015). These cells undergo epithelial-mesenchymal transition (EMT) as the epithelial cells contain mesenchymal properties, in order to invade into the mammary fat pad (Nelson *et al*., 2006; Kouros-Mehr & Werb, 2006). The production and activation of transforming growth factor beta (TGF-β) terminates branching morphogenesis into the fat pad, however, the exact mechanism is not known (Nelson *et al.*, 2006). During each menstrual cycle of virgin mice the epithelium proliferates and undergoes apoptosis (Fata, Chaudhary & Khokha, 2001).

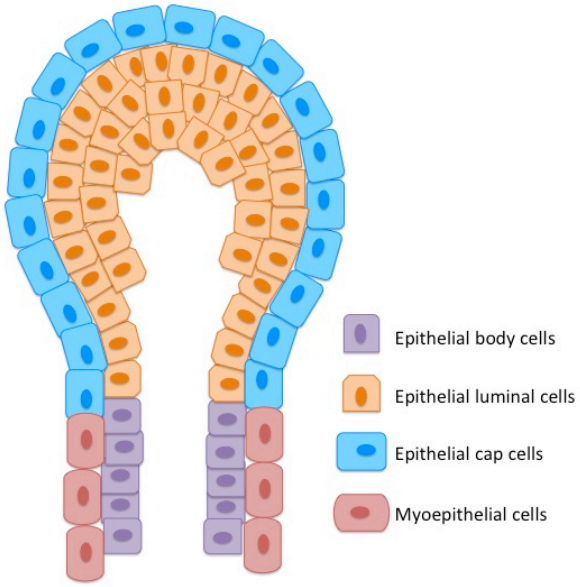

Figure 1.1: Structure of epithelial terminal end bud in mammary gland during branching morphogenesis at puberty development phase. The epithelial duct contains epithelial body cells surrounding by myoepithelial cells that attach to the epithelial terminal end bud. This bud contains epithelial luminal cells surrounded by epithelial cap cells that undergo transition during branching. Scheme reproduced from Inman *et al.* (2015).

1.1.3. Pregnancy development

During pregnancy, the circulating hormones initiate rapid proliferation of alveolar epithelium to form secretory alveoli. In the secretory alveoli of lactating females, the luminal epithelial cells that are apically orientated produce and secrete milk proteins into the lumen (Inman *et al.*, 2015). Once milk production is decreased due to weaning, the expanded epithelial compartments undergo apoptosis. This apoptotic process is known as involution and causes the remodeling of the epithelial compartment and surrounding tissue of the mammary gland (Monks *et al.*, 2008).

1.1.4. Mammary gland microenvironment

The microenvironment surrounding the mammary gland cells, such as the stroma and extra-cellular matrix (ECM), influences the development and function of the mammary gland epithelium throughout all phases of development. The ECM regulates epithelial structure and function in the mammary gland. Myoepithelial cells are smooth muscle-like cells with an epithelial origin and are found on a specialized layer of the ECM known as the basement membrane (Inman *et al.*, 2015). Stromal and myoepithelial cells are responsible for the synthesis of components of the ECM such as fibronectin, collagens, proteoglycans, and laminins. These compounds are not only incorporated into the ECM but also into the basement membrane.

Stromal compartments of the mammary gland consist of dense fat pad precursors during embryogenesis, which converts to white fat tissue after birth (Sakakura, Nishizuka & Dawe, 1976). A reduction in the lipid content of mammary adipocytes is observed during pregnancy and lactation. The reservoir of adipose tissue surrounding the epithelial compartments as seen in **Figure 1.2**, is therefore necessary for the production of milk as it is a demanding metabolic process (Hovey & Aimo, 2010; Gregor *et al.,* 2013). The endocrine functions of adipocytes are understood to influence epithelial growth, epithelium function, and communication with multiple cell types to regulate processes within the mammary gland (Hovey & Aimo, 2010).

Fibroblasts are implanted within the fat pad of the stromal compartments. During branching morphogenesis, fibroblasts communicate bi-directionally with the epithelium and releases proteases, growth factors, and other stimuli (Howard & Lu, 2014). The synthesis of ECM components fibronectin, proteoglycans, and collagens is also regulated by fibroblasts. In addition, fibroblasts synthesize matrix metalloproteinase's (MMP's); enzymes capable of

degrading the ECM and releasing growth factors or cytokines present within the ECM, in order to alter ECM composition or density (Lühr *et al.,* 2012).

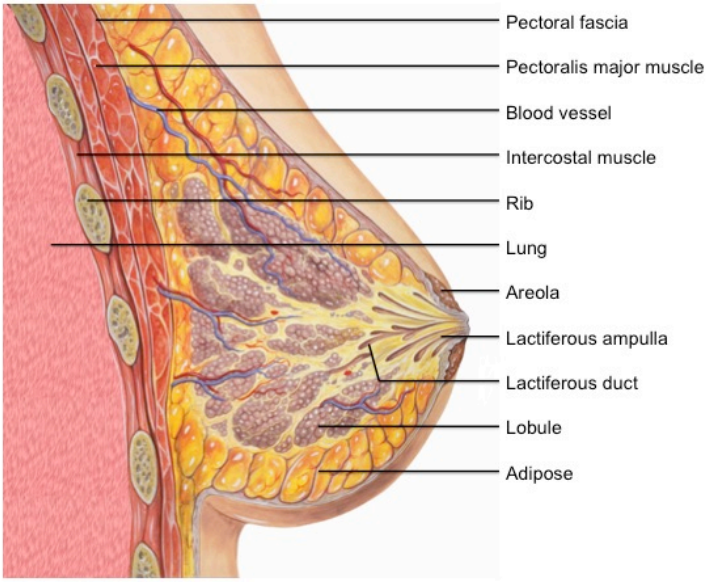

Figure 1.2: Anatomical structure of mammary gland and surrounding microenvironment. A mature mammary gland consists of lactiferous ducts, lactiferous ampulla and lobule. Adipocytes, fibroblasts and blood vessels within the surrounding microenvironment promote the development and function of the mammary gland. Scheme adapted from medical illustrator Patrick J. Lynch.

The skeletal muscle is located in close proximity to the mammary gland with vascular structures and adipocytes communicating between these microenvironments (**Figure 1.2**). During lactation, changes in skeletal muscle metabolism have been observed (Xiao, Grove & Smith, 2004), indicating interactions do occur during normal remodeling. The skeletal muscle microenvironment and interactions will be discussed later in this chapter.

1.2. Breast Cancer

Cancer develops due to mutations in genes responsible for the regulation of cell proliferation and differentiation (Tacar, Sriamrnsak & Dass, 2012). A tumour in the epithelium of the mammary gland is known as breast cancer and carcinomas commonly occur within the ducts, terminal ducts and lobules (Russo, Tay & Russo, 1982). According to the Cancer Association of South Africa and National Cancer Institute, breast cancer is the most common cancer found in women in South Africa with ±19.4 million women at risk (CANSA, 2010; National Cancer Institute, 2015). Globally, a reported 1.5 million new cases of breast cancer

is diagnosed every year with a prediction that in 2020, 1.7 million women will be diagnosed with breast cancer (CANSA, 2018). Factors such as inherited mutations, unsatisfactory diets, tobacco and radiation promote the possibility of developing cancer (Tacar, Sriamrnsak & Dass, 2012). The alterations in mammary cells and morphology during early menstruation induction, late pregnancy, and a nulliparous uterus are thought to be factors involved in increased risk of breast neoplastic development while early pregnancy induces a protective effect against neoplastic development (Russo, Tay & Russo, 1982). While there is an absence of updated registries in South Africa, it is still evident that breast cancer has a high mortality risk, therefore effective treatment strategies are required.

1.2.1. The structure of breast tumours

A breast tumour is composed of two compartments: an epithelial compartment that consists of proliferating cells while the stroma consists of blood vessels and connective tissue (Tacar, Sriamrnsak & Dass, 2012). The expression of molecules that is important for cell proliferation and other processes during embryogenesis are down regulated in adult tissue. These molecules, however, have been observed to be re-expressed in tumours (Mareel & Constantino, 2011). Tumour cell masses can be sub-divided into two categories, namely benign and malignant tumours. A benign tumour develops when cancer cells have not proceeded to disperse into tissue surrounding the tumour. The tumour is confined to a specific area of growth and maintains a lower risk to an individual. Malignant tumours are able to invade into surrounding tissue resulting in the development of more complex tumours and poor patient prognosis. Mutations in various signaling pathways may result in cancer and tumour development. Triple negative breast cancer (TNBC) is the most aggressive form of breast cancer and is commonly associated with advanced tumour grade, p53 and breast cancer 1 and 2 genes (BRCA 1/2) mutations as well as basal cytokeratin's alterations (Bernier & Poortmans, 2016). The tumour suppressor protein p53 regulates the cell cycle in normal cells and terminates proliferation when the cell has damage or physiological stress. Apoptosis is then induced to remove this harmful cell. In cancer conditions, p53 is dysfunctional allowing proliferation of damaged and stressed cells as well as inhibition of apoptosis (Hahn & Weinberg, 2002). Invasive breast cancer, such as TNBC, was observed to express markers often secreted by normal epithelial breast cells (Badve *et al.*, 2011). These aggressive cancers display increased necrotic areas with mitotic manifestations, recurrence of cancer, and the development of distant metastases (Bernier & Poortmans, 2016). Mutations within signaling pathways regulating cell proliferation, cell death or cell development promote the development and progression of cancer. The dysregulation of

these signaling pathways that promote tumour formation will be discussed in the proliferation section.

1.2.2. Classification

Breast tumours are classified according to the original tissue in which it develops, the morphology of the cell, and any molecular signatures that may be present. Adenocarcinoma is a broad term of cancer developing in glandular cells, these cells are found in the breast, prostate and lungs. Invasive ductal carcinoma is malignant cancer that develops in the epithelial lining of the mammary ducts, while the benign tumours are known as ductal carcinoma *in situ.* Cancer that progresses within the milk producing glands, the lobules, is known as a lobular carcinoma (Sakakura, Nishizuka & Dawe, 1976). This cancer may also be invasive or *in situ*.

Grading of breast cancer occurs according to the differentiated state of the cancer. Tumours with the worst prognoses are comprised of poorly differentiated or undifferentiated cells (Wong *et al.*, 2018). Ben-Porath *et al.,* (2008) analysed the expression profiles of 1211 breast tumours using six independent studies. They demonstrated that embryonic stem cell-like gene expression profiles in poorly differentiated tumours were associated with poor prognosis and patient survival. These findings were substantiated in bladder carcinomas and high-grade glioblastomas.

1.2.3. Treatments

Endocrine gland interactions modulate the normal development of the mammary gland therefore the hormones that regulate these processes may influence breast neoplasms and can serve as potential targets for effective cancer treatment (Mareel & Constantino, 2011). Cancer cells that are estrogen and/or progesterone positive contain receptors specific for these hormones. This enables them to be treated with hormone therapy while those expressing human epidermal growth factor receptor type 2 (HER2) receptors can be treated with interventions targeting this receptor (National Cancer Institute, 2015). TNBC does not express estrogen, progesterone, or HER2 receptors, thus rendering targeted hormonal therapies ineffective (Badve *et al.*, 2011; Foulkes, Smith & Reis-Filho, 2010; Bernier & Poortmans, 2016). Chemotherapy with the use of chemical agents has been successful in treating breast cancer including TNBC, however, cancer patients undergoing this treatment

can sometimes still have a poor outcome (Foulkes, Smith & Reis-Filho, 2010). Treatment of breast cancer using chemotherapy will be discussed in the doxorubicin section.

1.2.3. Metastasis

Cancer cells can exhibit metastatic properties, such as the secretion of MMP enzymes, which are able to disrupt the normal tissue (Croce, 2008). Cancer cells with these properties are able to invade into blood or lymphatic circulation systems and consequently spread throughout the body. It was found that gene expression profiles of metastatic breast cancer cell lines exhibit proteins that promote organ-specific metastasis (Mareel & Constantino, 2011). Sentinel lymph nodes are considered to be the initial step in breast cancer metastasis due to the nodes being the primary site where tumour antigens may be received (Mareel & Constantino, 2011). Metastatic cell lines, such as MDA-MB-231, may express high quantities of certain metastasis-associated molecules like the CD73 transmembrane protein. This protein is involved in normal lymphocyte homing processes and promotes lymph node metastasis (Lee *et al.*, 2003). Further discussion will be done of the invasive and metastatic properties of breast cancer in the invasion and metastatic section.

1.3. Doxorubicin

Chemotherapy, also known as anti-neoplastic therapy, remains the most common form of anti-cancer therapy for multiple cancer types. Treatment is given to patients through intravenous, intra-vesical, intra-arterial or oral diffusion depending on the type of cancer. For chemotherapy to be considered effective, cancer cells must show inhibition of cell proliferation and induction of cell death. Chemotherapeutic agents are classified into groups due to differences in chemical composition and anti-neoplastic function. Alkylating chemotherapeutic agents target and damage DNA directly to inhibit cancerous cell proliferation. Anti-metabolites target DNA and RNA synthesis where it substitutes the standard building blocks required for appropriate replication and transcription of DNA (Tacar, Sriamrnsak & Dass, 2012). Topoisomerase inhibitor agents target the topoisomerase enzyme preventing DNA double strand separation and mitotic inhibitor agents target the microtubule spindle machinery, thus inhibiting mitosis. Lastly, anti-tumour antibiotics, such as anthracyclines, target DNA replication enzymes, however, its function is not dependent on specific cell cycle phases (Shepherd, 2003).

Doxorubicin (DXR) is an anthracycline chemotherapeutic agent used to treat several different tumours including TNBC (Hudis & Gianni, 2011), lung (Melguizo *et al.*, 2015), ovarian (Ye, Karim & Loh, 2014) and colon cancer (Lüpertz *et al.*, 2010). DXR is observed to be one of the most effective chemotherapeutic agents approved by the Food and Drug Administration (FDA) (Carvalho *et al.,* 2009). Anti-neoplastic properties include targeting cells undergoing rapid proliferation and the reduction of cancer progression.

1.3.1. Structure and metabolism

DXR is chemically composed of an aglycone as well as a sugar moiety classifying it as a non-selective class I anthracycline. A tetracyclic ring with quinine-hydroquinone adjacent groups and a methoxy substituent short side chain trailed by a carbonyl group form the aglycone moiety (Hilmer *et al.,* 2004). Daunosamine, the sugar moiety, is characteristic of a 3-amino-2, 3, 4-trideoxy-L-fucosyl component attached to one of the tetracyclic rings of the aglycone with a glycosidic bond (**Figure 1.3**) (Hilmer *et al.,* 2004).

Following treatment, cells rapidly take up DXR as the chemical half-life of DXR is 3-5 minutes (New Zealand Medicines and Medical Devices Safety Authority, 2014). The elimination of DXR from tissue requires more time hence its terminal half-life is 20 - 48 hours. Injection of DXR into cancer patients is completed with a steady-state distribution flow of 20 to 30 L/kg (New Zealand Medicines and Medical Devices Safety Authority, 2014). This flow rate attempts to promote effective anti-cancer effects and decrease toxicity in patients (Zheng *et al.,* 2006). The liver chemically modifies DXR and its major metabolite, Doxorubicinol. Both these molecules undergo acid-catalyzed hydrolysis of their glycosidic bonds, eliminating the sugar component. This process forms doxorubicinone from DXR and doxorubicinolone from doxorubicinol.

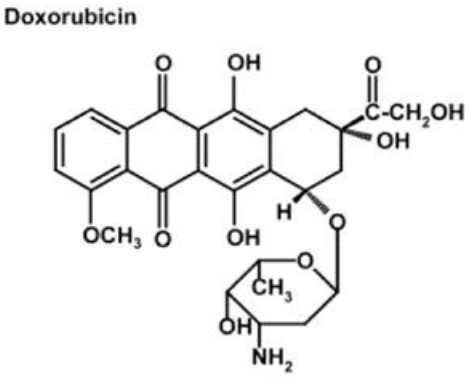

Figure 1.3: The chemical structure of the chemotherapeutic agent doxorubicin. Structure includes an aglycone attached to sugar moiety by a glycosidic bond. Sourced from Wang *et al.* (2001).

1.3.2. Mechanisms of action

After being injected into a patient, DXR passively diffused into cells until the extracellular concentration is less than the intracellular concentration (Wang *et al.,* 2000). While antracyclines customarily target DNA replication enzymes, DXR targets topoisomerase I and II, as well as intercalates itself into DNA to inhibit uncoiling (Tacar, Sriamrnsak & Dass, 2012).

Initial mechanism of action involves the binding of DXR to the 20S subunit of a proteasome in the cytoplasm, forming a DXR-proteasome complex **(Figure 1.4)**. The complex translocates into the nucleus through the nuclear pore. The affinity of DXR to bind to DNA is greater than the proteasome, therefore, DXR dissociates from the complex in order to bind to DNA (Hilmer *et al.,* 2004). It intercalates itself into DNA, which inhibits and dysregulates DNA and RNA polymerase functions, preventing DNA and RNA transcription (Volkova & Russell, 2011; Shaw & Cantley, 2006). Intercalation also prevents the uncoiling and separation of DNA (Minotti *et al.,* 2004). The lipophilic and DNA intercalating properties of DXR ensures it remain within the nucleus of the cells. DXR also has a high affinity for components associated with the mitochondria and the complexes of the electron transport chain (ETC) (Gilliam *et al.,* 2012). It has been observed that DXR binds to mitochondrial DNA, and not only nuclear DNA (Ashley & Poulton, 2009). The inability to pass the blood-brain barrier prevents DXR from being a viable treatment for brain cancer (Tacar, Sriamrnsak & Dass, 2012).

The production of reactive oxygen species (ROS) is another mechanism in which DXR induces its effects as shown in **Figure 1.4**. The chelation of intracellular iron with DXR activates a Fenton-type reaction and the production of highly reactive hydroxyl radicals. When molecular oxygen is present, redox cycle reactions occur with flavoprotein reductase that produces superoxide (Tacar, Sriamrnsak & Dass, 2012). Additionally, DXR binds directly to plasma proteins of the cell membrane inducing an enzymatic electron reduction that produces reactive hydroxyl free radicals that induce DNA damage and promote cell death (Tacar, Sriamrnsak & Dass, 2012). These effects make DXR an effective chemotherapeutic agent, however, it is also responsible for negative toxic effects.

The apoptotic pathway is directly influenced by DXR through Bcl-2/Bax interactions that will be discussed in the proliferation section (Leung & Wang, 1999). Additionally, the hyper-activation of poly (ADP-ribose) polymerase (PARP) can also occur promoting increased DNA repair and therefore avoidance of cell death (Tacar, Sriamrnsak & Dass, 2012).

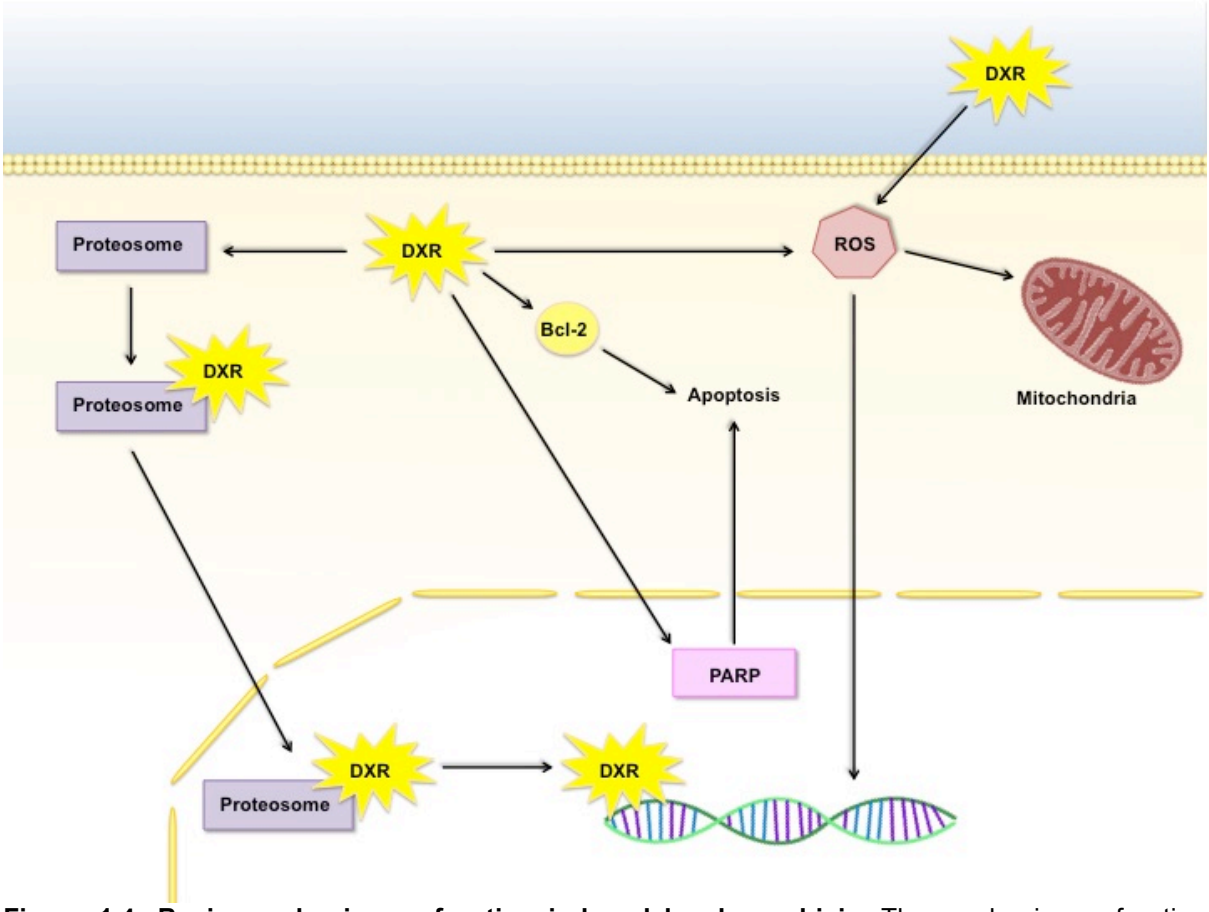

Figure 1.4: Basic mechanisms of action induced by doxorubicin. The mechanisms of action include the formation of a doxorubicin (DXR)-proteasome complex and translocation into the nucleus. Here DXR binds and intercalates into the DNA inhibiting transcription. The production of reactive oxygen species (ROS) is another mechanism in which the mitochondria and DNA damage occurs. Additionally, disruption of the Bcl-2/Bax ratio and hyper-activation of PARP inhibits apoptosis. Sourced from Tacar, Sriamrnsak & Dass (2012).

1.3.3. Negative side effects of chemotherapy

Chemotherapeutic drugs are not specialized agents that specifically target cancer cells. The systemic induction results in a systemic response affecting all tissues including healthy cells. Side effects, such as nausea, hair loss, fever, rashes and appetite alterations are a concern when treating patients with chemotherapeutic interventions (Coates *et al.*, 1983). The continuous administration of DXR into veins results in the thickening of vein walls, known as phlebosclerosis. The leakage of DXR out of the administration vein into the surrounding tissue is known as extravasation and causes an increase in fibrous components and inflammation in the tissue (Carvalho *et al.,* 2009). Cells that undergo rapid proliferation, such as mammary cells during pregnancy or immune cells, are easily targeted by chemotherapy and undergo cell death. (Shepherd, 2003). Leukocytes and bone marrow precursors are examples of rapid proliferating cells affected, as the concentration of DXR in these cells is ±

500 times greater than what is found in the plasma (Tacar, Sriamrnsak & Dass, 2012). This promotes immunosuppressive side effects in cancer patients (Weir, Liwski & Mansour, 2011). Due to the metabolic processes that occur in the liver, it has been observed to accumulate DXR (Tacar, Sriamrnsak & Dass, 2012). The metabolism results in significant ROS production that causes DNA damage and lipid peroxidation. This induces tissue damage and cell death in the liver. Accumulation of the drug within the heart results in cardiotoxicity, the most harmful consequence of this therapy. DXR targets brain natriuretic peptide (BNP) and atrial natriuretic peptide (ANP) within cardiomyocytes (Shi *et al.,* 2011). This induces cardiac hypertrophy in cancer patients. Mitochondria present within the cardiac muscle are also targeted by DXR by altering mitochondrial protein expression and ROS production (Sishi *et al.,* 2013). Cardiotoxicity may lead to pericarditis, arrhythmias and left ventricular dysfunction as well as stress-induced cardiomyopathy within these patients depending on severity of toxicity and individual parameters (Volkova & Russell, 2011). Mortality in breast cancer patients has been observed to occur due to heart failure decades after the last chemotherapeutic treatment was given (Harake *et al.*, 2012).

1.3.4. Resistance to chemotherapy

A concern in cancer intervention using current anti-cancer agents is the increased occurrence of drug resistance. Resistance to chemotherapeutic agents, especially doxorubicin, is common after prolonged treatment in patients including those with TNBC (McCubrey *et al*., 2007; Bernier & Poortmans, 2016). DXR and other chemotherapeutic agents require active proliferation of cancer cells as this exposes the DNA. Within tumours, cancer cells are at various phases within the cell cycle and sometimes even exhibit a reduced growth rate due to limitations of space and nutrients (Tacar, Sriamrnsak & Dass, 2012). This results in an ineffective response in cancer cells and the development of resistance. Drug resistance can also be induced where there is an increase in positive regulators of cell proliferation activity where cell death is inhibited, where tumour suppressors are reduced or where survival factors within cancer cells are increased (Chen *et al*., 2014). Signalling pathways that promote cell survival in response to ROS (McCubrey *et al*., 2007) may promote resistance and cell proliferation after DXR treatment. The influence of specific signalling pathways on the initiation of drug resistance will be discussed in the proliferation section.

1.4. Proliferation Signaling

Epithelial cells in the body undergo continuous cycles of growth and death. Damaged cells are normally repaired or removed during the cell cycle. However, defects in the cell cycle or gene mutations can lead to cells dividing uncontrollably. Hyperplasia is a condition where cells are able to proliferate at increased rates but where normal morphology remains (Sherwood, 2013). When these cells experience a change in morphology and structure within tissue, the condition is known as dysplasia (National Cancer Institute, 2015). Signaling pathways determine whether cells are proliferating or quiescent (Duronio & Xiong, 2013). Cancer cells develop when the cells are able to multiply unsuppressed and do not respond to signals within the body to cease growth (Peiris-Pagès *et al.,* 2016; Tacar, Sriamrnsak & Dass, 2012). Cell proliferation that is not regulated by appropriate signals and infinite replication are hallmarks of cancer (Hanahan & Weinberg, 2011).

1.4.1. The cell cycle

The cell cycle consists of the first gap (G_1) phase, DNA synthesis (S), second gap (G_2) phase and mitosis (M) phase. Each of these phases is controlled by certain cyclin-dependent kinases (CDKs) and their respective cyclins (Duronio & Xiong, 2013; Fei & Xu, 2018). Pathways involved in stress response, differentiation, quiescence, and senescence initiates the G_1 phase. At the end of this phase, Cyclin-D-CDK4/6 and cyclin-E-CDK2 initiates the G_1/S phase transition by phosphorylating proteins in the Retinoblastoma (RB) pathway (Ewen *et al*., 1993; Akiyama *et al*., 1992). If no DNA damage is present, the cell proceeds to enter the S phase, where the DNA is replicated. The G_2 phase follows where the cell ensures the successful completion of DNA synthesis and starts preparing for the next phase. The end of this phase and the beginning of the M phase is regulated by cyclin-B-CDK1 (Duronio & Xiong, 2013. The cell divides during the M phase before entering back to the G_1 phase. Quiescence is achieved when the cell exits the G_1 phase and enters into the G_0 phase. Differentiated cells such as skeletal muscle cells enter into the G_0 phase and remain metabolically active for a long period of time. Developmental defects and cancer may occur due to the disruption of this mechanism (Sherr, 1996) or other alterations in CDKs and cyclins (Fei & Xu, 2018). The phosphoinositide 3-kinase (PI3K)-Akt and the extracellular signal-regulated kinases (ERK) pathways regulate the expression and ubiquitination of the G_1 cyclins and therefore regulate the progression of the cell cycle.

1.4.2. PI3K/Akt pathway

The phosphoinositide-3-kinase (PI3K)/Akt pathway is composed of various components that regulate its multiple steps as indicated in **Figure 1.5**. This signaling pathway regulates downstream effects such as cell growth, cell proliferation, transcription, protein synthesis, cell survival, and cell death (Hemmings & Restuccia, 2012). Due to the numerous stimuli and targets of Akt, tumour development is significantly influenced by mutations or dysfunctions in the pathway.

The binding of the required cytokine or growth factor to specific receptor tyrosine kinases (RTK) on the cell membrane causes phosphorylation of the receptor. This causes a transformational change allowing the regulatory subunit of PI3K, subunit p85, to bind to the receptor (Blalock *et al.,* 1999). The catalytic subunit of PI3K, p110, is then also recruited and activated. Complete activation of PI3K induces the membrane localization and conversion of phosphatidylinositol 4,5 bisphosphate (PIP_2) into phosphatidylinositol 3, 4, 5 trisphosphate (PIP_3) (Chang *et al.,* 2003). This conversion localizes phosphoinositol-dependent kinase-1 (PDK1) to the cell membrane where it recruits Akt to the cell membrane and phosphorylates it on Thr308 (Hemmings & Restuccia, 2012). The Ser473 phosphorylation site on Akt is additionally phosphorylated by mammalian target of rapamycin complex 2 (mTORC2) in order for full activation (Manning & Toker, 2017) (**Figure 1.5**). Akt, also known as Protein Kinase B (PKB), is a significant protein in the PI3K-Akt pathway that has numerous downstream effects after it is phosphorylated that promote cell growth and proliferation. The growth-promoting effects of PI3K are regulated by phosphatases that dephosphorylate PIP_3, therefore, inhibiting downstream effects (Steelman, Bertrand & McCubrey, 2004). These phosphatases are PTEN (Phosphatase and tensin homologue deleted on chromosome 10) and SHIP-1/2 (Src homology 2 (SH2) containing phosphatases 1 and 2), which are encoded by tumor suppressor genes (Wu *et al.,* 1998; Taylor *et al.,* 2000).

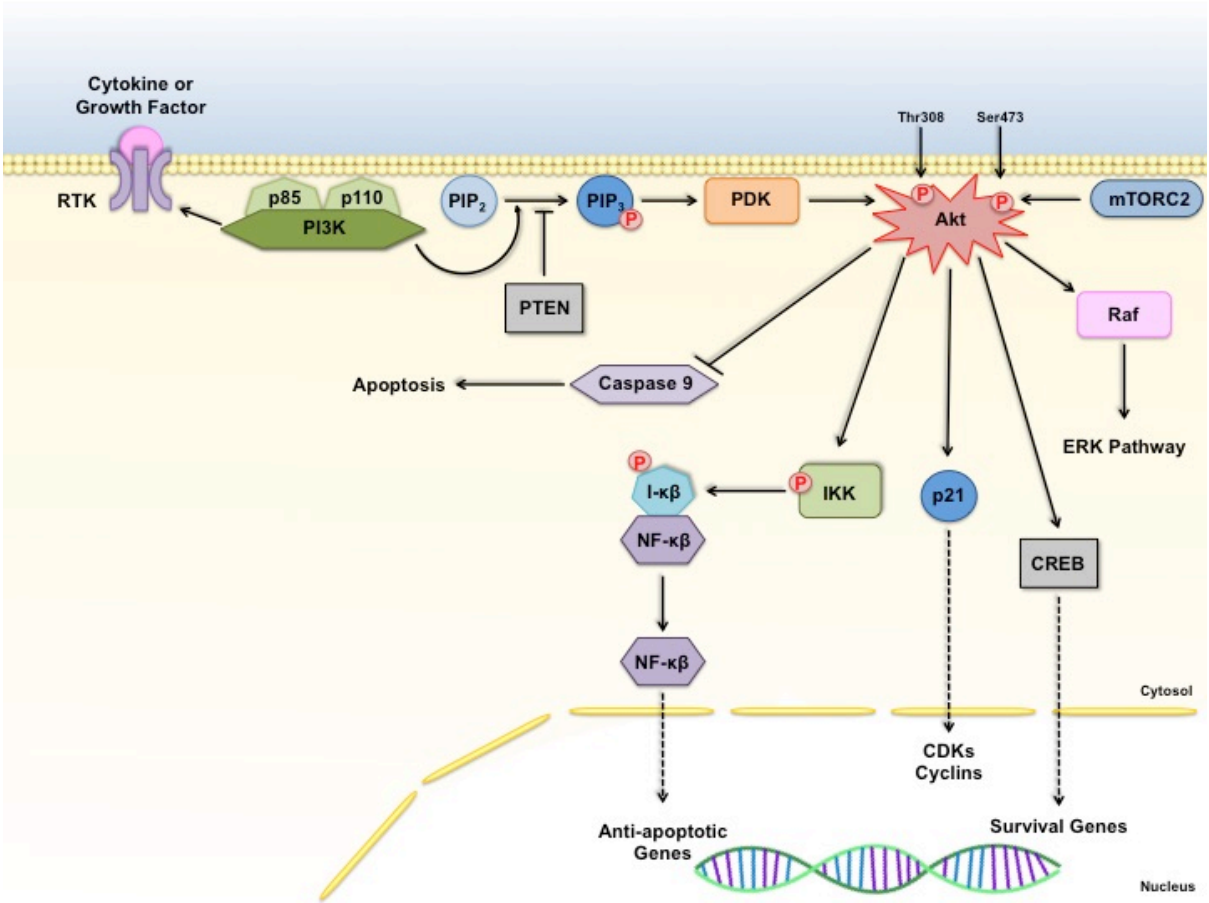

Figure 1.5: Activation of PI3K/Akt pathway and downstream effects. The PI3K/Akt pathway is initiated by a cytokine or growth factor binding to a RTK. PI3K then binds to the RTK and undergoes activation before phosphorylating PIP_2 into PIP_3. PDK localizes to the cell membrane and phosphorylates Akt at Thr308 while mTORC2 phosphorylates at Ser473. Following its activation, Akt is able to activate downstream effects including the ERK pathway, phosphorylation of p21 and IKK, transcription of CREB well as inhibition of caspase 9. Scheme reproduced from Hemmings & Restuccia (2012).

Selected downstream effects of activated Akt are represented in **Figure 1.5.** In mesenchymal cells, Akt has been shown to phosphorylate protein 21 (p21). Expression of p21 is responsible for the progression of the cell cycle and DNA synthesis through expression and activation of CDK and cyclins (Ghoudhury *et al.,* 1997). Activated Akt may also induce the transcription of cAMP response element-binding protein (CREB) and phosphorylation of inhibitor κβ kinase (IKK) (Nicholson & Anderson, 2002). Phosphorylated IKK induces phosphorylation and degradation of the protein inhibitor of κβ (I-κβ). This is significant as before phosphorylation, I-κβ binds to the transcription factor nuclear factor kappa-light-chain-enhancer of activated β cells (NF-κβ) and localizes it to the cytosol rendering it inactive (Chang *et al.,* 2003). Upon the degradation of I-κβ, NF-κβ is localized to the nucleus where transcription of targeted genes occurs. Anti-apoptotic genes are induced by NF-κβ activation thereby inhibiting apoptosis (Wang, Mayo & Baldwin, 1996). The

inactivation of Raf, Bad, pro-caspase 9, and other apoptotic proteins is also regulated by Akt activity (Chang *et al.,* 2003; McCubrey *et al*., 2007).

The dysregulation of PI3K has been observed in the development and progression of cancer such as breast cancer, prostate cancer, lung cancer, and melanomas (Chang *et al.,* 2003; McCubrey *et al*., 2007). Continuous phosphorylation of p21 by Akt induces an unregulated cell cycle due to high expression of CDK and cyclins (Ghoudhury *et al.,* 1997). Abnormal NF-κβ transcription of pro-apoptotic proteins due to the reduction in I-κβ inhibition also promotes cell survival (Wang, Mayo & Baldwin, 1996). Activated Akt additionally influences the regulation and expression of hormone receptors; therefore, high expression of Akt promotes resistance to hormone therapy (Shou *et al.,* 2004; Frogne *et al.,* 2005). Mutations in PI3K phosphatases may promote the continuous activation of PIP_3 and promote tumour development or progression (Wu *et al.,* 1998; Taylor *et al.,* 2000).

1.4.3. ERK pathway

The mitogen-activated protein kinase (MAPK) pathway is also known the ERK pathway. Cell growth and survival is promoted by the activation of the ERK pathway (Lu & Xu, 2006), however, pro-apoptotic induction has also been observed under certain conditions. This pathway is composed of a cascade of reactions from the cell membrane to the nucleus in order to phosphorylate and activate the transcription factors to induce specific gene expression such as cyclin D expression (Morrison, 2012; Yamaguchi *et al.,* 1995).

Specific integrins and growth factors that are involved in cell growth and differentiation induce the activation of the ERK signaling cascade represented in **Figure 1.6** (Yee, Weaver & Hammer, 2008; Renshaw, Ren & Schwartz, 1997). The binding of these molecules activate specific receptors on the cell membrane inducing the activation of the growth factor receptor-bound protein 2 (Grb2) / son of sevenless (SOS) coupling complex (McCubrey *et al*., 2007). This complex stimulates the exchange of guanine diphosphate (GDP) to guanosine triphosphate (GTP) by Ras. Ras is a GTP-binding protein that undergoes a conformational change and becomes active with the exchange of GDP. Raf, an enzyme from the serine/threonine-specific protein kinase family, contains multiple phosphorylation regulation sites that undergoes phosphorylation and dephosphorylating on various domains (Fabian, Daar & Morrison, 1993). After the activation of Ras, Raf is recruited to the plasma membrane and undergoes phosphorylation. Mitogen-activated protein kinase kinase 2 (MAP2K2), also known as mitogen-activated protein kinase/ERK kinase (MEK) is a duel specificity kinase that is activated by the phosphorylation of the serine residues in its

catalytic domain by Raf (Alessi *et al.,* 1994). Active MEK1 and MEK2 phosphorylate ERK 1 and 2 (McCubrey *et al*., 2007). ERK 1 and ERK 2 are regulated independently with ERK 2 being linked with proliferation while ERK 1 inhibits ERK 2 in specific cells (Pouysségur, Volmat & Lenormand, 2002). Phosphorylated-ERK downstream effects represented in **Figure 1.6** include activation of the transcription factor CREB and phosphorylation of IKK, which regulates the activation of NF-κβ (Nakano *et al.,* 1998).

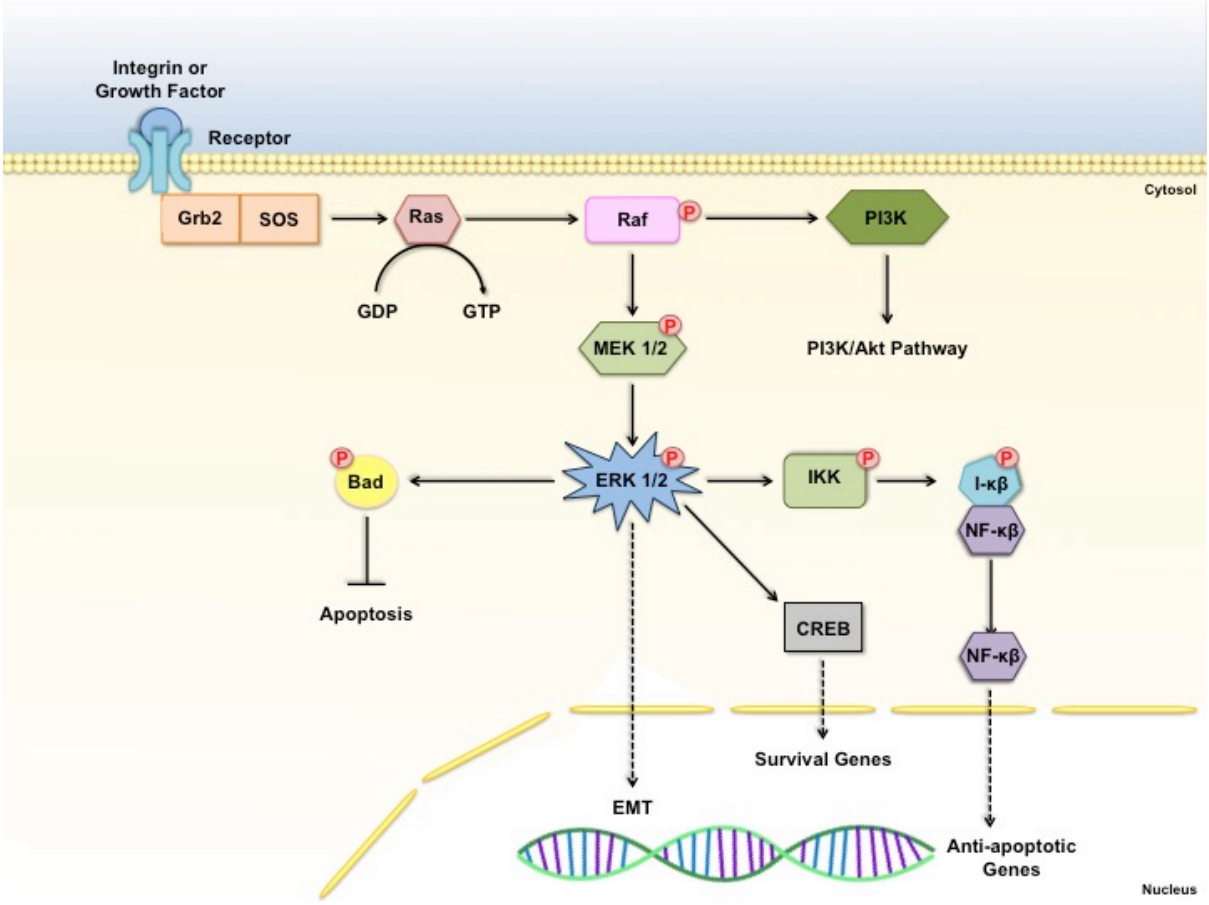

Figure 1.6: Activation of ERK pathway and downstream effects. The ERK pathway is initiation by the binding of an integrin or growth factor to a receptor that activates the Grb2/SOS coupling complex. This complex stimulates Ras to exchange GDP to GTP in order to become activated. Activated Ras phosphorylates Raf allowing for the stimulation of the PI3K/Akt pathway and phosphorylation of MEK1/2. Activated MEK1/2 phosphorylates and activates ERK 1/2 initiating its downstream effects, which include the transcription of CREB, phosphorylation of IKK and Bad as well as induction of EMT Scheme reproduced from Chang *et al.* (2003).

The dysregulation of ERK was observed to be involved in pathogenesis, progression and development of cancer (Zhu *et al.,* 2007; Fang & Richardson, 2005). Approximately 30% of human cancers are associated with constitutively active Ras proteins (McCubrey *et al*., 2007). Normal activation of Ras has been observed to influence the PI3K/Akt pathway as Ras promotes the localization of PI3K subunit p110 to the membrane and its activation

(Rodriguez-Viciana *et al.,* 1996). This promotes the downstream effects of the PI3K/Akt pathway. Cell growth, cell cycle arrest, and apoptosis are associated with an overexpression of active Raf proteins (Hoyle *et al.,* 2000). The variety of responses is a result of the specific isoform of Raf being overexpressed as A-Raf and Raf-1 promote cell proliferation while B-Raf promotes cell growth arrest (McCubrey *et al*., 2007). Mutation of B-Raf was observed in approximately 7% of cancers (Garnett & Marais, 2004). The post-translational phosphorylation of molecules involved in the regulation of apoptosis, such as Bad, caspase 9 and Bcl-2, is also influenced by Raf and ERK activity (Weinstein-Oppenheimer *et al.,* 2001). MEK regulates the protection of cells from oxidative stress and therefore dysfunction of MEK can promote resistance to ROS-dependent treatments, such as DXR (McCubrey *et al*., 2007). Additionally, epithelial cells, breast cancer cells, and fibroblasts have shown TGF-β facilitated activation of ERK which may promote the induction of EMT and cancer progression (Davies *et al*., 2005).

1.4.4. Mini-chromosome maintenance proteins

Replication of DNA consists of various components to maintain the integrity and stability of the genome. Mini-chromosome maintenance proteins (MCM) exhibit ATPase activity (Bochman & Schwacha, 2009) and play a role in recruitment of proteins involved in DNA replication as well as the formation of replication forks. The MCM proteins are responsible for the initiation and formation of pre-replicative complexes during the late M and early G_1 phase of the cell cycle. Following the formation of pre-replicative complexes, MCM proteins are phosphorylated by Dbf4-dependent kinase (DDK) and CDKs (Fei & Xu, 2018). Phosphorylation induces the recruitment of GINS (Go, Ichi, Ni, and San) and Cdc45 to the MCM proteins, which forms the Cdc45-MCMs-Gins (CMG) replicative helicase complex (Bruck & Kaplan, 2015; Yeeles *et al.,* 2015).

Replication checkpoints, transcription, and RNA splicing have also been observed to be regulated by MCM proteins (Stead *et al*., 2012; Li *et al.,* 2011; Chen *et al.,* 2014). The variety of downstream effects is due to MCM proteins containing several phosphorylation sites specific for kinases. The three kinases regulating MCM phosphorylation are cell division cycle (Cdc) kinases, CDKs, and ataxia telangiectasia/ ATM-and-RAD3-related proteins (ATM/ATR) (Fei & Xu, 2018). Each kinase phosphorylates specific sites within certain MCM proteins for the required function to occur. The phosphorylation of MCM2 by serine-threonine kinase Cdc7 at Ser27, Ser41, and Ser139 results in the initiation of DNA replication and promotion of ATPase activity while phosphorylation at Ser5 is needed for the pre-replicative complexes during the re-entry of the cell cycle (Stead *et al.,* 2012). The

MCM2 chromatin loading properties are regulated by Cdc7 phosphorylation of Ser40, Ser53, and Ser108 (Chen *et al.,* 2014). Cdc7 phosphorylation of MCM4 alternatively promotes the binding with CdC45 to the chromatin (Li *et al*., 2011), which is important for the induction of DNA replication and cell growth as previously described.

When the cell enters into the M phase, CDK2 phosphorylates MCM4 at Ser3, Thr7, Ser32, Ser54 and Thr110 in order to decrease MCM complex chromatin loading preventing DNA replication to re-occur during mitosis (Tudzarova *et al.,* 2016). Phosphorylation of MCM4 at Ser3, Thr7, Thr19, Ser54, Ser88, and Thr110 with Cdk2 further inhibits the MCM complex and reduces DNA helicase activity (Bochman & Schwacha, 2009; Moritani & Ishimi, 2013). The slowing or delaying of replication forks is known as replication stress (Fei & Xu, 2018). The majority of mutations resulting in genomic instability and tumour development occur as a result of replication stress (Tubbs & Nussenzweig, 2017).

ATM and ATR regulate this by stabilizing DNA replication forks and activating checkpoints in the cell cycle (Fei & Xu, 2018). DNA damage due to factors such as ultraviolet (UV) light and ionizing radiation (IR) induces replication stress that initiates the phosphorylation of Ser108 on MCM2. The replication fork is then a stabilized and delayed allowing cell to repair DNA damage (Cortez, Glick & Elledge, 2004). Abnormal MCM phosphorylation induces mutations in DNA replication and progression of the cell cycle, which influences development of diseases such as cancer (Fei *et al*., 2017). The upregulation of the PI3/Akt pathway has also been shown to directly phosphorylate MCM2 as a result of Akt activity (Chang *et al.,* 2003).

1.5. Evasion of Apoptosis

Apoptosis, first described by Kerr, Wylie & Currie (1972), is a cell death mechanism that ensures accurate embryogenesis and homeostasis in healthy tissue. This process is regarded as a form of programmed cell death as it is not only regulated by intracellular signals but also genetically (Nishida, Yamaguchi & Otsu, 2008). It is an energy-dependent mechanism composed of cysteine proteases known as caspases that require precise proteolysis for cleavage and activation (Kruidering & Evan, 2000; Martin & Green, 1995). Removal of old or DNA damaged cells occurs as a result of apoptotic mechanisms, with modest tissue disruption due to absence of inflammation induction (Elmore, 2007). Regulation of the apoptotic mechanism as shown in **Figure 1.7** is composed of three

pathways: extrinsic death receptor pathway, intrinsic mitochondrial pathway, and execution pathway.

1.5.1. Extrinsic death receptor pathway

Induction of the extrinsic death receptor pathway, represented in **Figure 1.7** is stimulated when the required extracellular death ligand binds to a death receptor on the plasma membrane of a cell. These receptors contain a cytoplasmic domain known as the death domain (DD). Combination of the ligand and receptor initiates trimerization of receptors forming a death complex (Ouyang *et al.,* 2002). A protein that contains a corresponding DD to the receptor and pro-caspase 8 is recruited to the death complex initiating formation of a death-inducing signaling complex (DISC) (Kischkel *et al.,* 1995). Cleavage and activation of pro-caspase 8 by DISC results in the formation of cleaved caspase 8. This active caspase protein contains a death effector domain (DED), which is able to induce the execution pathway, which will be discussed later (Ouyang *et al.*, 2012). The binding of cellular FLICE (FADD-like IL-1β-converting enzyme)-inhibitory protein (c-FLIP) to the death domains and pro-caspase 8 inhibits the extrinsic pathway (Scaffidi *et al.,* 1999).

1.5.2. Intrinsic mitochondrial pathway

Mitochondrial pro-enzymes regulate the intrinsic pathway. Induction of this pathway occurs by stimuli, such as toxins, free radicals or hypoxia, or due to the absence of growth factors, cytokines, and hormones that suppress cell death (Elmore, 2007). Bcl-2 (B-cell lymphoma 2) is a family of pro-apoptotic and anti-apoptotic molecules that regulate apoptosis (Ouyang *et al.*, 2012). The pro-apoptotic molecules include Bad, Bax, Bid, and Bcl-X_s while anti-apoptotic molecules are Bcl-2, Bfl-1, Mcl-1, and Bcl-X_L. An elevated Bcl-2/Bax ratio corresponds with the onset of apoptosis (Tacar, Sriamrnsak & Dass, 2012). Upon stimulation, the pro-apoptotic molecules are activated by dephosphorylation and cleavage before being translocated to the mitochondrial membrane (Shamas-Din *et al.,* 2011). These molecules, such as Bad, then promote the opening of the mitochondrial permeability transition (MPT) pore or bind to anti-apoptotic molecules rendering them ineffective (Yang *et al*., 1995; Elmore, 2007). Opening of the MPT leads to a reduction in the outer mitochondrial transmembrane potential resulting in the release of cytochrome c into the cytosol (Elmore, 2007). In the cytosol, apoptotic peptide activating factor-1 (Apaf-1) and pro-caspase 9, both containing caspase activation and recruitment domains (CARDs), bind each other through a CARD-CARD interaction and subsequently binds cytochrome c to form the apoptosome

complex (**Figure 1.7**) (Kurokawa & Kornbluth, 2009). The apoptosome cleaves pro-caspase 9 forming cleaved caspase 9. Similar to cleaved caspase 8, cleaved caspase 9 contains a DED that induces the execution pathway (Ouyang *et al.*, 2012).

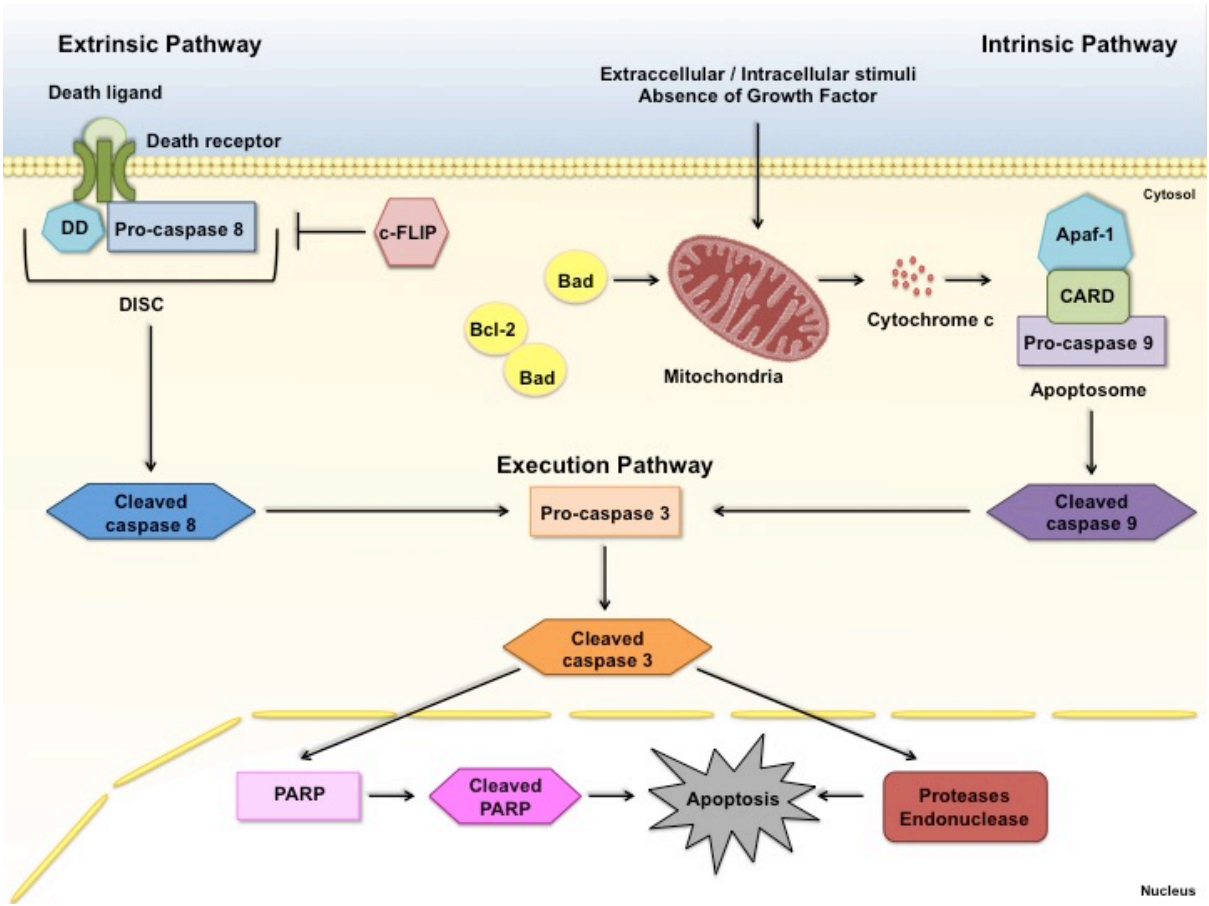

Figure 1.7: Regulation of apoptosis: extrinsic, intrinsic, and execution pathways. The extrinsic pathway is regulated by extracellular death ligands while the intrinsic pathway is regulated by mitochondrial pro-enzymes. Activation of these pathways may result in the activation of the execution pathway and induction of apoptosis. Scheme reproduced from Elmore (2007).

1.5.3. Execution pathway

The execution pathway is induced by cleaved caspase 8 from the extrinsic pathway and cleaved caspase 9 from the intrinsic pathway (**Figure 1.7**). These proteins activate pro-caspase 3 through cleavage forming cleaved caspase 3. Poly (ADP-ribose) polymerase (PARP) is found in the nucleus of a cell and regulates DNA repair by the modification of post-translated proteins in response to cell signaling (Herceg & Wang, 2001). Cleaved caspase 3 inactivates PARP by cleavage as cleaved PARP inhibits the repair of DNA (Ouyang *et al.*, 2012). Cleaved caspase 3 additionally activates proteases to degrade nuclear or cytoskeletal proteins or cytoplasmic endonucleases to degrade nuclear material

(Elmore, 2007). This allows for the final execution of apoptosis and morphological alterations.

The morphological alterations of the apoptotic process, described by Kerr, Wylie & Currie (1972), include shrinkage of cells in response to organelles becoming more tightly packaged and cytoplasm density changes. Nuclear condensation and the cleavage of chromosomal DNA into internucleosomal fragments is also observed (Renehan, Booth & Potten, 2001). The loss of cell-cell adhesion and ECM adhesion produces dynamic membrane blebbing. Due to these morphological changes, apoptotic bodies are formed that are degraded by non-inflammatory phagocytosis (Kerr, Wylie & Currie, 1972). The content of apoptotic bodies is dependent on cellular components that were located in areas where membranes underwent bledding.

1.5.4. Cancer and apoptosis

Mutations in the proliferation signaling of breast cells, such as increased expression of PI3K/Akt proteins and ERK proteins, promote cell survival gene expression as well as inhibit apoptosis (Weinstein-Oppenheimer *et al.,* 2001). This prevents damaged cells from being effectively removed, promoting cancer development and progression. Cell death avoidance, such as evasion of apoptosis, is a hallmark of cancer (Hanahan & Weinberg, 2011). Cancer cells display dysregulation of Bcl-2 proteins, such as an increase in anti-apoptotic Bcl-2 proteins or decrease in pro-apoptotic Bad protein, result in suppression of apoptosis which may lead to drug resistance (Kerr, Wylie & Currie, 1972). Chemotherapeutic agents, such as DXR, induce DNA damage and ROS to promote apoptotic cell death in cancer cells (Elmore, 2007). Additionally, DXR was observed to influence the apoptotic pathway through Bcl-2/Bax interactions (Leung & Wang, 1999). The concentration and treatment period of chemotherapeutic drugs to regulate this ratio therefore require to be optimized. The stimulation of the extrinsic apoptotic pathway by DXR has also been observed (Reed, 1994).

1.6. Invasion and Metastasis

The local occupation of tissue that is not the origin tissue of cancer cells is known as invasion while the occupation of distant organs by the cancer cells is known as metastasis (Mareel & Constantino, 2011). Surgery, endocrine therapy, radiotherapy or chemotherapy may stimulate signaling pathways in a tumour that promote invasion and metastasis (Ceelen

& Bracke, 2009; Mareel & Constantino, 2011). Invasion and metastasis are hallmarks of cancer and have been associated with the increase in therapy resistance and poor patient prognosis (Hanahan & Weinberg, 2011). Invasion and metastasis are multistep processes involving a large variety of cellular programs such as proliferation, cell-cell adhesion, cell-matrix adhesion, proteolysis, migration, and cell survival through the avoidance of cell death (Mareel & Constantino, 2011). The interactions occur between clusters of the same and different cell types, activation of several signaling pathways, and involves various sites within the body.

Bidard *et al*. (2008) described one possible mechanism of metastasis that occurs in three processes. Firstly, cells collectively migrate through the ECM, due to EMT activation, allowing the formation of gaps in the ECM. The migration of these initial cells may influence the direction and degree of metastasis. Secondly, there is a release of non-metastatic cancer cells, which have not undergone EMT, by the tumour into circulation by using the pathway formed by the initial invading cells. In combination with the initial cells, clusters of cells are formed and microenvironmental changes are made in the endothelium of the potential metastatic site. This develops a pre-metastatic niche. Finally, after the development of the pre-metastatic niche, circulating cells from the primary tumour populate and further alter the microenvironment of the secondary site to form final secondary tumours.

Tsuji, Ibaragi & Hu (2009) however proposed an alternative process in the mechanism of metastasis described by Bidard *et al*. (2008). They suggested that following invasion of EMT activated cancer cells into circulation these cells become dormant. The non-EMT cancer cells released into circulation are therefore solely responsible for adhesion to the endothelium of the secondary tumour site. These non-EMT cells alone are responsible for the development of the pre-metastatic niche and development of secondary tumours. This theory allowed for the elucidation of epithelial, E-cadherin positive phenotypes in these secondary tumours. Both the theories of Bidard *et al.* (2008) and Tsuji, Ibaragi & Hu (2009) highlighted the significant role that EMT has on the migration, invasion, and metastasis of cancer cells.

1.6.1. Epithelial-Mesenchymal Transition

The EMT is a highly conserved cellular process associated with one of the hallmarks and progression of cancer (Wong *et al.*, 2018). Based on the biological context in which the EMT can be found, it can be classified into three subtypes. Type I occurs within embryogenesis and organ development, Type II occurs in fibrosis and wound healing while being associated

with inflammation, and the final Type III occurs in cancer and will be the focus of this section (Zeisberg & Nelson, 2009). During EMT, epithelial cells that are attached to the basement membrane undergo various biochemical alterations that cause them to exhibit a mesenchymal phenotype (Kalluri & Weinberg, 2009). The mesenchymal phenotype promotes apoptotic resistance, cell migration, ECM component alterations as well as invasion and metastasis (Singh & Settleman, 2010). Apoptotic resistance as a result of EMT has also been observed to encourage drug resistance in cancer cells (Housman *et al.*, 2014). The plasticity of the EMT means that this process can be reversed with mesenchymal-epithelial-transition (MET) though little information is known about MET (Kalluri & Neilson, 2003). It has been shown that cancer cells which have undergone EMT and migrated to form secondary tumours at distant sites, do not maintain their mesenchymal phenotype (Zeisberg, Shah & Kalluri, 2004). The tumour at the secondary site is histopathologically similar to the primary tumour. The dissemination of secondary tumour cells to undergo MET is predicted to be due to the absence of signals in the primary tumour that induced EMT (Thiery, 2002).

During EMT various components are either induced or inhibited (**Figure 1.8**). These include reorganization and altered expression of the cytoskeletal proteins α-smooth muscle actin (α-SMA) and vimentin, the activation of transcription factors SNAIL, SLUG and TWIST (Guarino, Rubino & Ballabio, 2007), decreased expression of the cell surface protein E-cadherin as well as production of ECM-degrading enzymes and microRNA changes (Kalluri & Weinberg, 2009). Cancer cells that are the first to invade away from the primary tumour site have been found to express mesenchymal markers. These cells then enter into the invasion-metastasis cascade (Thiery, 2002). Although the mechanisms and signaling of EMT are not fully elucidated, molecules in the stroma associated with the tumour, such as hepatocyte growth factor (HGF), platelet-derived growth factor (PDGF), and TGF-β, induce EMT in two possible pathways. Smad proteins assisting the binding of TGF-β to activin receptor-like kinase-5 (ALK-5) receptor on the cell membrane induce motility activation. Autocine production of TGF-β is modulated by TGF-β and Smad that reinforces and up regulates EMT (Derynck, Akhurst & Balmain, 2001). Alternatively, significant evidence has indicated that TGF-β can induce EMT activation through the ERK pathway in mammary epithelial cells and hepatocytes (Kalluri & Weinberg, 2009; Zhang, Zhou & ten Dijke, 2013).

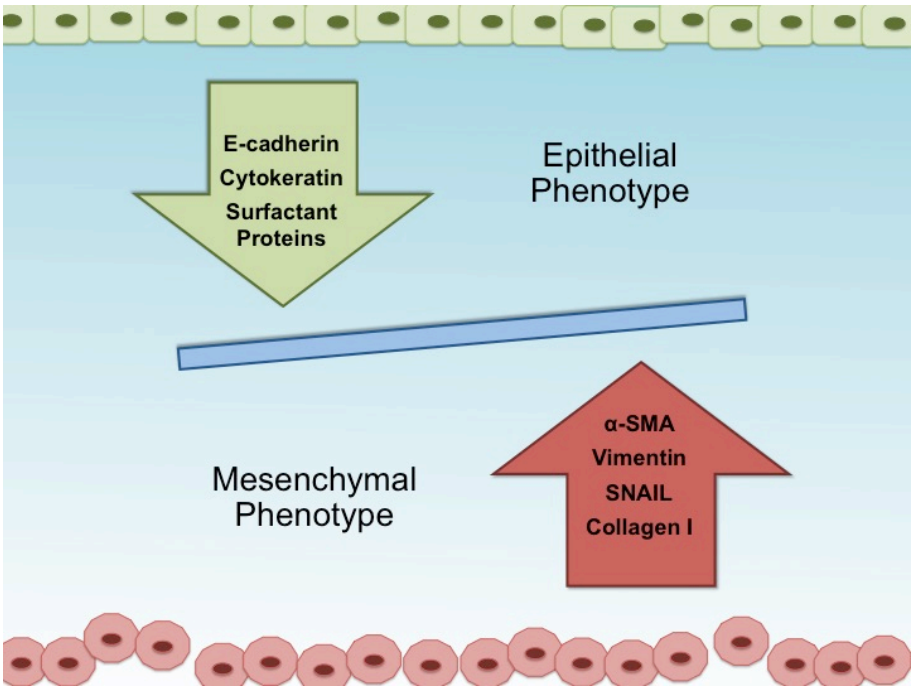

Figure 1.8: Markers of the Epithelial- Mesenchymal Transition (EMT) and Mesenchymal-Epithelial Transition (MET) dynamic processes. Increased expression of mesenchymal markers promotes a mesenchymal phenotype and the induction of Epithelial- Mesenchymal Transition (EMT) in epithelial cells while an increase expression of epithelial markers promotes an epithelial phenotype and the induction of Mesenchymal-Epithelial Transition (MET). Scheme reproduced from Hyun *et al.* (2016).

1.6.2. α-Smooth muscle actin

The protein α-SMA provides mechanical tension generated by the cell in order to maintain cell structure and motility. It is responsible for cell structure, integrity, and serves as an important component of the contractile apparatus. Fibrogenesis and the epithelial mesenchymal transition are influenced by the expression of α-SMA in cells and surrounding environments (Lee *et al.,* 2013). Due to the actin cytoskeleton influencing cell motility, alterations in actin expression promotes increased invasion and metastasis of cancer (Lambrechts, van Troys & Ampe, 2004). Lee *et al. (*2013) observed that EMT induction was influenced by α-SMA expression in lung adenocarcinoma. TGF-β was also observed to promote EMT in epithelial cancer cells that induces the expression of α-SMA (Masszi *et al.,* 2003). Smooth muscle cells and activated cancer-associated fibroblasts significantly express α-SMA, however, tumour cells are speculated to use actin bundles in order to invade surrounding tissue and metastases (Lambrechts, van Troys & Ampe, 2004).

1.6.3. Vimentin

Vimentin is the major cytoskeletal structural protein in mescenchymal cells. It is a type III intermediate filament (IF) that forms part of the cytoskeleton in combination with tubulin microtubules and actin microfilaments (Satelli & Li, 2011). Vimentin is responsible for the integrity of the cytoplasm, maintaining cell shape and the stabilization of interactions in the cytoskeleton. Vimentin expression is found in a variety of cell types including skeletal muscle (Sarnat, 1992). The influence of vimentin expression on cancer progression has not been fully investigated, however, vimentin has been shown to mediate migration of breast cancer cells through Ras activation (Vuoriluoto *et al.,* 2010). It has been shown that NF-κβ and TGF-β induction is important in the activation and maintenance of EMT as both these components bind to the promoter region of vimentin (Huber *et al.,* 2004; Wu *et al.,* 2007). E-cadherin expression has been observed to correlate with the expression of vimentin (Sommers *et al.,* 1994). Additionally, several aggressive breast cancer cell lines have been shown to exhibit increased expression of vimentin that correlated with increased migration and invasion (Gilles *et al.,* 2003). The induction of EMT is not the only process mediated by vimentin expression in epithelial cells, the induction of the reverse process, MET has also been shown to be mediated by vimentin (Satelli & Li, 2011).

1.6.4. SNAIL

SNAIL is a transcription factor associated with the suppression of E-cadherin as well as with neural differentiation and cell survival (Wang *et al.*, 2013). The family proteins of SNAIL include SNAIL 1 (SNAIL), SNAIL 2 (SLUG), and SNAIL 3 (SMUC), which are all transcriptional factors. These proteins consist of a highly conserved C-terminal domain that binds to the E-box motif (5'-CANNTG-3') present within targeted gene promoters (Nieto, 2002). The N-terminal consists of the conserved SNAG (SNAIL/Gfi) domain that is important for the binding of multiple transcriptional co-repressor complexes. Tumour grade, metastasis and poor patient prognosis have been found to positively correlate with SNAIL expression (Peinado, Olmeda & Cano, 2007; Chen *et al.,* 2010). Once TGF-β expression is up regulated, TGF-β induces activation of the transcription factors SNAIL, SLUG, and survival of motor neuron protein interacting protein 1 (SIP1). The PI3K-Akt pathway alternatively induces downstream effects on growth factors that activate receptor tyrosine kinases (RTKs). This activation then induces SNAIL activity (Wang *et al.,* 2013). Phosphorylation of NF-κβ, by Akt also up regulates SNAIL activity (Julien *et al.,* 2007).

1.6.5. E-cadherin

E-cadherin is a cell surface protein important for the formation and maintenance of adherent junctions within cell-cell adhesion. Within the mammary gland, E-cadherin is required for normal cell function of cells in the lactating gland (Boussadia *et al*., 2002). SNAIL mediates the methylation of the E-cadherin promoter with histone H3 lysine 9-methylation (H3K9me3) (Dong *et al.*, 2012). The repressor binding to the promoter region induces epigenetic alterations consequently blocking transcriptional machineries from accessing the promoter. Alterations in E-cadherin expression have been associated with increased invasion and progression of tumours in breast (Li *et al.,* 2017), ovarian (Sawada *et al.*, 2008), prostate (Umbas *et al.*, 1997), colorectal (Christou *et al.*, 2017), and gastric cancer (Liu & Chu, 2014). The decrease of E-cadherin expression can be a consequence of the alterations of EMT or it can be directly influenced by the EMT, such as the significant upregulation of the transcription factor SNAIL (Hollestelle *et al.*, 2013). Coding sequence mutations account for the minority of dysfunctional E-cadherin expression in cancer (Jeanes, Gottardi & Yap, 2008), while epigenetic alterations at various positions of the promoter region play a significant role in expression dysregulation (Wong *et al.,* 2018). Early studies reported that E-cadherin expression was an important contributor to the suppression of invasion and that the decrease in its expression induced invasion as well as dedifferentiated or poorly differentiated carcinomas (Wong *et al.*, 2018). Contradictory, recent studies observed breast cancer metastases or metastatic tumours originating from these cells, to express elevated E-cadherin expression and have induced the EMT (Chao, Shepard & Wells, 2010).

1.6.6. Hybrid phenotypes

The completion of EMT is characterized by the degradation of the epithelial basement membrane and the development of a mesenchymal phenotypic cell that is able to migrate to other locations, other than that of epithelium origin (Kalluri & Weinberg, 2009; Mareel & Constantino, 2011). Due to this, cancer cells were previously assumed to obtain fully epithelial or mesenchymal state following MET or EMT (Thiery, 2002). Current studies however have shown that these are not binary processes as cancer cells may consist of phenotypes that express both epithelial and mesenchymal markers (Jolly *et al*., 2017). Additionally, carcinoma cells have been shown to undergo partial transitions rather than a terminal epithelial or mesenchymal state (Lambert, Pattabiramn & Weinberg, 2017). This hybrid phenotype is significantly found more regularly in TNBC patients (Yu *et al.,* 2013). Cancer cells with hybrid phenotypes are able to rapidly enter back into the cell cycle and proliferate after metastasis to secondary sites. Cancer cells that undergo EMT or MET and

express an epithelial, mesenchymal or hybrid phenotype will have different responses to signaling pathways for cell growth, cell death, metastasis and drug resistance.

1.7. Skeletal Muscle

The contractile and metabolic properties of muscle fiber types are influenced by systemic and local microenvironments and are favorably plastic (Schiaffino & Reggiani, 2011). The mitochondria are linked to the regulation of cellular processes involved in remodeling and growth within skeletal muscle (Hardee, Montalvo & Carson, 2017). The disruption of oxidative metabolism will decrease basal protein synthesis within skeletal muscle (Hardee, Montalvo & Carson, 2017). The mitochondrial content and metabolic enzyme capacities of different fiber types vary. This allows the rate and capacity of protein synthesis in oxidative muscles to be greater than glycolytic muscles (Habets *et al.,* 1999). The human body consists of 50% skeletal muscle, however, cancer metastasis into skeletal muscle, including breast cancer, is uncommon (Surov *et al.,* 2009). Breast cancer patients have reported a reduction in body mass, loss of muscle strength, and muscle fatigue that are intensified during chemotherapy (Fox *et al.,* 2009; Klassen *et al.,* 2016).

1.7.1. Cancer Cachexia

Skeletal mass depletion is a wasting syndrome referred to as cachexia (Hardee, Montalvo & Carson, 2017). Increased susceptibility to treatment-induced toxicity, reduced physical function and psychosocial ability reduction have been observed with the depletion of muscle mass (Jung *et al.,* 2015). Cancer-induced cachectic muscles have interlinking processes that allow for interrupted muscle oxidative metabolism and protein turnover (Hardee, Montalvo & Carson, 2017). These small variations in daily protein synthesis induce a significant disruption in long-term skeletal muscle maintenance (Horstman *et al.,* 2016). Stimuli in both systemic and local environments induce a response in skeletal muscles that disturb the energy metabolism and proteostasis (Carson, Hardee & VanderVeen, 2016). These stimuli may be directly secreted from the cancer or be downstream stimuli from other mechanisms influenced by the cancer. Anabolic resistance is a term used to describe the inability to stimulate protein synthesis and plays a significant role in the regulation of muscle mass loss with aging (Fry & Rasmussen, 2011). The suppression of basal protein synthesis in cancer patients and preclinical cachexia models has been observed and attributed to muscle wasting (Dworzak *et al.,* 1998).

Wasting susceptibility is influenced by the oxidative metabolism capacity of skeletal muscles. Models of cancer cachexia demonstrated that mitochondrial dysfunction influences metabolic and energetic stress pathways that regulate protein synthesis (Hardee, Montalvo & Carson, 2017). The loss of skeletal muscle mass was directly associated with the morbidity and mortality of cancer patients as cachexia is credited to be the cause of death of 20-40% of cancer patients (Tisdale, 2009). In breast cancer patients however, a decrease in body weight and muscle mass was observed in only 24% of patients, while patients with gastric and pancreatic cancer experienced greater weight loss (Fox *et al.,* 2009). Mitochondrial dysfunction in skeletal muscle, due to tumour growth, has been observed indicating communication between the skeletal muscle microenvironment and cancer microenvironment (Tzika *et al.,* 2013). DXR treatment was shown to reduce muscle mass in cancer patients by targeting type 1 and type 2 fibers (Tozer *et al.,* 2008). The mechanism by which DXR is able to induce catabolism in muscles is currently undefined however, the production of ROS is shown to be significant in the process (Gilliam *et al*., 2011). In both skeletal and cardiac muscle, the ROS produced by DXR targets the complexes of the mitochondrial ETC (Min *et al.,* 2015). This results in muscle degradation by the activation of downstream pathways such as apoptosis, through Caspase 3 activity, and the ubiquitin-proteasome pathway (Jackman & Kandarian, 2004). A study completed by Bohlen *et al.* (2018) investigated the alterations in skeletal muscles of breast cancer patients. They observed that oxidative phosphorylation and mitochondrial pathways were dysfunctional in breast cancer patients that were not undergoing chemotherapeutic treatment as well as those that were. This was present within early stage breast cancer development of luminal, triple positive as well as triple negative breast cancer tumours. The activity of complexes in the mitochondrial ETC were down regulated as well as alterations in energy metabolism due to peroxisome proliferator-activated receptor (PPAR)-related signaling. The transcriptional alterations were not dependent on cancer type or treatment. The authors further speculated that cancer patients who experience significant weight and muscle loss undergo complete muscle atrophy while patients who experience minimum weight loss, such as breast cancer patients, exhibit dysregulation of oxidative phosphorylation pathways within skeletal muscle mitochondria (Bohlen *et al.,* 2018). While the influence of breast cancer and DXR on skeletal muscle has been investigated, the impact of skeletal muscle and DXR induced skeletal muscle dysfunction on breast cancer remains unclear. Investigating and elucidating the mechanisms linking cachexia and cancer could improve the treatment outcome of cancer patients.

1.8. Problem Statement

Although it is well established that cancer is a genetic disease, in the last decade our genetic view has expanded by the observation that tumours are thriving organs with multiple cell types which can affect tumour progression and response to therapy. This view has added significant complexity to the study of cancer when the effects of fibroblasts, mesothelial cells, immune cells, adipocytes, endothelial cells and muscle cells are taken into account. Since the pectoris muscle is in close proximity of the mammary gland, and chemotherapy also induces muscle wasting, it is important to investigate the interaction of skeletal muscle with cancer cells. The impact of the skeletal muscle microenvironment, in response to cancer and DXR treatment, on the efficiently of DXR to induce cell death in breast cancer cells has not been fully investigated. Understanding the mechanisms involved in the development of drug resistance and cancer metastasis is crucial to improve patient prognosis, especially since these two events have a significant impact on cancer mortality.

1.9. Hypothesis

We hypothesize that the skeletal muscle microenvironment of C2C12 myotubes will alter the response of E0771 breast cancer cells to DXR treatment resulting in increased resistance, promotion of proliferation, apoptosis avoidance, and metastasis induction.

1.10. Aims

1. To investigate the reciprocal interactions between mouse breast cancer cells (E0771) and mouse myotubes (C2C12).

2. To investigate the effects of DXR on the interactions between mouse breast cancer cells (E0771) and mouse myotubes (C2C12).

1.11. Objectives

- Determine the influence of E0771 conditioned media with/without DXR on mitochondrial oxidative stress and cell integrity in C2C12 myotubes.
- Determine the effect of myotube conditioned media with/without DXR on drug resistance and proliferation pathways in E0771 cells.
- Determine the effect of myotube conditioned media with/without DXR on the apoptotic pathway in E0771 cells.
- Determine the effect of myotube conditioned media with/without DXR on migratory and metastatic pathways in E0771 cells.

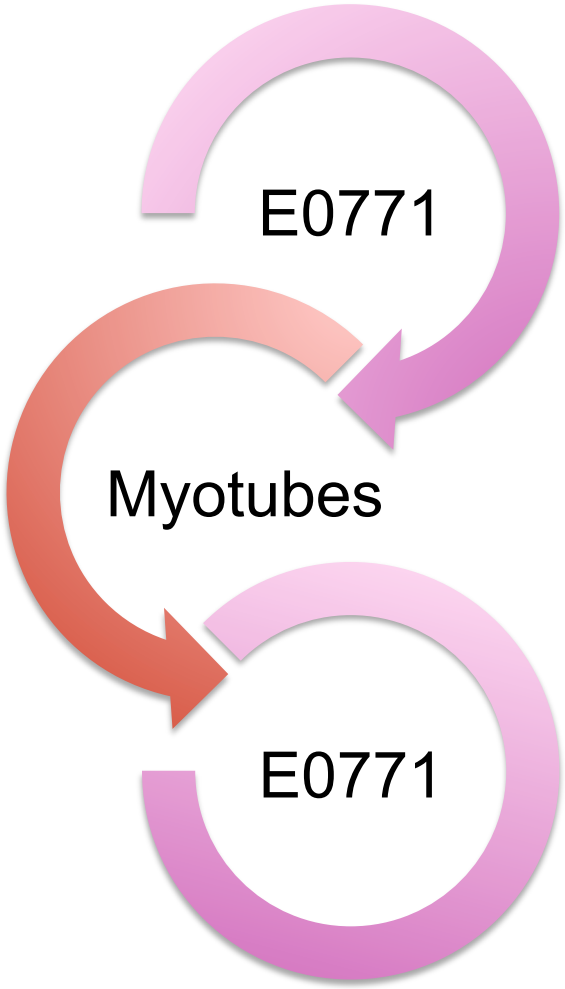

Figure 1.9: Scheme representing the reciprocal workflow for study. The investigation of the dynamic interacts between E0771 cells and myotubes consists of treatment cycles of conditioned media as represented.

Chapter 2: Materials and Methods

2.1. Cell Culture

A mouse metastatic mammary carcinoma cell line, E0771, and a mouse skeletal muscle cell line, C2C12, were used in this study. Cell lines were cultured in sterile Dulbecco's Modified Eagle's Medium (DMEM) (Gibco®, ThermoFisher Scientific®, #41965-062) supplemented with filtered 10% fetal bovine serum (FBS) (Capricorn Scientific®, ThermoFisher Scientific®, #FBS-G1-12A) and 1% Penicillin-Streptomycin (Gibco®, ThermoFisher Scientific®, #15140-122). Cells were incubated at 37°C and 5% CO_2 throughout the study. Cells were sub-cultured regularly once 70 – 80% confluency was achieved with the aid of 0.25% Trypsin-EDTA (Gibco®, ThermoFisher Scientific®, #25200072) followed by cell counting. E0771 cells were seeded, as required, at a density of 25 000 cells per well in a 96-well plate, 50 000 cells per well in a 24-well plate and 250 000 cells per well in a 6-well plate. The C2C12 cells were seeded at a density of 800 000 cells per T25 flask, and 50 000 cells in a 24-well plate. The C2C12 cells were allowed to grow to 70% confluency before being differentiated with 1% Horse Serum (Lonza, BioWhittaker®, #14-403F) for four days to induce myotube formation. After differentiation, media was removed and treatments commenced. Complete cell culture protocols for both E0771 cells and C2C12 cells can be found in **Appendix D.** For each experiment, the treatments for E0771 and C2C12 cell lines occurred in triplicate for a 24-hour time period. Each experiment was individually repeated three times in order to establish an n = 3.

2.2. Conditioned Media

Two individual treatment cycles of conditioned media were collected. The first cycle of conditioned media was collected from E0771 cells after a 24-hour treatment. Conditioned media was then centrifuged at 10 000 rpm for 10 minutes at 4°C. Media was finally filtered with a 0.2 micron syringe filter (Lasec®, #FLAS25AC2050) before being snap frozen in liquid nitrogen and stored at -80°C until use. The collection of the second cycle of conditioned media was collected from myotubes after a 24-hour treatment period. This conditioned media was harvested, purified and stored as the E0771 cells previously described.

2.3. Treatments

Treatment groups for the production of the first cycle of conditioned media from the E0771 cells included a **Control** group consisting only of serum free media (SFM) and a doxorubicin

(**DXR**) group consisting of SFM and DXR as seen at the top of **Figure 2.1**. DXR was prepared in DMSO as a stock solution of 3.4 µM (Lasec®, #FLAS25AC2050) before being added to SFM to obtain a final concentration of 1.6 µM.

The treatment for the second cycle of conditioned media to be harvested and for all myotube experiments indicated in the middle section of **Figure 2.1**. These treatments consisted of a control group **(Control)** containing 50% SFM and 50% differentiation media, a DXR group **(DXR)** containing 50% SFM, 50% differentiation media and 1.6 µM DXR, a conditioned media control group **(C.Control)** containing 50% SFM and 50% control conditioned media from E0771 cells, and a conditioned media DXR group **(C.DXR)** containing 50% SFM and 50% DXR conditioned media from E0771 cells.

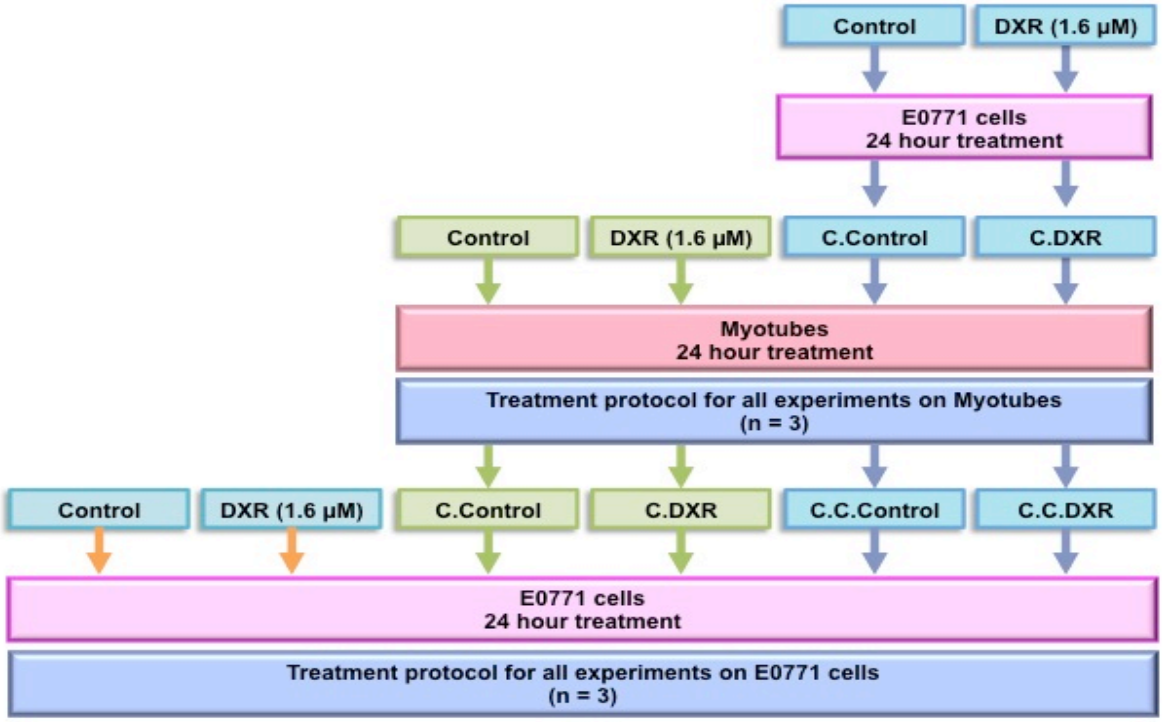

Figure 2.1: A visual representation of 24-hour treatments for the production of conditioned media and experiments on myotubes and E0771 cells. All treatments were prepared in a 1:1 ratio with serum free media and the relevant complete media or conditioned media. For both cell lines, Control consisted of serum free media and complete media while DXR consisted of serum free media, complete media and 1.6 µM. Myotube conditioned media treatments for experiments contained conditioned media harvested from Control and DXR treated E0771 cells. The conditioned media treatment of E0771 cells for experiments contained conditioned media harvested from Control and DXR treated myotubes as well as myotubes treated with conditioned media from E0771 cells.

Treatment of the E0771 cells for all experiments is indicated at the bottom of **Figure 2.1**. These treatment groups consisted of the following treatment groups: a control group **(Control)** containing only SFM, a DXR group **(DXR)** containing SFM and 1.6 µM DXR, a conditioned media control group **(C.Control)** containing 50% SFM and 50% control conditioned media from myotubes, a conditioned media DXR group **(C.DXR)** containing 50%

SFM and 50% DXR conditioned media from myotubes, an E0771 conditioned media control group **(C.C.Control)** containing 50% SFM and 50% control conditioned media from myotubes treated with E0771 conditioned media, and an E0771 conditioned media DXR group **(C.C.DXR)** containing 50% SFM and 50% DXR conditioned media from myotubes treated with E0771 conditioned media.

2.4. Assessment of Mitochondrial ROS Production (MitoSOX™)

MitoSOX™ (Invitrogen™, #M36009) is a fluorogenic dye that is able to permeate cells and target mitochondria. It is rapidly oxidized by super-oxide but no other reactive oxygen species. After the 24-hour treatment period of the myotubes, media was removed and cells washed with warm PBS (phosphate-buffered saline). A 5 µM MitoSOX™ working solution was prepared by dissolving the powder in PBS and 1% horse serum. The working solution was added to each well and allowed to incubate, covered in foil, under growth conditions for 15 minutes. Afterwards, MitoSOX™ solution was carefully removed, cells washed with warm PBS and a 5 µM Hoechst 33342 (Sigma-Aldrich®, #B2261) working solution, prepared with serum free media, was added to each well. The cells in the plate were incubated covered again under growth conditions for 10 minutes before being washed with warm PBS. A 4% paraformaldehyde solution was then used to fix cells for 10 minutes followed by another wash with PBS. Dako fluorescent mounting media was added to each well for improved imaging. A Nikon Eclipse E400 microscope equipped with DS-Fi2 colour digital camera with DAPI barrier filter (excitation 340-380 nm, emission 435-483 nm) and Tx Red barrier filter (excitation 540-580 nm, emission 600-650 nm) was used to capture 6 random fields for imaging at 10X objective. Processing and analyses of images were completed using Fiji software (Schindelin *et al.,* 2012) to determine florescent intensity as an indicator of mitochondria super-oxide production and mitochondrial function.

2.5. Assessment of myotube width (Cell Tracker™)

Myotubes are multi-nuclei cells and have high mitochondrial respiratory rates; therefore determining cell viability using a mitochondrial reductive assay, such as MTT, is inaccurate. Instead the viability and integrity of myotubes were determined based on alterations in myotube width and length, as a decrease in width indicates the presence of skeletal muscle catabolism (Gilliam *et al.,* 2012). Cell tracker™ Green, CMFDA (5-chloromethylfluorescein diacetate) (Invitrogen™, #C2925), is a fluorescent dye used to indicate cell location. The dye is able to permeate cell membranes where it is then transformed into cell membrane-

insoluble reaction products. C2C12 cells were grown, differentiated and treated in 24-well plates. After the 24-hour treatment period, media was removed and cells were washed with warm PBS. Warm Cell tracker™ working solution was prepared by dissolving the powder in serum free media to a final concentration of 5 µM, before being added to each well and allowed to incubate covered in foil under growth conditions for 30 minutes. A 5 µM Hoechst 33342 working solution, prepared in serum free media, was added to each well and allowed to incubate under growth conditions for another 10 minutes. The solution was removed and wells carefully washed with warm PBS. Fixation of cells was completed using 4% paraformaldehyde for 10 minutes followed by another wash with PBS. Dako fluorescent mounting media (Diagnostech®, #S302380) was added to each well for improved imaging. A Nikon Eclipse E400 microscope equipped with DS-Fi2 colour digital camera (Nikon, Japan) with DAPI barrier filter (excitation 340-380 nm, emission 435-483 nm) and FITC barrier filter (excitation 465-495 nm, emission 515-555 nm) was used to capture 6 random fields for imaging with the 10X objective. Images were processed and analysis completed using Fiji software (Schindelin *et al.,* 2012) to determine myotube width.

2.6. Cell Viability Assessment

A 3-(4, 5-dimethylthiazol-2-yl)-2, 5-diphenyltetrazoliumbromide (MTT) cell viability assay was conducted to assess mitochondrial reductive capacity, as an indication of the percentage of viable cells after treatments (Riss *et al*., 2004). The MTT powder and solution is light sensitive therefore it was covered and the lights were switched off in the working area. The MTT solution was prepared by dissolving MTT powder (Sigma-Aldrich®, #M2003) in PBS to a final concentration of 0.01 g/mL. Additional PBS was added to a final ratio of 1:3 (0.01 g/mL MTT:PBS) and mixed thoroughly. After the 24-hour treatment period, E0771 cells grown in 96-well plates were treated with MTT solution before being covered in foil and incubated for 1 hour under growth conditions. Viable respiring cells take up the yellow tetrazolium salt, present in the MTT solution, and produce purple formazan crystals. The crystals were then dissolved in an acidic Isopropanol/Triton-X 50:1 ratio solution and absorbance values read using a plate reader (EL 800 Universal Microplate Reader, Bio-Tek Instruments Inc) at 595 nm. Blank absorbance values were used to standardize treatment values and all values were analyzed as a percentage of the control.

2.7. Migration Scratch Assay

A migration scratch assay, also known as a wound-healing assay, was used to assess the migratory capacity of the E0771 cells. The E0771 cells were grown to 90-95% confluency in

a 6-well plate. Three individual scratch wounds were made using a sterile yellow pipette tip in each well. Cells were washed with warm sterile PBS to remove cellular debri before fresh growth media was added to each well. Due to the light sensitivity of DXR and Mitomycin C (MMC), treatment was completed after the initial images were acquired in order to prevent degrading of these products during initial set up. Brightfield images were acquired using the 4X objective on an Olympus® IX81 inverted fluorescence microscope with the Olympus® Cell^R software (Olympus®, GMBH Japan). This microscope allows for live cell imaging as it is equipped with an incubator system that is temperature-controlled at 37°C. The X, Y and Z coordinates of each image position can be saved onto the system and accessed at the different time points, this allows for improved accuracy. Three random positions, on three different scratches, were saved and imaged per group, while the experiment was also repeated three times. Once the 0 hour time point images for all treatment groups were completed, the cells were refreshed with the required treatment, indicated in **Figure 2.1,** and 10 µg/mL MMC (Sigma-Aldrich®, #M4287) dissolved in Dimethyl sulfoxide (DMSO) (Sigma-Aldrich®, #D2650). Cells were treated with the cytostatic agent MMC in combination with the treatments, as this compound is a strong DNA cross linker and inhibits the synthesis of DNA. This allowed for the exclusion of cellular proliferation during wound closure. A dose response of MMC on E0771 cells was completed by Mitchell (2017), which indicated the optimal concentration of MMC to be 10 µg/mL. Additional images were taken at time points of 6, 12 and 24 hours at the same positions saved at time point 0. Analysis of each image was completed by measuring the area (µm^2) of the wound (Justus *et al*, 2014), using Fiji software (Schindelin *et al.,* 2012). Wound closure over time was determined using the equations in **Figure 2.2** adapted from Davis (2016) and Mitchell (2017).

$$\%\ wound\ closure\ at\ x\ hour = \frac{Wound\ area\ at\ 0\ hour - Wound\ area\ at\ x\ hour}{Wound\ area\ at\ 0\ hour} \times 100$$

$$rate\ of\ wound\ closure\ at\ xhour(\%.hour^{-1}) = \frac{\%\ wound\ closure\ (x\ hour)}{x}$$

Figure 2.2: Equations used for analyses of wound closure in migration scratch assay. Calculation of the percentage of wound closure over time and rate of wound closure using wound area measurement at timepoints following treatment of E0771 cells. Adapted from Davis (2016) and Mitchell (2017).

2.8. Protein Extraction

Myotubes for protein extraction were grown, differentiated and treated in T25 flasks while E0771 cells were grown and treated in 6-well plates. Modified radioimmunoprecipitation (RIPA) buffer with pH 7.4 was prepared containing 65 mM Tris-base, 154 mM sodium chloride (NaCl), 1% nonyl phenoxypolyethoxylethanol (NP-40), 1% sodium deoxycholate, 5 mM ethylenediamine tetraacetic acid (EDTA), 5 mM ethylene glycol-bis(β-aminoethyl ether)-N,N,N',N'-tetraacetic acid (EGTA), and 0.1% sodium dodecyl sulfate (SDS). Protease inhibitor cocktail at 1X dilution in dH_2O (Roche, #11893580001), 1 mM sodium orthovanadate (Na_3VO_4), 1 mM sodium fluoride (NaF) and 1 mM Phenylmethylsulfonyl Flouoride (PMSF) was added to RIPA buffer immediately before use. Media from cells was removed and flasks/wells were washed twice with ice-cold PBS before adding RIPA buffer to all flasks/wells. A cell scraper was used to scrape cells loose from flasks/wells and cell suspensions from triplicate flasks/wells of the same treatment group were pooled into pre-cooled microtubes. Sample lysates were kept on ice and sonicated (Sonicator S-4000, Ultrasonic Liquid Processors, Misonix) at amplitude of 5A for 5 seconds. Sonicated lysates were placed on ice to allow the foam to settle before being centrifuged at 16.3 g for 2 minutes at 4°C. The supernatant was then collected in a clean-labeled pre-cooled centrifuge tube and kept on ice before being used for protein determination.

2.9. Protein Determination & Sample Preparation

The Bradford assay (Bradford, 1976) was used to determine the total quantity of protein within each lysate to ensure that equal amounts of protein were loaded into each well for electrophoresis. A bovine serum albumin (BSA) (Roche, #10735078001) working solution with a final concentration of 200 µg/mL was used to prepare standards on ice (0 µg/mL, 2 µg/mL, 4 µg/mL, 8 µg/mL, 12 µg/mL, 16 µg/mL, and 20 µg/mL) in duplicate in order to establish a standard curve. The Bradford working solution containing Coomassie Brilliant Blue G-250 (Sigma-Aldrich®, #27815-25G), ethanol, phosphoric acid and dH_2O was used at a ratio of 9:1 with the standards as well as in the sample lysates. A Cecil CE 2021 (2000 Series) spectrophotometer, set to 595 nm and zeroed using a blank, was used to measure the absorbance of the standards and sample lysates. A standard curve was drawn in Microsoft® Excel and the protein concentration for each sample lysate was determined.

While working on ice, the appropriate volumes of protein sample from each treatment group was added to the appropriate volume of Laemmil's sample buffer, with a final concentration of 62.5 mM Tris with pH 6.8, 4% SDS, 10% glycerol, 0.03% Bromophenol blue, and 5% β-

mercaptoethanol, as determined in the Bradford Assay. Prepared samples were mixed thoroughly and stored in the -80°C freezer until use.

2.10. SDS-PAGE & Western blot

Separations of protein samples were done with sodium dodecyl sulphate polyacrylamide gel electrophoresis (SDS-PAGE). Stain free self-cast gels were prepared using 12% resolving solution, supplemented with 1% Trichloroethylene (TCE) (Sigma-Aldrich®, # T54801), and 4% stacking solution. TCE binds to proteins and emits a fluorescent signal after activation using ultraviolet (UV) light allowing proteins to be visible without the requirement of a staining step, therefore stain free. Prepared samples were thawed on ice before being briefly vortexed, heated at 95°C for 5 minutes and kept on ice. BLUeye Prestained Protein Ladder (GeneDirex®, #PM007-0500) was loaded into first well of all gels in order to determine the molecular weights of specific bands. A standard sample was then loaded followed by the required protein samples. Proteins were separated at 90 V for 10 minutes until samples had passed through the stacking gel followed by separation at 100 V until completion. Gels were activated using the stain-free gel protocol: 2.5 minutes activation and 5-second exposure using the ChemiDoc™ MP Imaging System with Image Lab™ Software (Bio-Rad®). Proteins were transferred from the gel onto polyvinylidene fluoride (PVDF) membranes using the Bio-Rad® RTA Midi PVDF Transfer Kit (Bio-Rad®, #1704273), the TransBlot® Turbo™ Transfer System (Bio-Rad®) and the mixed molecular weight protocol for 7 minutes. PVDF membranes were washed with Tris-buffered saline and Tween-20 (Sigma-Aldrich®, #P1379) (TBS-T) before being blocked using a solution of 5% fat free milk or 5% BSA for 2-hours. Membranes were washed and incubated in the required primary antibody solution and incubated for 36-hours at 4°C. The complete list of antibodies given can be found in **Appendix C.** Once incubation was completed, membranes were washed before incubated in secondary antibodies at room temperature for 1 hour. PDVF membranes were developed using the Bio-Rad ChemiDoc™ MR Imaging system with Image Lab™ Software after the enhanced chemiluminescence (ECL) western blotting substrate (Bio-Rad®, #1705061) was applied. ECL is light sensitive therefore all lights in work area were switched off with ECL remaining covered during use. Normalization of protein loading was achieved by using the total protein content of each lane and a protein standard on Image Lab™ Version 7 Software for Mac®. Protein expression in visualized bands on membranes was expressed as a percentage (%) of control.

2.11. Statistical analyses

Statistical analyses of data were performed with the use of GraphPad Prism® Version 5 for Windows® (GraphPad Software, San Diego, CA). All values represent percentage of control for mean ± standard error of mean. One-way ANOVA was performed with a Fisher's least significant difference (LSD) post-hoc test. A p-value <0.05 was considered as statistically significant. All treatments were completed in triplicate and each experiment was repeated three times resulting in an $n = 3$.

Chapter 3 – Results I

Introduction

The muscle wasting syndrome, cachexia, is stimulated by stimuli from cancer cells or tumours as well as treatment-induced toxicity (Hardee, Montalvo & Carson. 2017). Mitochondrial dysfunction of skeletal muscle is also a result of tumour growth (Tzika *et al.,* 2013). In this chapter, the results are shown where the effects of DXR and E0771 conditioned media on mitochondrial ROS production in myotubes were investigated. These experiments were done to ensure that a cachexia phenotype was introduced in the myotubes. A mouse breast adenocarcinoma cell line, E0771, and mouse myoblast cell line, C2C12, were chosen for this study as the cell lines are syngeneic to one another. DXR is the chemotherapeutic agent regularly used in South Africa for the treatment of various cancers including breast cancer and was used as our treatment of interest. Previous studies within our research group by determined that a dose of 1.6 µM (IC50 value) DXR induced ±50% cell death compared to control in E0771 cells. Conditioned media used to treat myotubes was harvested from E0771 cells after Control and DXR treatments, as previously described in chapter 3.3, and are indicated as C.Control and C.DXR.

3.1. Induction of oxidative stress in myotubes

Breast cancer has been observed to induce mitochondrial dysfunction and increase ROS production in skeletal muscle independent of chemotherapy (Bohlen *et al.,* 2018). Additionally, DXR has a high affinity for components associated with the mitochondria and the complexes of the ETC that promote ROS production (Gilliam *et al.,* 2012). In order to investigate ROS production in myotubes a MitoSOX™ assay was performed.

3.1.1. Assessment of Mitochondrial ROS Production (MitoSOX™)

Mitochondrial superoxide oxidizes MitoSOX™ within cells to produce a fluorescent signal. Alterations in fluorescent signal indicate changes in mitochondrial superoxide within the cells as observed in representational images of **Figure 3.1**. The auto-fluorescence signal of DXR was accounted and adjusted for in results presented in **Figure 3.2.**

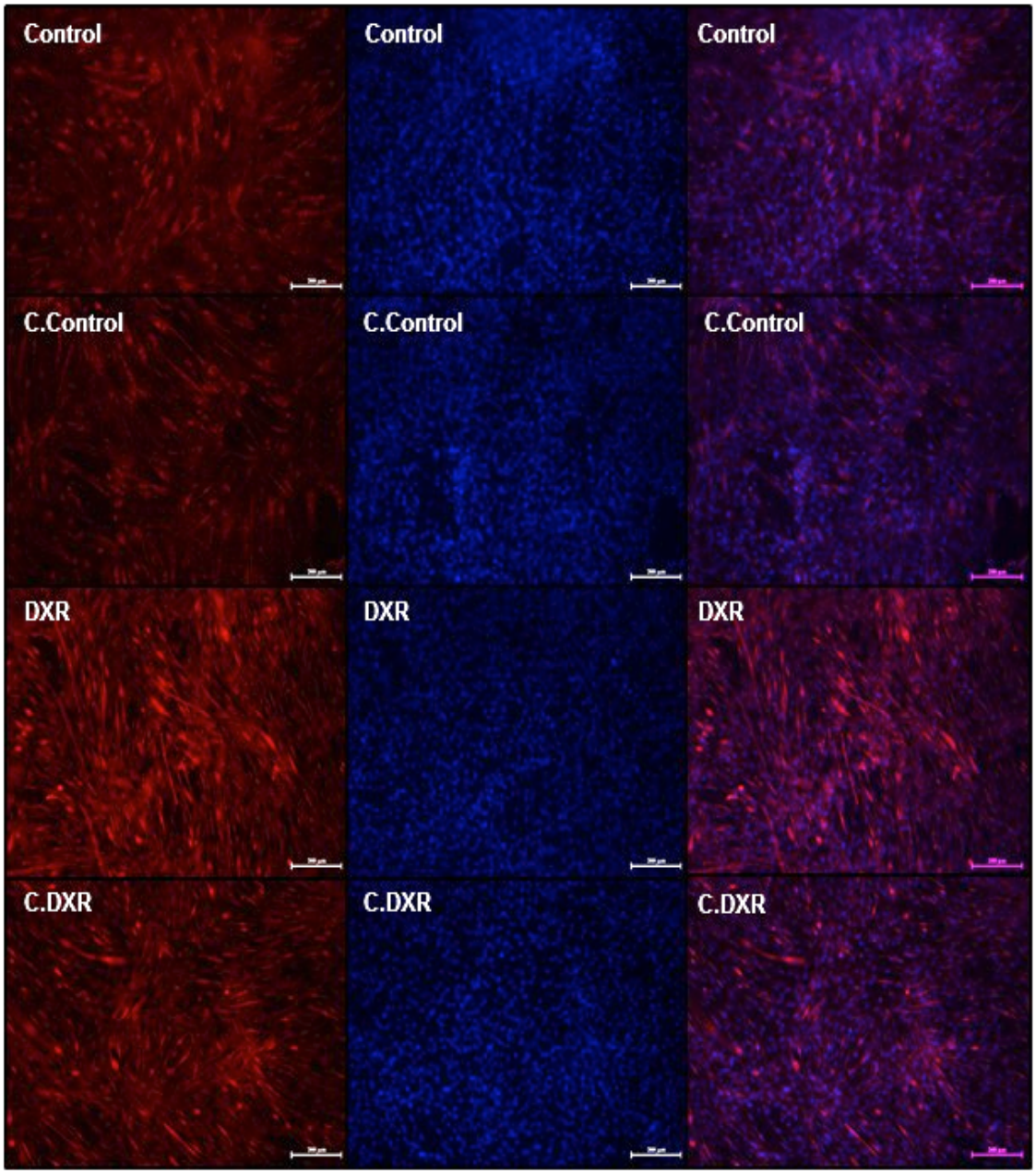

Figure 3.1: Representative images of MitoSOX™ assay after 24-hour treatment of myotubes. Myotubes were treated for 24-hours with the following treatments: 1) Control consisting of serum free media and complete media in 1:1 ratio. 2) C.Control consisting of serum free media and conditioned media harvested from E0771 cells after Control treatment in 1:1 ratio. 3) DXR consisting of serum free media and complete media in 1:1 ratio, and 1.6 μM DXR. 4) C.DXR consisting of serum free media and conditioned media harvested from E0771 cells after DXR treatment in 1:1 ratio. Tx Red filter indicates MitoSOX™, DAPI blue filter indicates nuclear DNA with Hoechst 33342, and combinational image indicates MitoSOX™ and Hoechst 33342. Images acquired with 40X objective. Scale = 200 μm.

The mean fluorescent intensity (**Figure 3.2)** of C.Control exhibited no difference when compared to Control (4.285 ± 0.086 and 4.101 ± 0.152 respectively). The intensity of mitochondrial ROS significantly increased in DXR when compared to Control (5.580 ± 0.4, $p<0.001$) indicating DXR did promote ROS production. Additionally, while the intensity in

C.DXR (4.812 ± 0.122) exhibited no significant differences compared to C.Control, there was a significant increase of $p<0.05$ compared to Control, however, the mitochondrial ROS production was significantly lower compared to DXR ($p<0.05$).

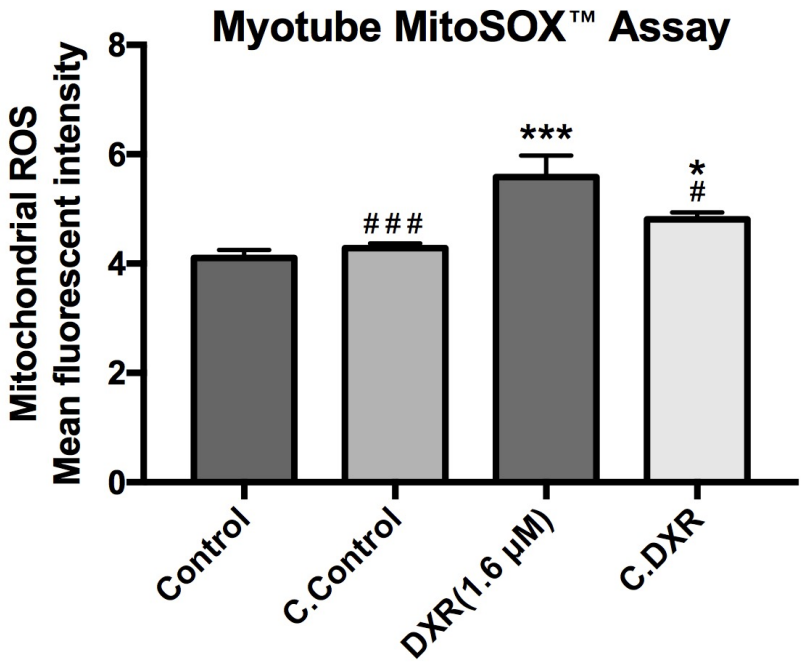

Figure 3.2: Mitochondrial ROS analysis from MitoSOX™ assay after 24-hour treatment of myotubes. Myotubes were treated for 24-hours with the following treatments: 1) Control consisting of serum free media and complete media in 1:1 ratio. 2) C.Control consisting of serum free media and conditioned media harvested from E0771 cells after Control treatment in 1:1 ratio. 3) DXR consisting of serum free media and complete media in 1:1 ratio, and 1.6 µM DXR. 4) C.DXR consisting of serum free media and conditioned media harvested from E0771 cells after DXR treatment in 1:1 ratio. Values expressed as mean fluorescent intensity with statistical representation as mean ±SEM with n = 3. *p<0.05 compared to Control, ***p<0.001 compared to Control, #p<0.05 compared to DXR, ###p<0.001 compared to DXR.

3.2. Maintenance of myotube integrity

Minimal weight and muscle loss have been observed in breast cancer patients with cachexia and was reported to be associated with mitochondrial dysfunction of muscle and not complete muscle atrophy (Bohlen *et al.,* 2018). In order to determine whether concentration of DXR selected and E0771 conditioned media induced muscle atrophy, the integrity and morphology was observed using a Cell Tracker™ Assay and western blot analyses. Due to time constraints analysis of apoptotic and autophagic markers in myotubes could not be completely investigated, however, preliminary results can be found in **Appendix A, Figures A-D**.

3.2.1. Assessment of myotube width (Cell Tracker™)

Cell Tracker™ produces insoluble products within the cytosol allowing the entire cell to be fluorescently stained (**Figure 3.3**). This enables the measuring of myotube width in μm^2 to determine alterations in myotube morphology and integrity.

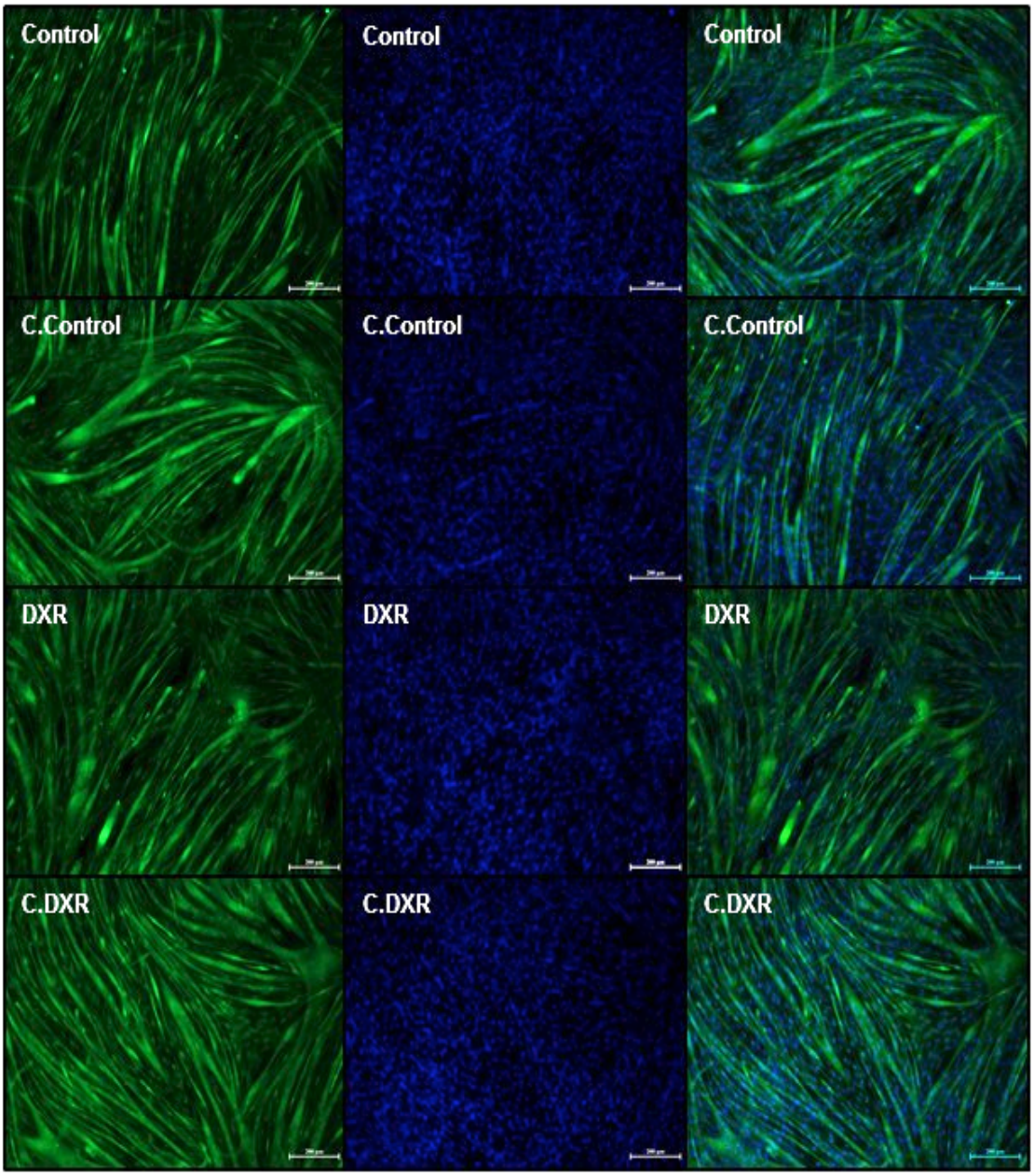

Figure 3.3: Representative images of Cell Tracker™ assay after 24-hour treatment of myotubes. Myotubes were treated for 24-hours with the following treatments: 1) Control consisting of serum free media and complete media in 1:1 ratio. 2) C.Control consisting of serum free media and conditioned media harvested from E0771 cells after Control treatment in 1:1 ratio. 3) DXR consisting of serum free media and complete media in 1:1 ratio, and 1.6 µM DXR. 4) C.DXR consisting of serum free media and conditioned media harvested from E0771 cells after DXR treatment in 1:1 ratio. FITC green filter indicates Cell Tracker™, DAPI blue filter indicates nuclear DNA with Hoescht.33342, and combinational image indicates Cell Tracker™ and Hoescht.33342. Images acquired with 40X objective. Scale = 200 µm.

Analysis of Cell Tracker™ Assay (**Figure 3.4)** indicated that no difference was observed in the myotube width (μm^2) between Control (15.250 μm^2 ± 1.024) and C.Control (15.740 μm^2 ± 1.709) indicating no loss of muscle integrity. While a decrease was observed in DXR (13.185 μm^2 ± 1.271) compared to Control and in C.DXR (13.340 μm^2 ± 0.995) compared to C.Control this was not significant. Minimal loss of myotube width was therefore observed in response to treatments.

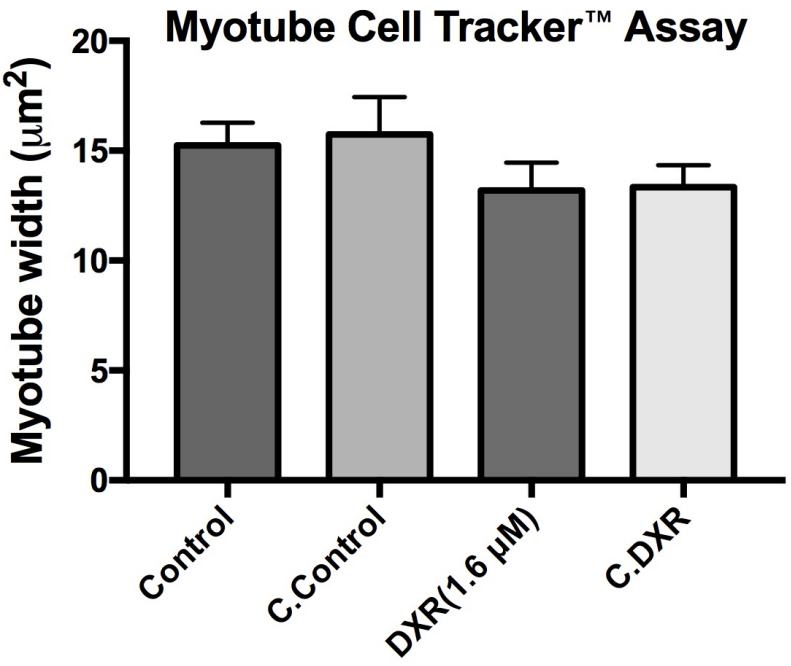

Figure 3.4: Myotube width (μm^2) analysis from Cell Tracker™ assay after 24-hour treatment of myotubes. Myotubes were treated for 24-hours with the following treatments: 1) Control consisting of serum free media and complete media in 1:1 ratio. 2) C.Control consisting of serum free media and conditioned media harvested from E0771 cells after Control treatment in 1:1 ratio. 3) DXR consisting of serum free media and complete media in 1:1 ratio, and 1.6 μM DXR. 4) C.DXR consisting of serum free media and conditioned media harvested from E0771 cells after DXR treatment in 1:1 ratio. Values expressed as myotube width (μm^2) with statistical representation as mean ±SEM with n = 3.

Chapter 4 – Results II

Introduction

The development and progression of breast cancer is a complex process involving various mutations and dysfunctional signaling pathways responsible for cell proliferation, cell growth, cell death, and differentiation. The release of cytokines and growth factors by skeletal muscle in response to stimuli from cancer cells, chemotherapy treatment, or a combination of both, may inhibit or induce signaling pathways in breast cancer cells. In this chapter we assessed the influence of DXR and myotube conditioned media on mechanisms associated with drug resistance, cell proliferation, apoptosis, and metastasis. As previously described in chapter 2.3, conditioned media used to treat E0771 cells was harvested from myotubes following basic Control and DXR treatments, indicated as C.Control and C.DXR, as well as treatment of myotubes with E0771 conditioned media, indicated as C.C.Control and C.C.DXR.

4.1. Conditioned media induce resistance in E0771 cells

Due to the induction of adaptive or survival responses in cancer cells following treatment, cancer cells can develop drug resistance. As previously stated, the appropriate dose of 1.6 µM DXR was chosen over a 24-hour treatment period. Cell viability was firstly assessed to determine if the intervention of a myotube microenvironment promoted more effective cell death or increased drug resistance in breast cancer cells after DXR treatment. As the myotube condition media contains >25% differentiation media, which contains horse serum, an additional MTT assay was completed and can be found in **Appendix A, Figure E**. This ensured that an increase in cell viability was due to cytokines and growth factors excreted by the myotubes and not due to stimulation directly from horse serum.

4.1.1. Cell Viability Assessment

An increase in the mitochondrial reductive capacity of an MTT assay is correlated with cell proliferation and an increase in cell viability. Alternatively, a decrease of reductive capacity is correlated with cell death and a decrease in cell viability. When compared to Control (± 1.689) in **Figure 4.1,** C.Control exhibited a significant increase of $p<0.01$ in mitochondrial reductive capacity (116.731% ± 5.374) while no difference was observed in C.C.Control (108.687% ± 5.819). Additionally, no difference was observed between C.Control and

C.C.Control. A significant decrease in reductive capacity to 60.354% was observed in DXR (± 1.237) when compared to Control ($p<0.001$) indicating a loss of viable cells.

Alternatively, when compared to DXR in **Figure 4.1**, a significant increase of $p<0.01$ was observed in C.DXR (115.443% ± 3.02) and $p<0.001$ in C.C.DXR (121.743% ± 3.442). The mitochondrial reductive capacity of C.DXR and C.C.DXR exhibited no differences, however, a significant difference was observed when comparing C.C.Control and C.C.DXR ($p<0.05$).

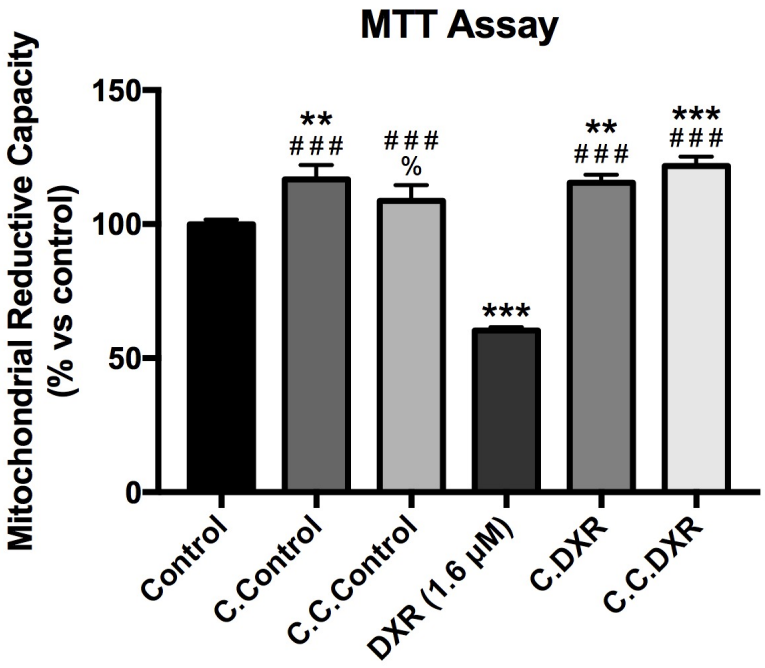

Figure 4.1: Mitochondrial reductive capacity assessed from MTT assay after 24-hour treatment of E0771 cells as an indicator of cell viability. E0771 cells were treated for 24-hours with the following treatments: 1) Control consisting of serum free media and complete media in 1:1 ratio. 2) C.Control consisting of serum free media and conditioned media harvested from myotubes after Control treatment in 1:1 ratio. 3) C.C.Control consisting of serum free media and conditioned media harvested from myotubes after E0771 Control treatment in 1:1 ratio. 4) DXR consisting of serum free media and complete media in 1:1 ratio, and 1.6 µM DXR. 5) C.DXR consisting of serum free media and conditioned media harvested from myotubes after DXR treatment in 1:1 ratio. 6) C.C.DXR consisting of serum free media and conditioned media harvested from myotubes after E0771 DXR treatment in 1:1 ratio. Values expressed as percentage (%) of control with statistical representation as mean ±SEM with n = 3. **p<0.01 compared to Control, ***p<0.001 compared to Control, ###p<0.001 compared to DXR, %p<0.05 compared to C.C.DXR.

4.2. The effect of conditioned media on markers of cell proliferation

Cell proliferation is a complex process and various signaling pathways are involved in its regulation. Breast cancer cells display dysregulation in one or more of these pathways, which promote unsuppressed growth. The PI3K/Akt and ERK pathways play important roles in the cell proliferation and inhibition of apoptosis in cancer cells. To support the results obtained in the cell viability assay, the protein expression of a marker from each pathway, as well as a member of the MCM protein family, were determined by means of western blot experiments.

4.2.1. PI3K/Akt Pathway

Akt is a significant protein in the PI3K/Akt pathway. Once activated, Akt mediates downstream effects on multiple intracellular proteins that influence cell survival, cell proliferation, cell growth, cell migration as well as angiogenesis. Unfortunately, due to the poor quality of the antibody, phosphorylated Akt could not be analysed and a fold change in the phosphor-Akt and total Akt ratio could not be established. A decrease in total Akt expression in C.Control (81.159% ± 1.745) was observed while no difference in expression in C.C.Control (100.53% ± 4.307) was observed when compared to Control (±15.75) (**Figure 4.2**). Akt expression was also decreased in DXR (77.568% ± 2.534) when compared to Control. When compared to DXR, no differences were observed in C.DXR (84.778% ± 10.13) and C.C.DXR (65.554% ± 17.55). Additionally, C.C.DXR exhibited a significant decreased in Akt expression when compared to C.C.Control ($p<0.05$).

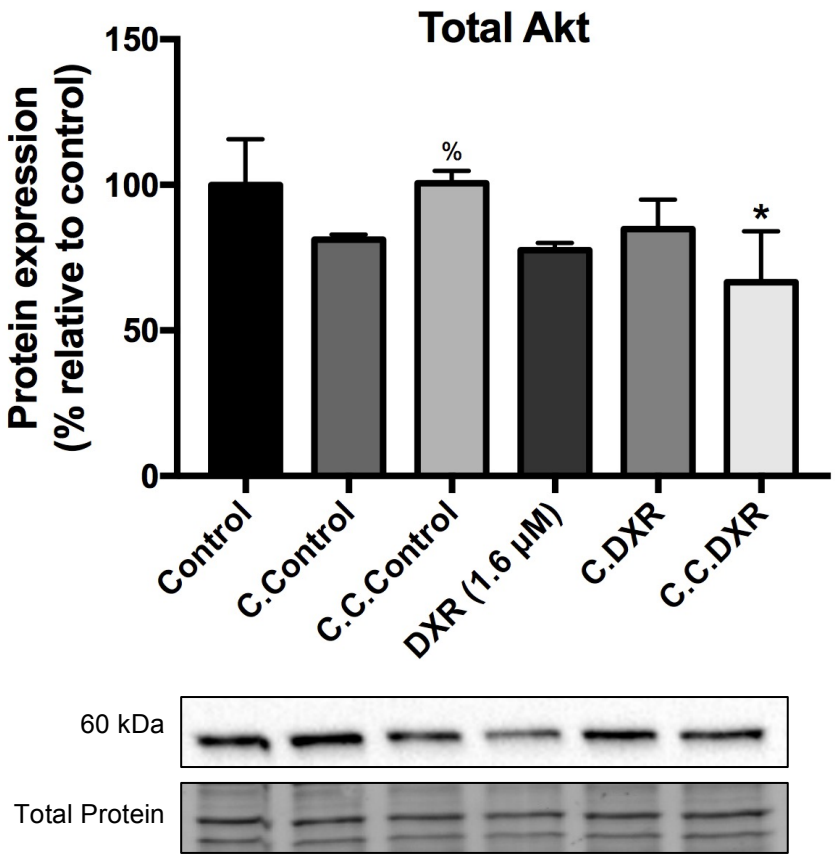

Figure 4.2: Protein expression of total Akt from western blot analysis after 24-hour treatment of E0771 cells. E0771 cells were treated for 24-hours with the following treatments: 1) Control consisting of serum free media and complete media in 1:1 ratio. 2) C.Control consisting of serum free media and conditioned media harvested from myotubes after Control treatment in 1:1 ratio. 3) C.C.Control consisting of serum free media and conditioned media harvested from myotubes after E0771 Control treatment in 1:1 ratio. 4) DXR consisting of serum free media and complete media in 1:1 ratio, and 1.6 µM DXR. 5) C.DXR consisting of serum free media and conditioned media harvested from myotubes after DXR treatment in 1:1 ratio. 6) C.C.DXR consisting of serum free media and conditioned media harvested from myotubes after E0771 DXR treatment in 1:1 ratio. Values expressed as percentage (%) of control with statistical representation as mean ±SEM with n = 3. *$p<0.05$ compared to Control, %$p<0.05$ compared to C.C.DXR.

4.2.2. ERK pathway

ERK proteins are responsible for the activation and regulation of processes involved in meiosis, mitosis and cell survival and proliferation. A ratio comparing the expression of phospho-ERK 2 and Total ERK indicates the activation of this protein. An increase in the ratio represents an increase in the activation of ERK through phosphorylation. C.Control and C.C.Control exhibited an increase in fold change of phospho-ERK 2 over total ERK 2 in **Figure 4.3** when compared to Control (1.406 ± 0.137 and 1.785 ± 0.181). Additionally, DXR exhibited a statistically significant fold change to 3.946 (± 0.520, $p<0.001$) when compared to Control. While the ratio's in C.DXR and C.C.DXR was significantly decreased compared to DXR (1.710 ± 0.272, $p<0.001$ and 1.822 ± 0.176, $p<0.001$), there were no differences observed during comparison of C.Control and C.DXR or C.C.Control and C.C.DXR.

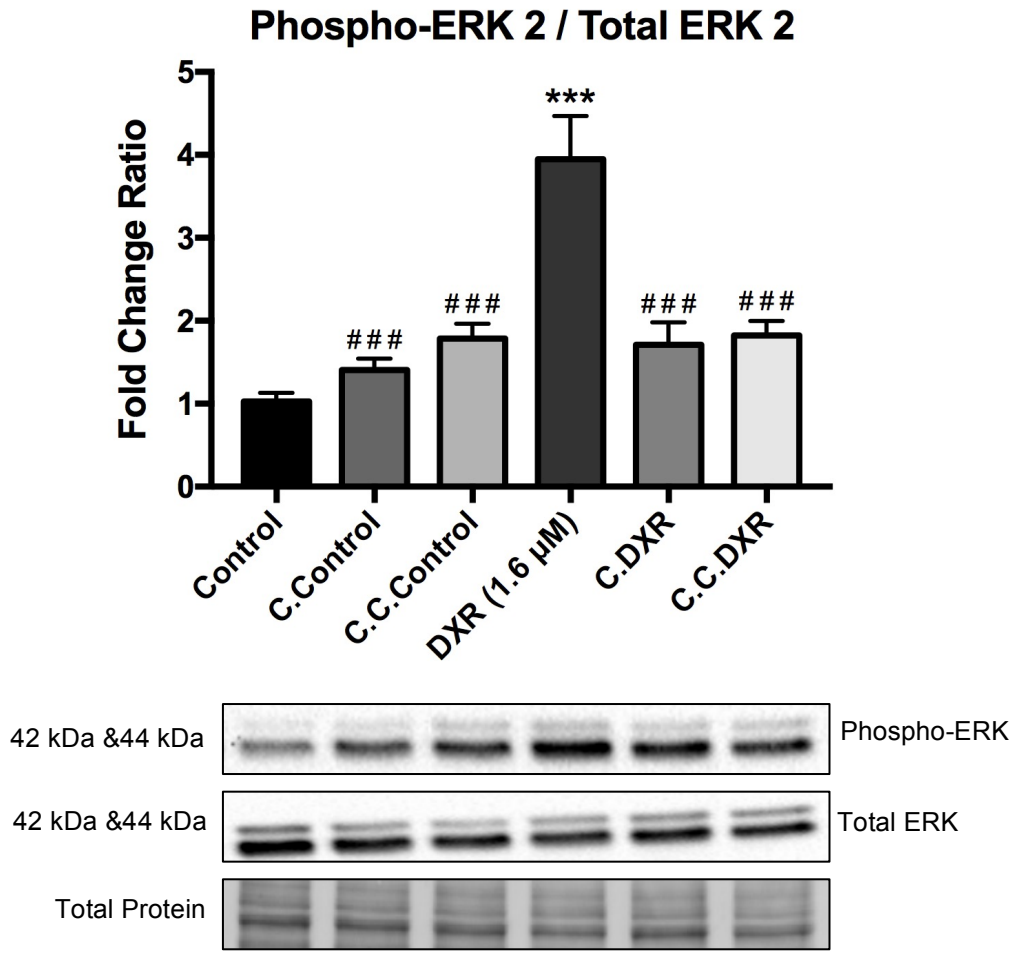

Figure 4.3: Ratio of protein expression of phospho-ERK2 / Total ERK2 from western blot analysis after 24-hour treatment of E0771 cells. E0771 cells were treated for 24-hours with the following treatments: 1) Control consisting of serum free media and complete media in 1:1 ratio. 2) C.Control consisting of serum free media and conditioned media harvested from myotubes after Control treatment in 1:1 ratio. 3) C.C.Control consisting of serum free media and conditioned media harvested from myotubes after E0771 Control treatment in 1:1 ratio. 4) DXR consisting of serum free media and complete media in 1:1 ratio, and 1.6 µM DXR. 5) C.DXR consisting of serum free media and conditioned media harvested from myotubes after DXR treatment in 1:1 ratio. 6) C.C.DXR consisting of serum free media and conditioned media harvested from myotubes after E0771 DXR treatment in 1:1 ratio. Values expressed as percentage (%) of control with statistical representation as mean ±SEM with n = 3. ***p<0.001 compared to Control, ###p<0.001 compared to DXR.

4.2.3. Mini-chromosome maintenance (MCM) proteins

MCM2, a member of the MCM protein family, plays an important role in DNA replication by recruiting other essential proteins as well as the formation of replication forks and serves thus as a marker of cellular proliferation. An increase in the expression of MCM2 indicates an increase in proliferation activity. Comparison of MCM2 expression to Control (± 9.153) in **Figure 4.4** exhibited no difference in C.Control (102.109% ± 9.047), DXR (110.711% ± 7.145) or C.DXR (96.897% ± 8.494). A decrease in expression to 89.121% (± 2.028) was however observed in C.C.Control when compared to Control. The expression of MCM2 was

significantly decreased in C.C.DXR (55.167% ± 14.64) when compared to DXR ($p<0.01$) and C.C.Control ($p<0.01$).

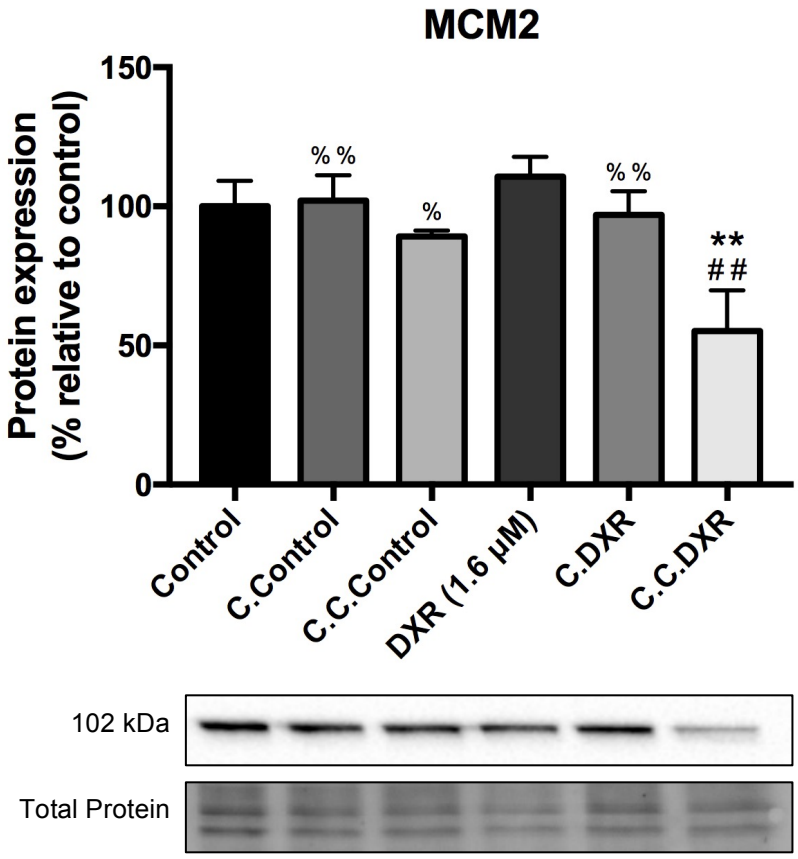

Figure 4.4: Protein expression of MCM2 from western blot analysis after 24-hour treatment of E0771 cells. E0771 cells were treated for 24-hours with the following treatments: 1) Control consisting of serum free media and complete media in 1:1 ratio. 2) C.Control consisting of serum free media and conditioned media harvested from myotubes after Control treatment in 1:1 ratio. 3) C.C.Control consisting of serum free media and conditioned media harvested from myotubes after E0771 Control treatment in 1:1 ratio. 4) DXR consisting of serum free media and complete media in 1:1 ratio, and 1.6 µM DXR. 5) C.DXR consisting of serum free media and conditioned media harvested from myotubes after DXR treatment in 1:1 ratio. 6) C.C.DXR consisting of serum free media and conditioned media harvested from myotubes after E0771 DXR treatment in 1:1 ratio. Values expressed as percentage (%) of control with statistical representation as mean ±SEM with n = 3. **p<0.01 compared to Control, ##p<0.01 compared to DXR, %p<0.05 compared to C.C.DXR, %%p<0.01 compared to C.C.DXR.

4.3. The effect of conditioned media on apoptosis

Effective treatment of cancer with DXR induces apoptosis (Tacar, Sriamornsak & Dass, 2012), however as discussed, drug resistant cells are able to evade apoptosis. Intervention of microenvironments may directly or indirectly, with the use of previously mentioned signaling pathways, inhibited apoptosis from occurring (Weinstein-Oppenheimer *et al.,* 2001). To determine whether DXR was capable of inducing cell death in the context of the

myotube microenvironment, the protein expression of apoptotic markers caspase 3 and PARP was determined using western blot analysis.

4.3.1. Caspase 3

Within the apoptotic pathway, both the extrinsic and intrinsic pathways are involved in the activation of caspase 3. Cleavage of this protein executes the final steps in the apoptotic process allowing for programmed cell death. An increase in the fold change ratio of the expression of cleaved caspase 3 and total caspase 3 indicates induction of this proteins cleavage, therefore activation of Caspase 3 activity. This increased cleavage activity of Caspase 3 represents the induction of the execution pathway, which may induce downstream cell death effects. Cleaved caspase 3 and total caspase 3 fold change in **Figure 4.5** exhibited no differences between Control (± 0.567), C. Control (1.521 ± 0.792), C.C.Control (1.367 ± 0.661), and DXR (1.761 ± 0.522). There was an increase in fold change observed in C.DXR (2.962 ± 1.109) compared to DXR and C.Control, however this was not significant. The ratio observed in C.C.DXR (0.993 ± 0.209) was non-significantly decreased compared to DXR and C.DXR, however, not when compared to C.C.Control. The large variation exhibited in the ratio change of cleaved and total Caspase 3 attributed to non-significance being observed.

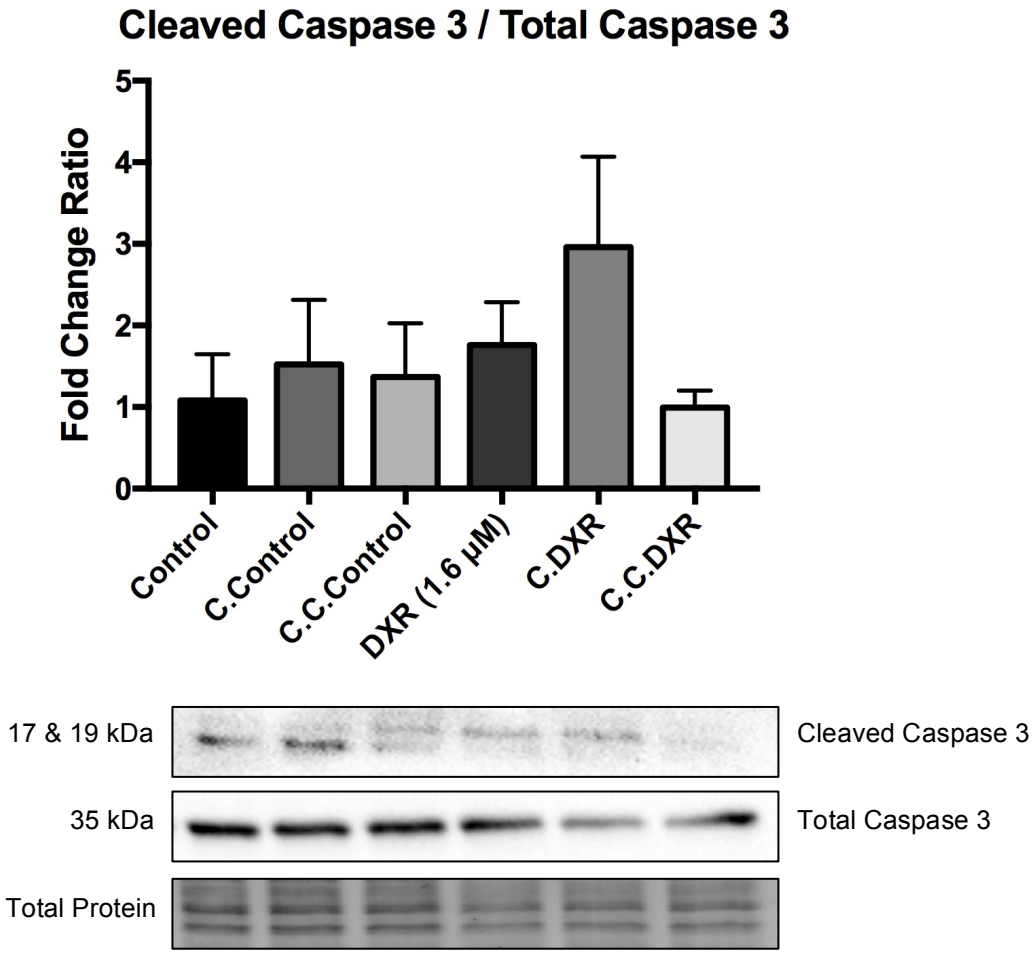

Figure 4.5: Ratio of protein expression of cleaved Caspase 3 / total Caspase 3 from western blot analysis after 24-hour treatment of E0771 cells. E0771 cells were treated for 24-hours with the following treatments: 1) Control consisting of serum free media and complete media in 1:1 ratio. 2) C.Control consisting of serum free media and conditioned media harvested from myotubes after Control treatment in 1:1 ratio. 3) C.C.Control consisting of serum free media and conditioned media harvested from myotubes after E0771 Control treatment in 1:1 ratio. 4) DXR consisting of serum free media and complete media in 1:1 ratio, and 1.6 µM DXR. 5) C.DXR consisting of serum free media and conditioned media harvested from myotubes after DXR treatment in 1:1 ratio. 6) C.C.DXR consisting of serum free media and conditioned media harvested from myotubes after E0771 DXR treatment in 1:1 ratio. Values expressed as percentage (%) of control with statistical representation as mean ±SEM with n = 3.

4.3.2. Poly ADP ribose polymerase (PARP)

Poly ADP ribose polymerase (PARP) is a protein found in the nucleus of a cell, where it is able to detect alterations in single-strand DNA and promotes apoptosis, genomic stability or DNA repair. Cleavage of PARP by caspase 3 causes inactivation of PARP activity. The increase expression of cleaved PARP compared to total PARP, thus the increase in fold change ratio, indicates the inhibition of PARP and induction of apoptosis. The fold change ratio of cleaved and total PARP is shown in **Figure 4.6.** Comparison of Control (1.018 ± 0.075), C.Control (1.038 ± 0.068), and C.C.Control (1.064 ± 0.091) exhibited no difference in fold change ratio. Compared to Control, a significant decrease was observed in DXR with

the ratio decreasing to 0.651 (± 0.027, p<0.01). The decrease of fold change ratio in C.DXR (0.662 ± 0.097) was significant compared to C.Control (p<0.01) while the decrease in C.C.DXR (0.456 ± 0.111) was significant when compared to C.C.Control (p<0.001).

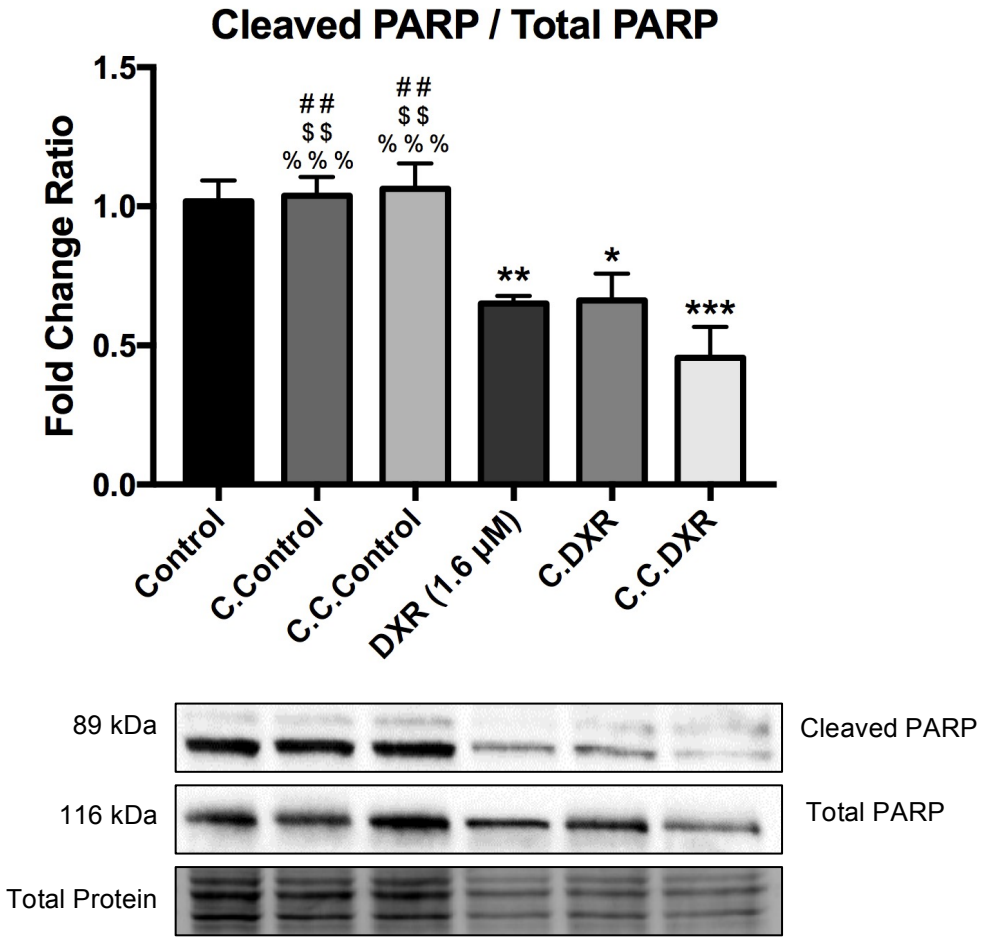

Figure 4.6: Ratio of protein expression of cleaved PARP / total PARP from western blot analysis after 24-hour treatment of E0771 cells. E0771 cells were treated for 24-hours with the following treatments: 1) Control consisting of serum free media and complete media in 1:1 ratio. 2) C.Control consisting of serum free media and conditioned media harvested from myotubes after Control treatment in 1:1 ratio. 3) C.C.Control consisting of serum free media and conditioned media harvested from myotubes after E0771 Control treatment in 1:1 ratio. 4) DXR consisting of serum free media and complete media in 1:1 ratio, and 1.6 µM DXR. 5) C.DXR consisting of serum free media and conditioned media harvested from myotubes after DXR treatment in 1:1 ratio. 6) C.C.DXR consisting of serum free media and conditioned media harvested from myotubes after E0771 DXR treatment in 1:1 ratio. Values expressed as percentage (%) of control with statistical representation as mean ±SEM with n = 3. *p<0.05 compared to Control, **p<0.01 compared to Control, ***p<0.001 compared to Control, ##p<0.01 compared to DXR, $$p<0.01 compared to C.DXR. %%%p<0.001 compared to C.C.DXR.

4.4. The effect of conditioned media on cell migration

Chemotherapy and microenvironments have been shown to stimulate migration activity in cancer cells, therefore promoting invasion and metastatic properties (Ceelen & Bracke, 2009; Mareel & Constantino, 2011). To investigate the influence of the myotube

microenvironment on breast cancer cell migration, a migration scratch assay was completed by making a scratch within a monolayer of cells and monitoring cell migration into the scratch over a period of 24-hours. Representative images of the scratches are shown in **Figure 4.7**.

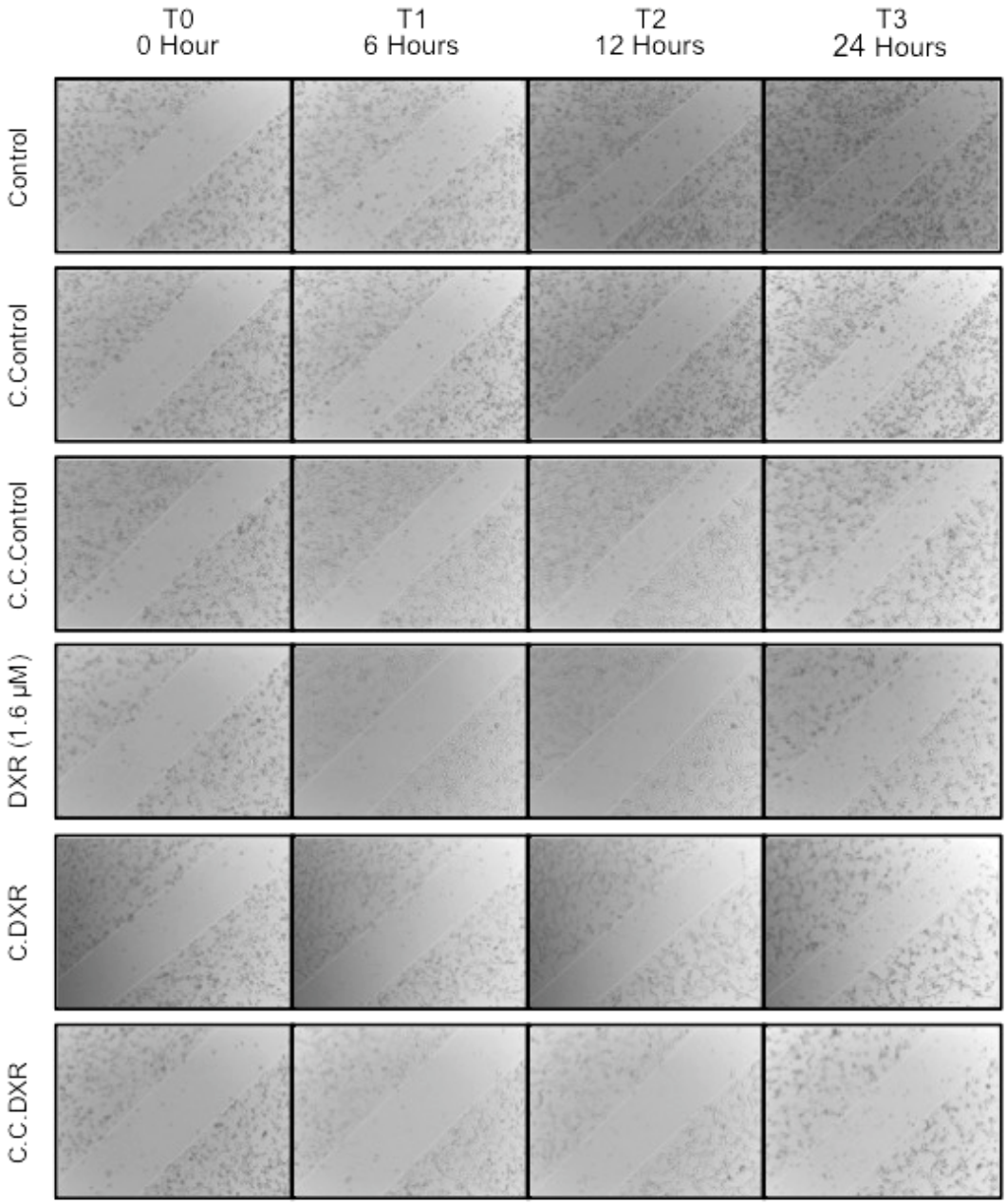

Figure 4.7: Representative images of migration scratch assay over 24-hours of treatment of E0771 cells. E0771 cells were treated for 24-hours with the following treatments: 1) Control consisting of serum free media and complete media in 1:1 ratio. 2) C.Control consisting of serum free media and conditioned media harvested from myotubes after Control treatment in 1:1 ratio. 3) C.C.Control consisting of serum free media and conditioned media harvested from myotubes after E0771 Control treatment in 1:1 ratio. 4) DXR consisting of serum free media and complete media in 1:1 ratio, and 1.6 µM DXR. 5) C.DXR consisting of serum free media and conditioned media harvested from myotubes after DXR treatment in 1:1 ratio. 6) C.C.DXR consisting of serum free media and conditioned media harvested from myotubes after E0771 DXR treatment in 1:1 ratio. Images were captured at 0 Hour, 6 Hours, 12 Hours and 24 Hours in order to measure area of the wound. Images acquired with 40X objective.

4.4.1. Percentage (%) of wound closure

The percentage (%) of wound closure at each time point was calculated relative to the initial scratch (**Figure 4.8)**. Mitomycin C was used to inhibit cell proliferation, therefore wound closure was an indicator of wound closure due to only cell migration and not proliferation. After 6-hours of treatment, the lowest percentage of wound closure was observed in C.Control with 4.123% (± 0.629), which was significantly lower to C.C.Control (8.093 ± 0.955, $p<0.001$) and C.DXR ($p<0.001$). The highest percentage of closure was observed in DXR with 9.628% (± 0.628), which was significantly higher compared to Control (6.212% ± 0.471, $p<0.01$). A significant difference was also observed between C.Control and C.DXR ($p<0.001$) but not between C.C.Control and C.C.DXR.

Percentage of wound closure at 12-hours of treatment was increased among all treatments. C.Control continued to exhibit the lowest percentage of wound closure that was significant compared to C.C.Control (14.631% ± 1.804, $p<0.01$). A significant difference was observed between DXR (14.59% ± 0.946) and Control (8.128% ± 0.875, $p<0.001$). Finally, a significant difference was observed between C.Control and C.DXR (13.04 ± 0.801, $p<0.001$).

C.Control continued to have the lowest significant wound closure percentage (10.713%, ± 0.896) after 24-hours of treatment. The difference was observed to be significant when compared to C.C.Control (14.985% ± 1.024, $p<0.01$). Compared to DXR (16.049% ± 1.11), a significant difference was observed in Control (12.009% ± 1.278, $p<0.01$). Additionally, C.Control and C.DXR (17.19 ± 0.758) observed a significant difference in percentage of wound closure ($p<0.001$).

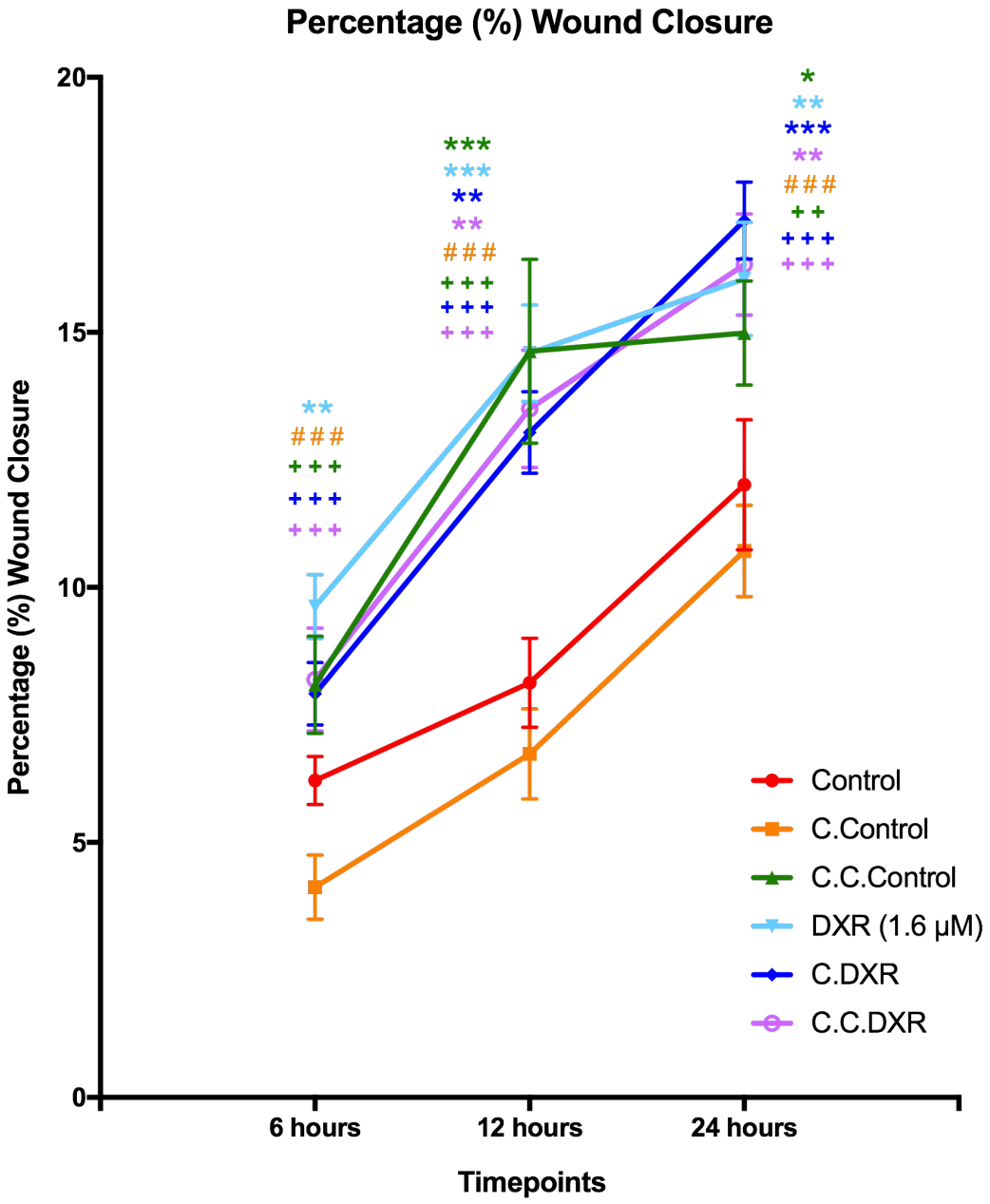

Figure 4.8: Percentage wound closure from migration scratch assay analysis over 24-hours of treatment of E0771 cells. E0771 cells were treated for 24-hours with the following treatments: 1) Control consisting of serum free media and complete media in 1:1 ratio. 2) C.Control consisting of serum free media and conditioned media harvested from myotubes after Control treatment in 1:1 ratio. 3) C.C.Control consisting of serum free media and conditioned media harvested from myotubes after E0771 Control treatment in 1:1 ratio. 4) DXR consisting of serum free media and complete media in 1:1 ratio, and 1.6 µM DXR. 5) C.DXR consisting of serum free media and conditioned media harvested from myotubes after DXR treatment in 1:1 ratio. 6) C.C.DXR consisting of serum free media and conditioned media harvested from myotubes after E0771 DXR treatment in 1:1 ratio. Values expressed as percentage (%) of wound closure over time with statistical representation as mean ±SEM with n = 3. *p<0.05 compared to control, **p<0.01 compared to control, ***p<0.001 compared to control, ###p<0.001 compared to DXR, ++p<0.01 compared to C.Control, +++p<0.001 compared to C.Control.

4.4.2. Rate of wound closure

The rate of wound closure (%.hr^{-1}) for each treatment in **Figure 4.9** was calculated as a percentage over time for each time point. After 6-hours of treatment, the lowest rate of wound closure was observed with 0.628 %.hr^{-1} (± 0.098) in C.Control. This rate was significantly lower when compared to Control (1.035 ± 0.079, $p<0.05$) and C.C.Control (1.349 ± 0.159, $p<0.001$). The highest rate of closure was observed in DXR with 1.605 %.hr^{-1} (± 0.105), which was significantly different when compared to Control ($p<0.01$) and C.Control ($p<0.001$).

All treatments showed a decrease in the rate of wound closure at the 12-hour time point with C.Control continuing to have the lowest rate with 0.561 %.hr^{-1} (± 0.074) that was significant when compared to C.C.Control (1.000 %.hr^{1} ± 0.129, $p<0.01$). Compared to Control (0.677 %.hr^{1} ± 0.073), the difference in wound closure rate was no longer significant compared to C.Control, however there was a significant difference compared to C.C.Control (1.000 %.hr^{1} ± 0.129, $p<0.05$) and DXR (1.216 %.hr^{1} ± 0.079, $p<0.001$). Additionally, a significant difference was observed between C.Control and C.DXR (1.319 ± 0.102, $p<0.001$).

The rate of wound closure was observed to decrease further after 24-hours in all treatments. C.Control continued to exhibit the lowest rate with 0.446 %.hr^{1} (± 0.034) that was significant when compared to C.C.Control (0.624 %.hr^{1} ± 0.043, $p<0.001$). The difference in wound closure rate in Control was significant when compared to C.C.Control ($p<0.05$) and DXR (0.669 %.hr^{1} ± 0.046, $p<0.01$). The comparison between C.Control and C.DXR was also observed to be significant ($p<0.001$).

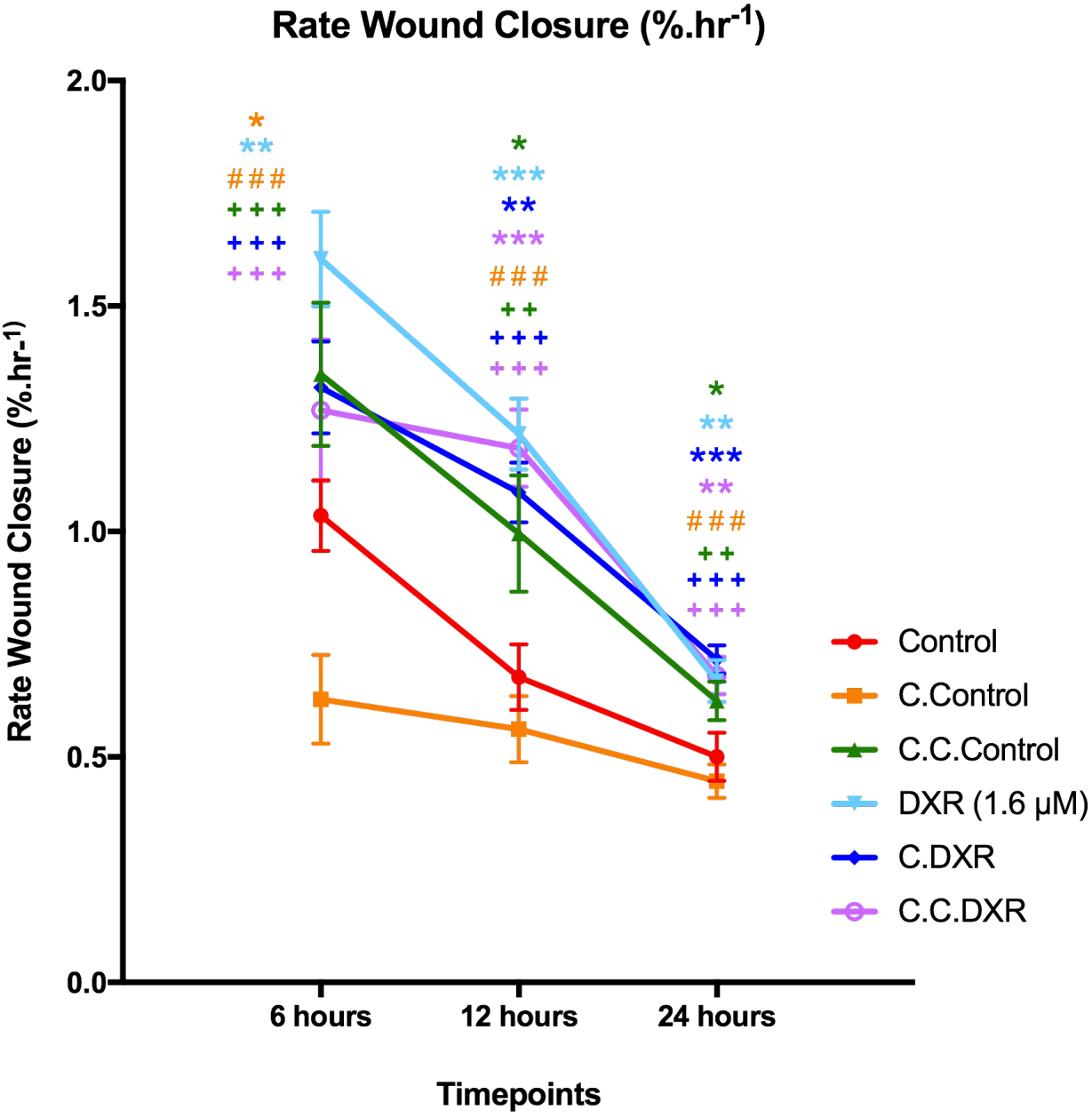

Figure 4.9: Rate wound closure (%.hr^{-1}) from migration scratch assay analysis over 24-hours of treatment of E0771 cells. E0771 cells were treated for 24-hours with the following treatments: 1) Control consisting of serum free media and complete media in 1:1 ratio. 2) C.Control consisting of serum free media and conditioned media harvested from myotubes after Control treatment in 1:1 ratio. 3) C.C.Control consisting of serum free media and conditioned media harvested from myotubes after E0771 Control treatment in 1:1 ratio. 4) DXR consisting of serum free media and complete media in 1:1 ratio, and 1.6 µM DXR. 5) C.DXR consisting of serum free media and conditioned media harvested from myotubes after DXR treatment in 1:1 ratio. 6) C.C.DXR consisting of serum free media and conditioned media harvested from myotubes after E0771 DXR treatment in 1:1 ratio. Values expressed as rate wound closure over time (%.hr^{-1}) with statistical representation as mean ±SEM with n = 3. *p<0.05 compared to control, **p<0.01 compared to control, ***p<0.001 compared to control, ###p<0.001 compared to DXR, ++p<0.01 compared to C.Control, +++p<0.001 compared to C.Control.

4.5. The effect of conditioned media on markers of Epithelial-Mesenchymal Transition (EMT)

EMT is an important process in the normal development and remodeling of the mammary gland (Nelson *et al*., 2006; Kouros-Mehr & Werb, 2006). However, dysregulation of this process in breast cancer can also promote invasion of tumours into surrounding tissue. EMT is also important to maintaining skeletal muscle functions and integrity since they have a plastic phenotype. Western blot analyses of epithelial and mesenchymal markers were performed to investigate alterations in cancer cell phenotype due to the myotube microenvironment. Time constraints prevented the complete investigation of EMT expression alterations in the myotubes due to E0771 conditioned media, although preliminary results of cytoskeleton EMT markers are indicated in **Appendix A, Figures F-G.**

4.5.1. α-Smooth muscle actin

The protein α-Smooth muscle actin (α-SMA) is responsible for cell structure and integrity as well as being an important component of the contractile apparatus. It is regarded as a mesenchymal marker and its expression is expected to increase during EMT. The protein expression of α-SMA in **Figure 4.10** showed a decrease in C.Control (65.038% ± 12.86) and a significant decrease in C.C.Control (53.607% ± 12.63, $p<0.05$) compared to Control (± 20.82). Additionally, compared to Control, no difference in expression was observed in DXR (102.127% ± 19.58). C.DXR exhibited decreased expression (65.574% ± 7.699) compared to DXR with no difference when compared to C.Control. A significant decrease in expression was observed in C.C.DXR (35.889% ± 8.666, $p<0.01$) compared to DXR while no alteration of expression was observed between C.C.DXR and C.C.Control.

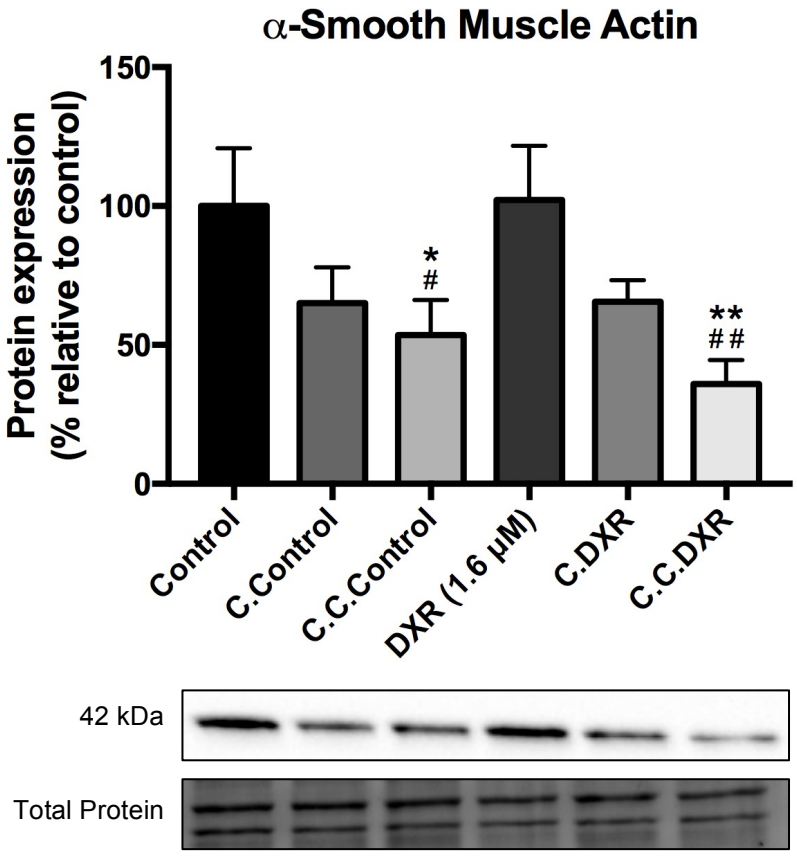

Figure 4.10: Protein expression of α-Smooth Muscle Actin from western blot analysis after 24-hour treatment of E0771 cells. E0771 cells were treated for 24-hours with the following treatments: 1) Control consisting of serum free media and complete media in 1:1 ratio. 2) C.Control consisting of serum free media and conditioned media harvested from myotubes after Control treatment in 1:1 ratio. 3) C.C.Control consisting of serum free media and conditioned media harvested from myotubes after E0771 Control treatment in 1:1 ratio. 4) DXR consisting of serum free media and complete media in 1:1 ratio, and 1.6 µM DXR. 5) C.DXR consisting of serum free media and conditioned media harvested from myotubes after DXR treatment in 1:1 ratio. 6) C.C.DXR consisting of serum free media and conditioned media harvested from myotubes after E0771 DXR treatment in 1:1 ratio. Values expressed as percentage (%) of control with statistical representation as mean ±SEM with n = 3. *p<0.05 compared to Control, **p<0.01 compared to Control, #p<0.05 compared to DXR, ##p<0.01 compared to DXR.

4.5.2. Vimentin

Vimentin is a major cytoskeletal structural protein in mesenchymal cells responsible for the integrity of the cytoplasm, maintaining cell shape and the stabilization of interactions in the cytoskeleton. An increased expression of vimentin is observed during a mesenchymal state compared to an epithelial state. The protein expression of vimentin in C.Control and C.C.Control was observed to increase to 118.227% (± 5.585) and 118.723% (± 5.9), respectively, when compare to Control (± 13.32) (**Figure 4.11**) however, this was not significant. Comparison of C.Control and C.C.Control as well as Control and DXR (90.181% ± 4.42) showed no difference in expression. The expression of vimentin in C.DXR

(128.996% ± 13.75) was significantly increased when compared to DXR ($p<0.05$) with a slight increase observed when compared to C.Control. While C.C.DXR (115.44% ± 15.11) exhibited an increase in expression when compared to DXR, no difference was observed when compared to C.C.Control.

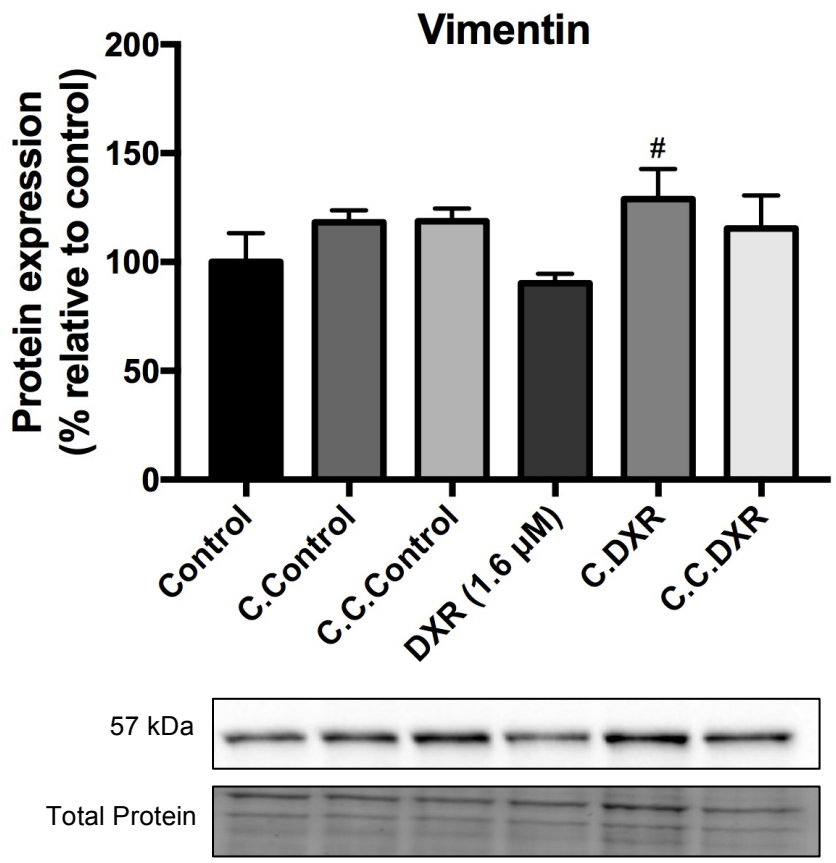

Figure 4.11: Protein expression of Vimentin from western blot analysis after 24-hour treatment of E0771 cells. E0771 cells were treated for 24-hours with the following treatments: 1) Control consisting of serum free media and complete media in 1:1 ratio. 2) C.Control consisting of serum free media and conditioned media harvested from myotubes after Control treatment in 1:1 ratio. 3) C.C.Control consisting of serum free media and conditioned media harvested from myotubes after E0771 Control treatment in 1:1 ratio. 4) DXR consisting of serum free media and complete media in 1:1 ratio, and 1.6 µM DXR. 5) C.DXR consisting of serum free media and conditioned media harvested from myotubes after DXR treatment in 1:1 ratio. 6) C.C.DXR consisting of serum free media and conditioned media harvested from myotubes after E0771 DXR treatment in 1:1 ratio. Values expressed as percentage (%) of control with statistical representation as mean ±SEM with n = 3. #$p<0.05$ compared to DXR.

4.5.3. SNAIL

SNAIL is a transcription factor important in the regulation of EMT. During EMT, increased SNAIL expression modulates the expression of several EMT markers, including E-cadherin. In **Figure 4.12,** no differences were observed between Control (± 11.96), C.Control (102.947% ± 12.69), C.DXR (102.524% ± 23.92), and C.C.DXR (104.461% ± 17.4). DXR

exhibited a decrease in expression of SNAIL to 74.337% (± 17.05) compared to Control (± 11.96) that was also decreased compared to C.DXR and C.C.DXR. SNAIL expression in C.C.Control was increased (129.219% ± 23.21) compared to Control and C.C.DXR.

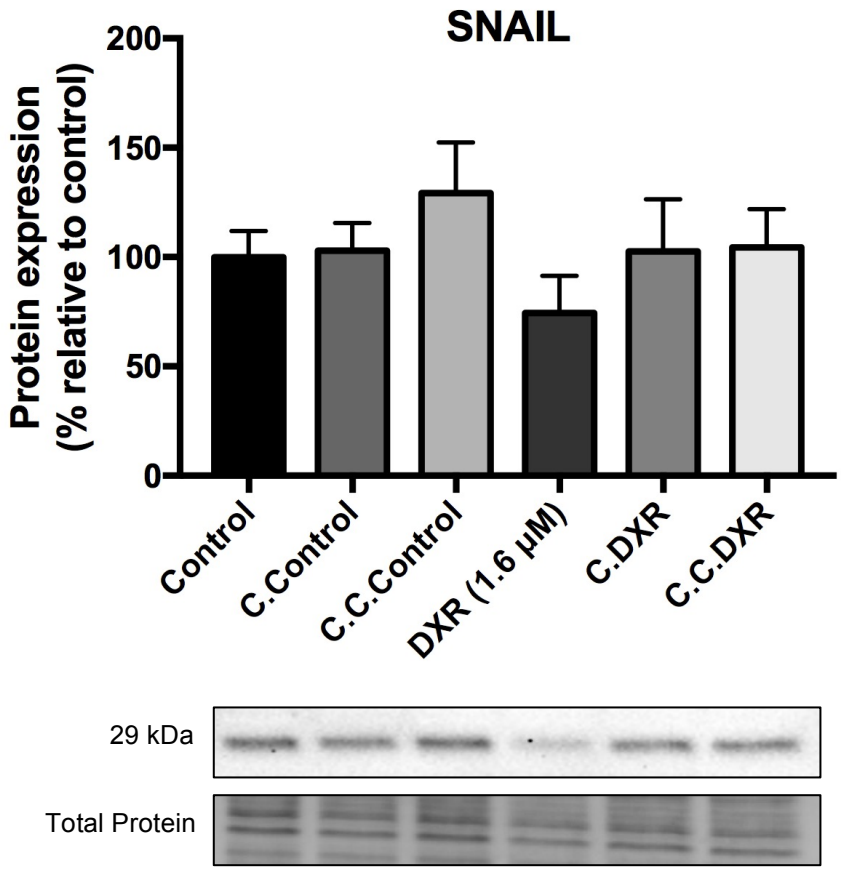

Figure 4.12: Protein expression of SNAIL from western blot analysis after 24-hour treatment of E0771 cells. E0771 cells were treated for 24-hours with the following treatments: 1) Control consisting of serum free media and complete media in 1:1 ratio. 2) C.Control consisting of serum free media and conditioned media harvested from myotubes after Control treatment in 1:1 ratio. 3) C.C.Control consisting of serum free media and conditioned media harvested from myotubes after E0771 Control treatment in 1:1 ratio. 4) DXR consisting of serum free media and complete media in 1:1 ratio, and 1.6 µM DXR. 5) C.DXR consisting of serum free media and conditioned media harvested from myotubes after DXR treatment in 1:1 ratio. 6) C.C.DXR consisting of serum free media and conditioned media harvested from myotubes after E0771 DXR treatment in 1:1 ratio. Values expressed as percentage (%) of control with statistical representation as mean ±SEM with n = 3.

4.5.4. E-cadherin

E-cadherin is a cell surface protein important for the formation and maintenance of adherent junctions within cell-cell adhesion. The loss of expression indicates an increase of metastatic properties of the cell. The expression of E-cadherin represented in **Figure 4.12** indicated the when compared to Control (± 19.03), an increase of expression in C.Control (199.903% ± 78.84), C.Control (200.649% ± 14.9) and DXR (237.571% ± 85.82) was observed. The

expression observed in C.DXR (112.349% ± 5.994) was less than DXR and C.Control while no difference was observed when comparing C.C.DXR (202.854% ± 72.29) to DXR or C.C.Control. Variation was observed in E-cadherin expression among treatments represented in **Figure 4.13** preventing significant changes to be observed.

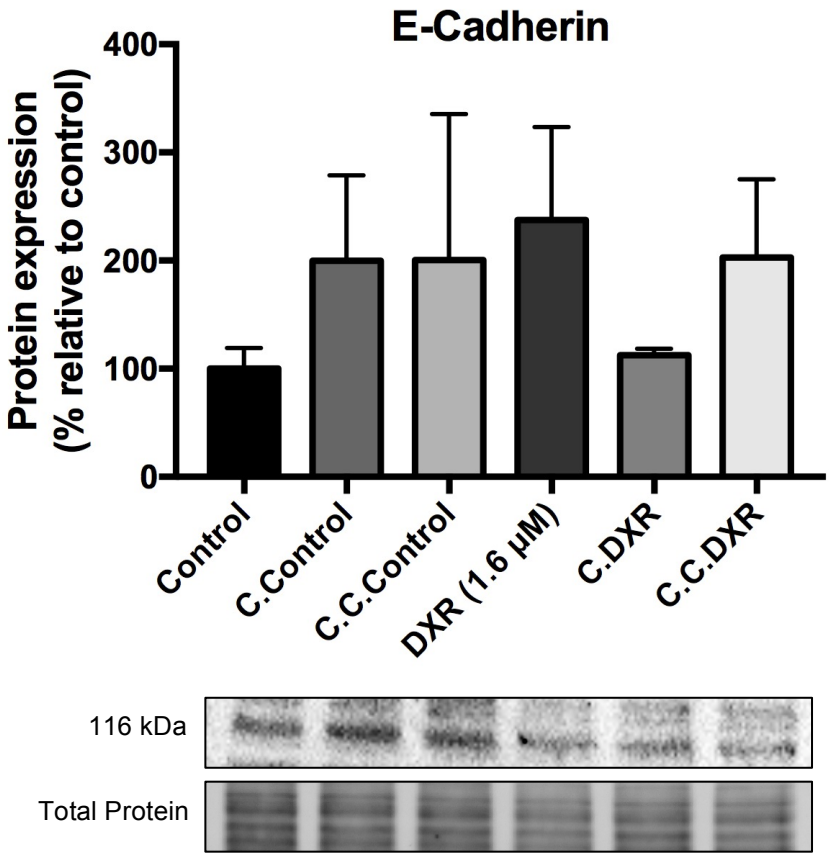

Figure 4.13: Protein expression of E-cadherin from western blot analysis after 24-hour treatment of E0771 cells. E0771 cells were treated for 24-hours with the following treatments: 1) Control consisting of serum free media and complete media in 1:1 ratio. 2) C.Control consisting of serum free media and conditioned media harvested from myotubes after Control treatment in 1:1 ratio. 3) C.C.Control consisting of serum free media and conditioned media harvested from myotubes after E0771 Control treatment in 1:1 ratio. 4) DXR consisting of serum free media and complete media in 1:1 ratio, and 1.6 µM DXR. 5) C.DXR consisting of serum free media and conditioned media harvested from myotubes after DXR treatment in 1:1 ratio. 6) C.C.DXR consisting of serum free media and conditioned media harvested from myotubes after E0771 DXR treatment in 1:1 ratio. Values expressed as percentage (%) of control with statistical representation as mean ±SEM with n = 3.

Chapter 5 – Discussion

Introduction

Dysregulation of signaling pathways in breast cancer cells promotes cancer development and progression. Mutations and alterations in proliferation pathways promote infinite replication, abnormal cell growth, and avoidance of growth suppression while dysfunctional cell death mechanisms inhibit the effective removal of cancerous cells by the body (Hanahan & Weinberg, 2011). Invasion and metastasis of cancer cells is also upregulated by dysregulation of EMT. These mechanisms each play a role in the development of drug resistance and cancer metastasis. Complex cancer microenvironment has observed to be influenced by various other factors, cells and microenvironments (Howard & Lu, 2014). The absence of information regarding the reciprocal interactions between breast cancer cells and skeletal muscle could provide essential information regarding breast cancer progression. Chemotherapeutic treatment targets various cells, tissues, and organs of cancer patients each of which respond differently (Tacar, Sriamrnsak & Dass, 2012). Understanding these responses and the mechanisms involved improve patient prognosis and lower mortality rate by ensuring effective chemotherapeutic treatment and preventing metastasis. This chapter will discuss the impact of the skeletal muscle microenvironment, in response to breast cancer and DXR treatment, on the efficiently of DXR to induce cell death and reduce progression of breast cancer cells.

5.1. Myotube Mitochondrial Oxidative Stress

Investigation of mitochondrial ROS production in myotubes was done using the MitoSOX™ assay. There were no differences in mean fluorescent intensity between the Control group and the group treated with cancer conditioned media obtained from E0771 cells (C.Control) **(Figure 3.2)**. Therefore in our study, factors released from the breast cancer microenvironment did not result in increased production of mitochondrial ROS in myotubes. Our results contradict the results of McLean, Moylan & Andrade (2014) who observed that treatment of C2C12 myotubes with conditioned media harvested from Lewis lung carcinoma cells increased the production of ROS and induced alterations in the mitochondrial ETC. Additionally, Bohlen *et al.* (2018) observed an increase in ROS production in the skeletal muscle of breast cancer patients. The difference observed in our results might be due to different cancer types that were investigated. Various cancer cells secrete different factors therefore specific signaling pathways in the myotubes are activated in response to this.

The production of free radicals and ROS is one of the mechanisms in which DXR induces its anti-neoplastic and cytotoxic effects on healthy cells or tissues, including skeletal muscle (Tacar, Sriamornsak & Dass, 2012). In the skeletal muscle, DXR targets mitochondrial ETC complexes and induces ROS production (Min *et al.,* 2015). In our study, treatment of the myotubes with 1.6 µM DXR did induce a significant increase ($p<0.001$) in mitochondrial ROS compared to Control (**Figure 3.2**). These results correlate with DXR induction of mitochondrial stress in the myotubes observed by Gilliam *et al*. (2011).

Our results showed that mitochondrial ROS in C.DXR was significantly decreased when compared to DXR ($p<0.05$) and that no difference was observed when compared to C.Control (**Figure 3.2**). This finding might suggest that the breast cancer cells were able to mediate DXR mitochondrial ROS production that reduced the amount of mitochondrial ROS produced in the myotubes. Cancer cells have been shown to maintain ROS homeostasis and increase anti-oxidant capacity in response to elevated ROS production (Kumari *et al*., 2018). The mechanism of action in C.DXR may be an anti-oxidant response of the cancer cells to DXR however, further analysis of oxidative stress in both E0771 cells and myotubes will be required.

5.2. Myotubes Integrity

Cachexia is the skeletal muscle-wasting syndrome that has been accredited to be the cause of death for 20-40% of cancer patients (Tisdale, 2009). The extent of cancer cachexia that is induced in breast cancer patients is not fully established. Investigation of myotube atrophy, integrity, and morphology was completed with myotube width measurement (μm^2) using the Cell Tracker™ Assay. Our findings showed no differences between Control and C.Control (**Figure 3.4**) therefore E0771 conditioned media did not alter myotube morphology and integrity after 24-hour treatment. DXR and C.DXR (**Figure 3.4**) did not significantly reduce myotube width however Gilliam *et al*. (2011) observed a significant decrease in myotube integrity when treated with 2 µM of DXR after 24-hours. While the concentration of DXR used by Gilliam *et al*. (2011) was considerably different, it may account for alterations in myotube due to sensitivity of *in vivo* studies. The downstream effects in protein expression and mitochondrial dysfunction, induced by cancer cells and chemotherapy, may therefore not have been significantly induced yet. Further analyses with longer treatment periods or at higher DXR concentrations will be required to determine if alterations in myotube integrity will occur.

5.3. Resistance

Cancer cells must undergo inhibition of cell proliferation and induction of cell death in order for chemotherapy to be considered effective. The ability of cancer cells or tumours to withstand the intended anti-neoplastic and cytotoxic effects of chemotherapy is known as resistance. Mitochondrial reductive capacity, analyzed with a MTT assay in **Figure 4.1,** indicated the metabolic activity of active viable cells**.**

Myotube conditioned media (C.Control) was observed to significantly promote cell proliferation and increase cell viability of breast cancer cells when compared to Control ($p<0.01$)(**Figure 4.1**). The introduction of the E0771 conditioned media onto myotubes did eliminate the influence myotubes had on cell proliferation as no alteration in cell viability was observed in C.C.Control when compared to Control. This was observed to be a novel finding which may indicate that the release of cytokines and growth factors by skeletal muscle promoted cancer cell proliferation. Additionally, stimuli from breast cancer cells prevented myotubes from releasing the factors that increased proliferation in breast cancer cells.

The use of DXR to induced effective cytotoxic effects in breast cancer was validated as treatment with DXR at 1.6 µM dose in breast cancer cells significantly decreased cell viability ($p<0.001$)(**Figure 4.1**). As DXR produces ROS for its cytotoxic and neo-plastic effects (Tacar, Sriamrnsak & Dass, 2012), the increase in mitochondrial ROS observed in DXR (**Figure 3.2)** would likely have reduced the cell viability in E0771 cells (**Figure 4.1**). Unexpectedly, a significant increase in viability was observed in C.DXR ($p<0.01$) compared to DXR, however no difference in viability was observed when compared to C.Control **(Figure 4.1)**. This novel finding indicates that even though mitochondrial ROS production was increased in myotubes following treatment of DXR, the treatment of E0771 cells with DXR reduced ROS production. Further analysis of oxidative stress in E0771 cells will determine if the mechanism is due to the anti-oxidant capacity as previously described (Kumari *et al*., 2018). Additionally, the potential factors released by myotubes that increased the cell viability in C.Control, in response to E0771 conditioned media, were not altered when myotubes were treated with DXR as equal cell viability was observed between these groups (**Figure 4.1**). Further investigation of conditioned media is required to identify the markers that resulted in breast cancer cell viability maintenance.

Cell viability in E0771 cells (**Figure 4.1**) treated with DXR treated E0771 conditioned media (C.C.DXR), was observed to be significantly increased when compared to DXR ($p<0.001$) and to C.C.Control ($p<0.05$). As mitochondrial ROS production was not observed to be significantly increased in myotubes (C.DXR) (**Figure 3.2**), it is presumed that induction of

survival pathways was not due to ROS stimuli. Alternatively, the increase of cell viability in C.C.DXR may be due to reciprocal alterations of factors between the breast cancer cells and myotubes. DXR treatment of E0771 cells has been shown to release proteins that stimulate survival pathways such as NF-κβ, PI3K/Akt, and ERK (Buchholz *et al.,* 2005; Zhang *et al.,* 2016). These proteins in the E0771 conditioned media can interact with the myotubes resulting in the release of additional or alternative proteins in response. When the breast cancer cells are treated with this myotube conditioned media, significant alterations in protein expression or signaling pathways were induced in the breast cancer cells. Downstream results of these interactions resulted in the significant increase of E0771 cell viability. Investigation of proliferation and apoptotic pathways will elude the modifications in cancer signaling pathways, that upregulated the cell viability of breast cancer cells.

5.4. Proliferation

Dysregulation in one or more proliferation pathways has been shown to promote unsuppressed growth. To validate the E0771 cell viability results, protein expression of cell proliferation markers in the PI3K/Akt pathway, ERK pathway, and a member of the MCM protein family was analyzed using western blot. Akt is phosphorylated for its activation and is a significant protein in the PI3K/Akt pathway that induces various effects that promote cell survival, cell proliferation, cell growth, and cell migration. Meiosis, mitosis and cell survival are promoted by the activation of the ERK pathway. The phospho-ERK and total ERK ratio indicates a fold change in the phosphorylation and activation of ERK. Increases in the ratio correlates to upregulation of ERK activation and downstream effects. Finally, MCM proteins recruit proteins involved in DNA replication and the formation of replication forks. An increase in MCM2 expression indicates increased induction of genome replication. The interactions between the PI3K/Akt pathway, ERK pathway, MCM proteins and their contributions to cancer progression are illustrated in **Figure 5.1.**

The PI3K/Akt pathway was shown to regulate skeletal muscle atrophy *in vivo*, but the mechanism has not been fully investigated (Bodine *et al.,* 2001). The expression of total Akt in Control, C.Control and C.C.Control was however observed not to be significantly different in our study (**Figure 4.2**). Accurate analysis of the activation of Akt activity and the PI3K/Akt pathway however could not be completed without the expression of phosphorylated Akt. ERK expression in skeletal muscles promotes proliferation of myoblasts as well as differentiation of myocytes into myotubes (VanHook, 2014). No significant difference was observed in the ERK fold change ratio between Control, C.Control and C.C.Control (**Figure**

4.3) therefore, even though the muscle cells were differentiated myotubes, ERK expression in myotubes did not cause alterations in expression in E0771 cells. Additionally, no difference of MCM2 expression was observed between these groups (**Figure 4.4**). These changes are noteworthy due to the significant increase of cell viability in C.Control ($p<0.01$) but not C.C.Control when compared to Control (**Figure 4.1**). Further investigation of the expression of phosphorylated Akt may reveal alterations in Akt activity that correlate with the increase in proliferation observed.

DXR has been shown to trigger Akt activation in breast cancer cells (Brown *et al.,* 2015) however no difference in total Akt expression was observed in our study (**Figure 4.2**). As previously discussed, future investigation of phosphorylated Akt expression may reveal alterations in activity. The ROS produced from DXR can stimulate growth factors, Ras activity and ERK 1/2 protein phosphorylation causing significant activation of the ERK pathway (McCubrey *et al*., 2007; Cheruku *et al.,* 2015). The alterations in expression of ERK and phosphorylated ERK in MDA-MB-231 and MCF-7 cells due to DXR treatment were investigated by Taherian & Mazoochi (2012). They showed that MDA-MB-231 cells were more sensitive to DXR and induced a decrease in ERK 1/2 and phosphorylated ERK 1/2 expression while alternatively, MCF-7 cells were seen to have an increase in ERK 1/2 and phosphorylated ERK 1/2 expression. Our results observed a significant increase in the ERK fold change ratio when compared to Control ($p<0.001$) that may reduce the sensitivity to DXR treatment (**Figure 4.2**), however significant cell death was observed (**Figure 4.1**). While activation of the ERK pathway is associated with cell growth and survival, pro-apoptotic induction has also been observed under certain conditions (Lu & Xu, 2006). Currently there is little evidence of alterations in MCM2 expression due to DXR however DXR forms clusters of replication forks that decrease transcription (Im *et al.,* 2014). Our results did not correlate with this, as no difference in MCM2 expression was observed (**Figure 4.4**).

When C.DXR and C.C.DXR were compared to DXR, an equal and significant increase in cell viability was observed ($p<0.001$) (**Figure 4.1**) with no alterations in total Akt expression (**Figure 4.2**) and a significant reduction in the ERK expression ratio (**Figure 4.3**). These results show that the activation of the ERK pathway in cancer cells from DXR-induced ROS production (McCubrey *et al*., 2007) is eliminated, further supporting that ROS production and its downstream effects can be mediated by the anti-oxidant capacity of cancer cells. Alternatively, a significant decrease in MCM2 expression in C.C.DXR was observed compared to DXR ($p<0.01$) as well as C.DXR ($p<0.01$) (**Figure 4.4**). Our results indicate that the cells which DXR initially targets, and induces a response in, is able to mediate a

difference in MCM2 protein expression in breast cancer cells. This may be due to these microenvironments promoting replication fork cluster formation.

An equal increase in cell viability was observed between C.Control and C.DXR (**Figure 4.1**) was supported by no difference being observed, between these groups, in the expression of total Akt, the ERK ratio, and MCM2. This novel finding indicated that an alteration in proliferation signaling and increased cell growth of breast cancer cells was a result of stimuli from the myotubes, irrespective of chemotherapy treatment, however the exact mechanism is not known. The cell viability in C.C.DXR was significantly increased when compared to C.C.Control ($p<0.05$) (**Figure 4.1**). This significant increase in cell viability is substantiated with a significant decrease in total Akt expression in C.C.DXR when compared to C.C.Control (**Figure 4.2**). As no difference in the ERK expression ratio was observed in these groups, our results show that the ERK pathway is not influenced by alterations between breast cancer cells, myotubes, and DXR (**Figure 4.3**). Finally, the comparison of C.C.Control and C.C.DXR exhibited a significant decrease in the expression of MCM2 ($p<0.01$) (**Figure 4.4**). These findings contradict results of the significant increase in cell viability, as MCM proteins are responsible for transcription and regulation of the cell cycle, are reduced therefore a reduction of replication forks and cell proliferation. Furthermore, the downregulation of Akt activity has also been shown to reduce the phosphorylation of MCM2 (Chang *et al.,* 2003). This interaction was observed in total Akt expression of the E0771 cells following treatment of DXR treated E0771 conditioned media, however comprehensive Akt activity analysis is required. The novel findings in proliferation pathways emphasize the need of systemic consideration during chemotherapy as cancer cells treated with DXR prompt a response in myotube microenvironments with reciprocal upregulation of proliferation signaling in cancer cells. Further investigation into the factors present in myotube-conditioned media will assist with potential targets to reduce cancer cell growth.

5.5. Apoptosis

A mutation that promotes rapid cell proliferation or inhibits apoptosis promotes the development and progression of tumours, as the damaged cells are not effectively removed. Apoptosis is mediated by an extrinsic and an intrinsic pathway that converge into the execution pathway. Chemotherapeutic drugs, including DXR, modulate apoptosis with multiple pathways and the increased presence of apoptotic markers in tumours after chemotherapy indicates induction of apoptosis (Kerr, Wylie & Currie, 1972). DXR directly targets components of the intrinsic pathway (Leung & Wang, 1999) and the extrinsic

pathway (Reed, 1994). Our study did not focus on the mechanism of induction but rather on the final execution of apoptosis. The fold change ratio of cleaved caspase 3 and total caspase 3 (**Figure 4.5**) as well as cleaved PARP and total PARP (**Figure 4.6**) indicated no activation of the execution pathway in C.Control or C.C.Control compared to Control. These results are supported by cell death not being observed in the E0771 cells (**Figure 4.1**)**.** These novel finding indicates that myotube conditioned media components do not directly, or through downstream signaling pathways, induce apoptosis in breast cancer cells irrespective of initial stimuli from breast cancer cells.

DXR treatment of E0771 cells did not alter the fold change ratio of caspase 3 (**Figure 4.5**); however, a significant decrease was observed in the PARP fold change ratio ($p<0.01$) compared to Control (**Figure 4.6**). This fold change ratio reduction indicates a decrease in apoptotic induction. PARP is the active form of this protein and its functions are inactivated by cleavage (Ouyang *et al.*, 2012). The decrease in PARP fold change may indicate a reduction in the cleavage of PARP through upstream pathways or a higher expression of activated PARP. Hyper-activation of PARP, and thus an increase in total PARP expression, has been shown to a direct response of DXR activity (Tacar, Sriamrnsak & Dass, 2012). While a decrease of cell viability in the DXR group was observed in **Figure 4.1**, the significant decrease in the ratio of PARP expression (**Figure 4.6**) could be an attempt by the E0771 cells to repair the DNA induced by DXR for cell survival. Alternatively, an alternative cell death mechanism may have been induced by DXR resulting in the reduction of viability.

Intervention of microenvironments may directly or indirectly, with the use of signaling pathways, inhibit apoptosis from occurring (Weinstein-Oppenheimer *et al.,* 2001). During protein degradation of muscle, downstream activation of caspase 3 and the ubiquitin-proteasome pathway have been observed (Jackman & Kandarian, 2004). A study by Gilliam *et al*. (2012) observed that exposure of myotubes to DXR has been shown to promote skeletal muscle catabolism with the upregulation of caspase 3 activity. In the C.DXR group, an increase in the fold change ratio of caspase 3 was observed but this was not significant due to the considerable variation observed (**Figure 4.5**). Additionally, cell death was not observed in the MTT assay (**Figure 4.1**) and this could possibly be explained with changes in PARP activity. The fold change ratio of cleaved PARP and total PARP (**Figure 4.6**) was significantly decreased when compared to C.Control ($p<0.01$) indicating an upregulation of DNA repair and a decrease in the induction of apoptosis. This repair prevented the cells from undergoing apoptosis and maintaining cell viability (Elmore, 2007). This novel finding indicated that contradictory alterations of protein expression in breast cancer cells were induced due to factors released by myotubes in response to chemotherapy. Additionally, the

hyper-activation of total PARP activity by DXR, thus reduction in PARP cleavage, is maintained in downstream effects irrespective of cell type and concentration.

The fold change ratio of caspase 3 in C.C.DXR remained unaltered when compared to C.C.Control (**Figure 4.5)** indicating that there were no alterations in the factors released by the myotubes in response to cancer stimuli with and without DXR treatment that could induce apoptosis. The factors released by myotubes in response to DXR-treated cancer cells however, did result in alterations in DNA repair. The PARP fold change ratio observed in **Figure 4.6** was significantly reduced compared to C.C.Control ($p<0.001$) but remain constant with expression in DXR and C.DXR. Our findings observed that DXR treatment decreases apoptotic signaling in both cancer cells and myotubes that can promote upegulation of survival signals and chemotherapy resistance in breast cancer cells.

5.6. Invasion and Metastasis

In epithelial breast cancer cells, the induction of EMT induces a mesenchymal phenotype that promotes migration of tumour cells and their invasion into surrounding tissue. EMT activation has also been shown to stimulate apoptotic resistance, thereby encouraging resistance to chemotherapeutic agents. The mesenchymal markers α-SMA and vimentin are important proteins within the cytoskeleton. An increase in these markers has been shown to correspond to alterations in the cell structure that increases migratory capabilities of cells. The upregulation of the transcription factor SNAIL suppresses the transcription and expression of the epithelial marker E-cadherin. Cell-cell adhesions are broken down with the loss of E-cadherin promoting metastatic properties of the cell.

No difference in the percentage of wound closure was observed between Control and C.Control or Control and C.C.Control (**Figure 4.8**). The percentage of wound closure in C.Control however was observed to be significantly lower compared to C.C.Control after 6-hours ($p<0.001$), 12-hours ($p<0.01$), and 24-hours ($p<0.01$). The highest percentage of wound closure for C.C.Control was observed at 12-hour time point but closure remained unchanged after 24-hours. Comparison of α-SMA expression to Control exhibited a decrease in C.Control and a significant reduction in C.C.Control ($p<0.05$) (**Figure 4.10**). The significant reduction of α-SMA indicates a more epithelial phenotype in the breast cancer cells. These results are contradictory as migration and invasion of epithelial cancers were shown to correlate with an increase in α-SMA expression (Birchmeier *et al.,* 2003). When observing the expression of vimentin and SNAIL (**Figure 4.11 and 4.12**), no difference was observed when comparing Control, C.Control and C.C.Control. Additionally, E-cadherin

expression was observed to be increased in C.Control and C.C.Control (**Figure 4.13**) when compared to Control but significance could not be determined due to variation in expression. Our novel findings indicate that treatment of breast cancer cells with myotube conditioned media could possibly induce a more epithelial phenotype, however, the significant increase in the percentage of wound closure of C.C.Control exhibits that reciprocal interactions between E0771 cells and myotubes did promote migration of the cancer cells.

DXR percentage of wound closure was significantly higher when compared to Control at all time points ($p<0.05$, $p<0.001$) (**Figure 4.8**). No significant difference was observed in the expression of α-SMA, vimentin or SNAIL when compared to Control (**Figure 4.10-4.12**). These results indicate that during migration of cancer cells, the cell phenotype was not permanently altered to one state. An increase in E-cadherin expression was observed when compared to Control but as previously discussed, significance could not be accurately obtained due to variation (**Figure 4.13**). A study by Bandyopadhyay *et al.* (2010) has shown that TGF- β is upregulated by doxorubicin in metastatic murine breast cancer. Upregulation of TGF-β due to DXR correlates with significant dysregulation of ERK activation we observed in our results as an alternative induction of EMT. Investigation of TGF-β is however required to determine the mechanisms in which DXR induces the effects observed.

Comparison of DXR, C.DXR and C.C.DXR exhibited no difference in percentage or rate of wound closure (**Figure 4.8 and 4.9**). Compared to DXR, the expression of α-SMA was decreased in C.DXR and significantly decreased in C.C.DXR ($p<0.01$) (**Figure 4.10**). As previously described, an increase in α-SMA is associated with increased invasion of epithelial cancers (Birchmeier *et al.,* 2003) however our studies observed significant decrease when cancer cells were treated with E0771 treated myotube conditioned media with and without DXR. This novel finding indicates that myotube conditioned media was able to reduce α-SMA expression in E0771 cells and that this response was independent of chemotherapy. Additionally, the reciprocal stimulations between myotubes and E0771 cells further reduced the expression of α-SMA. A significant alteration in expression of any protein will result in alterations in cell functions therefore a significant loss of a protein responsible for structure and integrity (Lee *et al.,* 2013) may result in dysfunctional morphology. This may additionally reduce adhesion to neighbouring cells however further investigation is required. Vimentin expression was observed to have been significantly increased in C.DXR compared to DXR ($p<0.05$) (**Figure 4.11**). An upregulation of vimentin has been shown to correlate with increased tumour growth and invasion (Satelli & Li, 2011). This increase in vimentin expression may be a downstream activation of Ras due to the significant increase in mitochondrial ROS in the myotubes during treatment (Vuoriluoto *et al.,* 2010). This will

correlate to why no difference in expression was observed in the other treatment groups, however further investigation into oxidative stress within both myotubes and cancer cells is required. No differences were observed in SNAIL expression in a comparison between DXR, C.DXR and C.C.DXR (**Figure 4.12**). Finally, C.DXR expression of E-cadherin non-significantly decreased compared to DXR however, no difference of expression was observed between DXR and C.DXR (**Figure 4.13**). Additionally, the E-cadherin expression in C.DXR was observed to be non-significantly decreased when compared to C.Control.

A significant increase in percentage of wound closure was observed in C.DXR at all time points when compared to C.Control ($p<0.001$) (**Figures 4.8**). Comparison between C.DXR and C.Control, however exhibited no significant difference in the mesenchymal markers α-SMA, vimentin and SNAIL (**Figure 4.10-4.12**). The decrease in the epithelial marker E-cadherin observed in C.DXR (**Figure 4.13**) was insignificant therefore this finding indicates that the phenotypical profile of E0771 cells remain even though significant migration was induced in C.DXR. Comparison of C.C.Control and C.C.DXR exhibited no differences in percentage of wound closure (**Figure 4.8**). Alternatively, no alterations observed in the expression of α-SMA, vimentin, SNAIL or E-cadherin between C.C.Control and C.C.DXR (**Figure 4.10-4.13**). These findings indicate that myotubes treated with E0771 conditioned media, independent of DXR treatment, initiated the same migratory and EMT phenotype in breast cancer cells. These findings may help to understand mechanisms of metastasis and correlate with a study by Velikova *et al* (1998). They observed that while E-cadherin expression at tumour sites was significantly increased in patients with liver, stomach, colon, pancreas, ovarian, and rectal cancer, the soluble expression of E-cadherin was not significantly increased in the colorectal cancer patients compared to the healthy control.

Significant differences were observed in the percentage of wound closure and rate of wound closure during our study (**Figure 4.8-4.9**) however no significant alterations in the EMT markers were observed (**Figure 4.10-4.13**). As we used Mitomycin C during our scratch assay, the migration observed could not have resulted due to proliferation. Breast cancer cell lines have been shown to undergo partial transitions rather than a terminal epithelial or mesenchymal state (Grosse-Wilde *et al*., 2015; Lambert, Pattabiraman & Weinberg, 2017). Additionally a study conducted by Chao *et al.* (2012) had shown that breast cancer metastases expressed E-cadherin at cellular membranes as well as retaining the expression of the mesenchymal marker vimentin. Partial transitions between EMT and MET could account for these alterations and hybrid co-expression of epithelial and mesenchymal markers. Control and C.Control observed very little migration after the 24-hour treatment period, however significant migration in wound closure was observed in C.C.Control

($p<0.001$). In this treatment group, an increase in the percentage of wound closure was observed after 12-hours of treatment that was then maintained until after 24-hours of treatment. Additionally the rate of wound closure $\%.hr^{1}$) was observed to steadily decrease for all treatments at each time point (**Figures 4.8**). This indicates that at the time point protein expression was analysed, the cells may potentially be in a hybrid phase as migration rate was decreasing. The rapid alteration may be due to stimuli from nutrients depleting or space restriction. In cancer cells, phenotypic plasticity is maintained to promote quick transition between MET and EMT in order to promote cell growth and resistance to chemotherapeutic treatments in metastases. Additionally, the tumour microenvironment is able to influence phenotypic plasticity of cancer cells and induce EMT (Jolly *et al*., 2017). The decrease of E-cadherin expression in cancer cells was observed to induce EMT and the promotion of invasion, however, the induction of MET and the increase of E-cadherin expression was necessary for the survival and migration of secondary metastasis (Louie *et al.*, 2013; Ya, Peng & Dai, 2013). The significant variation of E-cadherin expression observed in some of our treatments groups may be a result of these alterations in the hybrid phenotypes. Skeletal muscle microenvironments are favorably plastic to promote rapid contraction and wound healing of muscle fibres (Schiaffino & Reggiani, 2011). This plastic microenvironment may be promoting an increased plastic phenotype in the cancer cells enabling migration through rapid induction of EMT followed by MET induction. The proximity of microenvironments has been shown to promote metastasis is correlated with the risk of cancer metastasis (Robinson *et al.,* 2009). Investigation of markers at additional time points may reveal the dynamic alterations of EMT and MET induction in cancer cells, the influence of skeletal muscle plasticity on these alterations and responses to chemotherapeutic treatment.

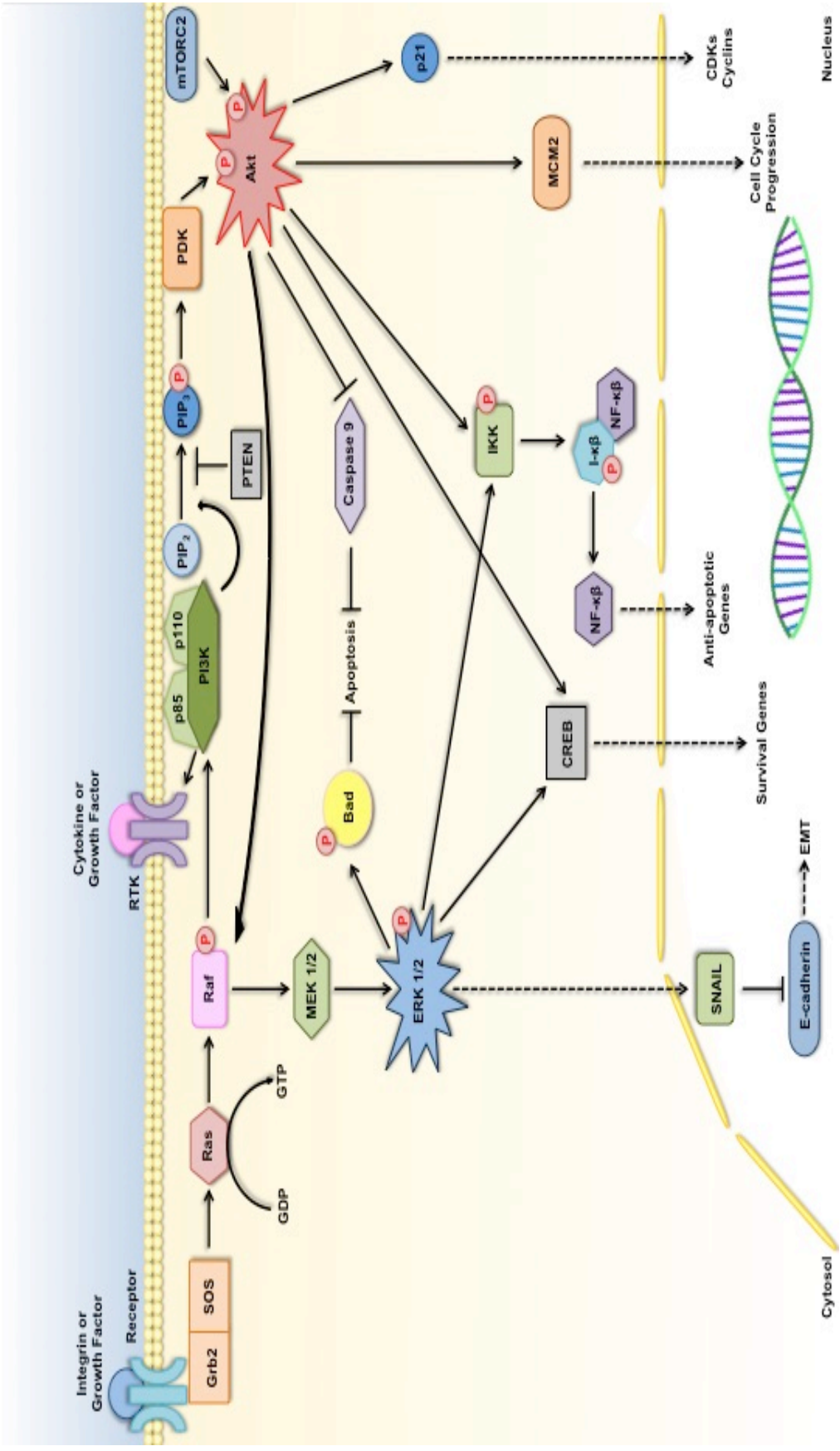

Figure 5.1: Interactions between PI3K/Akt pathway, ERK pathway, Apoptosis, and EMT. Molecular pathways interact with eachother in order to regulate proliferation, cell death and migration of a cell. Dysfunction of one or more proteins in a pathway may alter activation as well as the downstream effects of another promoting cancer development and progression. Scheme reproduced from Larue & Bellacosa (2005), Hemmings & Restuccia (2012) and Chang *et al.* (2003).

Chapter 6 – Conclusion

The investigation of the influence of myotube microenvironments on cancer progression and the chemotherapeutic response is important to reduce chemotherapy resistance and metastasis as these factors significantly reduce patient survival. Our study investigated the dynamic interactions between skeletal muscle and breast cancer following chemotherapeutic treatment (**Figure 6.1**). In our study, following treatment of myotubes with 1.6 μM DXR, a significant increase in mitochondrial ROS production was observed when compared to Control ($p<0.001$) while myotube integrity was preserved. Treatment of E0771 cells with DXR-treated myotube conditioned media (C.DXR) significantly increased the percentage of wound closure after 24-hours ($p<0.01$) and decreased the cleaved/total PARP ratio ($p<0.001$), indicating a decrease in the induction of apoptosis, when compared to the myotube conditioned media (C.Control). These novel findings indicated that significant alterations in E0771 cells by myotube-conditioned media were dependent on chemotherapy-induced alterations, possibly as a mechanism of mitochondrial ROS production.

Treatment of E0771 cells with 1.6 μM DXR compared to Control significantly decrease cell viability ($p<0.001$), increases the phospho/total ERK ratio ($p<0.001$) and decreases the cleaved/total PARP ratio ($p<0.01$). This indicates that although there was a reduction of viable cells, a survival pathway was induced and apoptosis reduced. Additionally, a significant increase in the percentage of wound closure after 24-hours ($p<0.01$) was observed indicating migration of the cells. These findings correlated with interactions and mechanisms of action previously observed as a result of DXR in cancer cells. Treatment of myotubes with DXR-treated E0771 conditioned media (C.DXR) did not result in any significant changes in mitochondrial ROS production or myotube integrity. Finally, following treatment of E0771 cells with DXR-treated E0771 myotube conditioned media (C.C.DXR), a significant increase in cell viability ($p<0.05$) and a significant decrease in expression of total Akt ($p<0.05$), MCM2 ($p<0.05$), and the cleaved/total PARP ratio ($p<0.001$) was observed when compared to Control-treated E0771 myotube conditioned media (C.C.Control). These novel findings exhibited that significant alterations in breast cancer signaling pathways were induced due to reciprocal interactions between breast cancer cells and myotubes as well as their responses to DXR.

Our novel investigation of the dynamic interactions between myotubes and breast cancer cells revealed evidence of alterations in breast cancer signaling pathways that promoted cancer progression and cell survival. Our study also revealed novel evidence that this myotube microenvironment significantly affected the response of breast cancer cells to the

chemotherapeutic treatment of DXR. These alterations were also significantly influenced when the dynamic cancer-myotube-cancer interactions were investigated. While the exact mechanisms and responses have not yet been fully elucidated in our study, we have identified new target mechanisms that may reduce drug resistance and breast cancer metastases as these processes significantly impact the mortality of cancer patients.

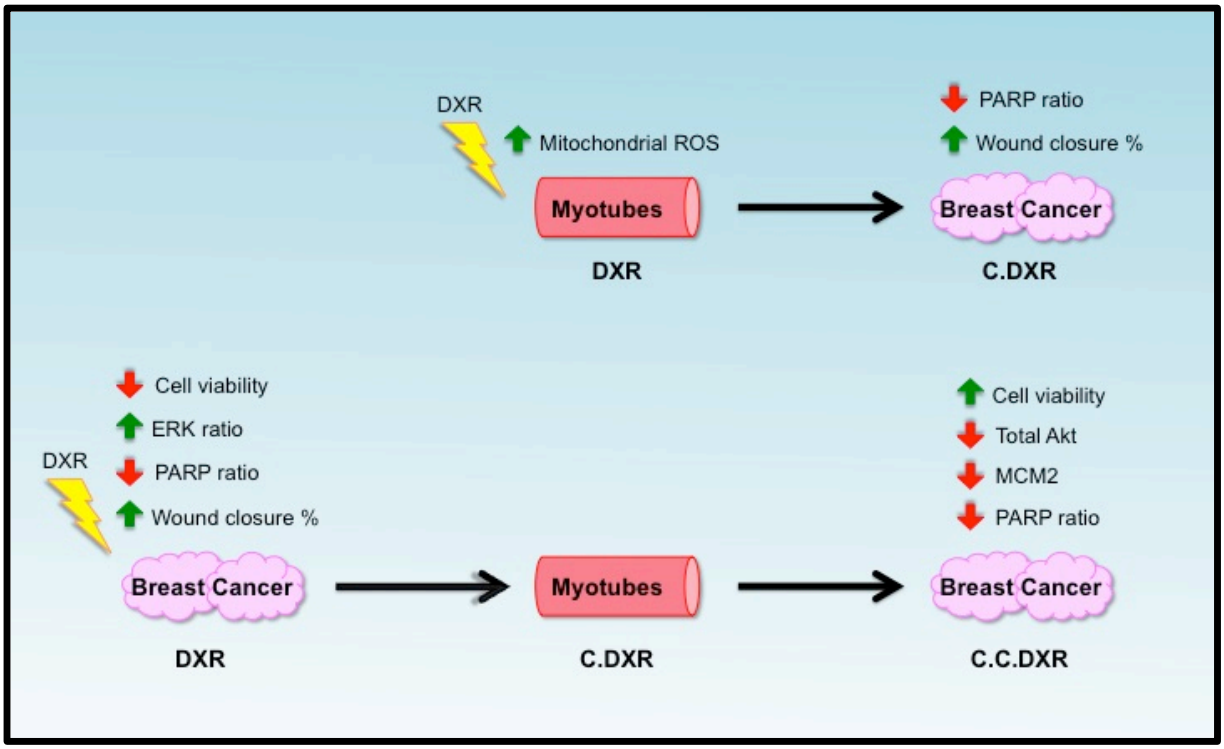

Figure 6.1: Proposed alterations in signaling pathways due to the dynamic relationships between E0771 cells, myotubes and DXR treatment. Significant results observed in myotubes when DXR treatment was compared to Control and E0771 cell conditioned media C.DXR treatment to C.Control. Treatment of E0771 cells showed significant results when DXR treatment was compared to Control, myotube conditioned media C.DXR treatment compared to C.Control as well as myotube conditioned media following treatment of E0771 cell condition media C.C.DXR compared to C.C.Control.

Chapter 7 – Limitations and Future Studies

Limitations of this study include that only one time point of cell viability and protein expression was investigated. This resulted in observation of alterations at that specific time point and not the dynamic interactions that change over time. This study only used a cancerous epithelial cell line, therefore comparisons to healthy mammary epithelial cells could not be completed. Alternate cell death mechanisms were not studied therefore only alterations regarding apoptosis could be investigated. Additionally, only one or two markers were investigated within a signaling pathway that do not accurately represent if complete activation of the pathway has occurred.

Future studies that should be considered following our study include examining the alterations with myotubes as a consequence of cancer and DXR. Due to the mechanism of action induced by DXR, analyses of mitochondrial dynamics and oxidative stress within the myotubes and cancer cells would increase understanding the mechanisms of drug resistance to DXR. Determining alterations in the cell cycle phases of cancer cells and investigation of TGF-β and p53 regulation should also be considered as these components play significant roles in drug resistance and metastasis. An additional treatment of cancer cells with DXR, after stimulation by myotube conditioned media with/without cachexia phenotype, is required for future studies. This will investigate alterations in chemotherapeutic response of breast cancer cells due to pre-stimulation by a healthy and diseased myotube microenvironment. Proteomics analyses of all conditioned media collected and used will provide more information regarding proteins and signaling pathways activated due to stimuli from different microenvironments.

References

Akiyama, T., Ohuchi, T., Sumida, S., Matsumoto, K. & Toyoshima, K. (1992). Phosphorylation of the retinoblastoma protein by cdk2. *Proceedings of the National Academy of Sciences*, 89(17), pp.7900-7904.

Alessi, D., Saito, Y., Campbell, D., Cohen, P., Sithanandam, G., Rapp, U., Ashworth, A., Marshall, C. & Cowley, S. (1994). Identification of the sites in MAP kinase kinase-1 phosphorylated by p74raf-1. *The EMBO Journal*, 13(7), pp.1610-1619.

Ashley, N. & Poulton, J. (2009). Mitochondrial DNA is a direct target of anti-cancer anthracycline drugs. *Biochemical and Biophysical Research Communications*, 378(3), pp.450-455.

Badve, S., Dabbs, D., Schnitt, S., Baehner, F., Decker, T., Eusebi, V., Fox, S., Ichihara, S., Jacquemier, J., Lakhani, S., Palacios, J., Rakha, E., Richardson, A., Schmitt, F., Tan, P., Tse, G., Weigelt, B., Ellis, I. & Reis-Filho, J. (2010). Basal-like and triple-negative breast cancers: a critical review with an emphasis on the implications for pathologists and oncologists. *Modern Pathology*, 24(2), pp.157-167.

Bandyopadhyay, A., Wang, L., Agyin, J., Tang, Y., Lin, S., Yeh, I., De, K. & Sun, L. (2010). Doxorubicin in Combination with a Small TGFβ Inhibitor: A Potential Novel Therapy for Metastatic Breast Cancer in Mouse Models. *PLoS ONE*, 5(4), p.e10365.

Ben-Porath, I., Thomson, M., Carey, V., Ge, R., Bell, G., Regev, A. & Weinberg, R. (2008). An embryonic stem cell–like gene expression signature in poorly differentiated aggressive human tumors. *Nature Genetics*, 40(5), pp.499-507.

Bernier, J. & Poortmans, P. (2016). Surgery and radiation therapy of triple-negative breast cancers: From biology to clinics. *The Breast*, 28, pp.148-155.

Bidard, F., Pierga, J., Vincent-Salomon, A. & Poupon, M. (2007). A “class action” against the microenvironment: do cancer cells cooperate in metastasis?. *Cancer and Metastasis Reviews*, 27(1), pp.5-10.

Birchmeier, C., Birchmeier, W., Gherardi, E. & Vande Woude, G. (2003). Met, metastasis, motility and more. *Nature Reviews Molecular Cell Biology*, 4(12), pp.915-925.

Bissell, M. & Hines, W. (2011). Why don't we get more cancer? A proposed role of the microenvironment in restraining cancer progression. *Nature Medicine*, 17(3), pp.320-329.

Blalock, W., Weinstein-Oppenheimer, C., Chang, F., Hoyle, P., Wang, X., Algate, P., Franklin, R., Oberhaus, S., Steelman, L. & McCubrey, J. (1999). Signal transduction, cell cycle regulatory, and anti-apoptotic pathways regulated by IL-3 in hematopoietic cells: possible sites for intervention with anti-neoplastic drugs. *Leukemia*, 13(8), pp.1109-1166.

Bochman, M. & Schwacha, A. (2009). The Mcm Complex: Unwinding the Mechanism of a Replicative Helicase. *Microbiology and Molecular Biology Reviews*, 73(4), pp.652-683.

Bodine, S., Stitt, T., Gonzalez, M., Kline, W., Stover, G., Bauerlein, R., Zlotchenko, E., Scrimgeour, A., Lawrence, J., Glass, D. & Yancopoulos, G. (2001). Akt/mTOR pathway is a crucial regulator of skeletal muscle hypertrophy and can prevent muscle atrophy in vivo. *Nature Cell Biology*, 3(11), pp.1014-1019.

Bohlen, J., McLaughlin, S., Hazard-Jenkins, H., Infante, A., Montgomery, C., Davis, M. & Pistilli, E. (2018). Dysregulation of metabolic-associated pathways in muscle of breast cancer patients: preclinical evaluation of interleukin-15 targeting fatigue. *Journal of Cachexia, Sarcopenia and Muscle*, 9(4), pp.701-714.

Boussadia, O., Kutsch, S., Hierholzer, A., Delmas, V. & Kemler, R. (2002). E-cadherin is a survival factor for the lactating mouse mammary gland. *Mechanisms of Development*, 115(1-2), pp.53-62.

Bradford, M. (1976). A Rapid and Sensitive Method for the Quantitation of Microgram Quantities of Protein Utilizing the Principle of Protein-Dye Binding. *Analytical Biochemistry*, 72(1-2), pp.248-254.

Brown, K., Montaser-Kouhsari, L., Beck, A. & Toker, A. (2015). MERIT40 Is an Akt Substrate that Promotes Resolution of DNA Damage Induced by Chemotherapy. *Cell Reports*, 11(9), pp.1358-1366.

Bruck, I. & Kaplan, D. (2015). Conserved mechanism for coordinating replication fork helicase assembly with phosphorylation of the helicase. *Proceedings of the National Academy of Sciences*, 112(36), pp.11223-11228.

Buchholz, T., Garg, A., Chakravarti, N., Aggarwal, B., Esteva, F., Kuerer, H., Eva Singletary, S., Hortobagyi, G., Pusztai, L., Cristofanilli, M. & Sahin, A. (2005). The Nuclear Transcription Factor B/bcl-2 Pathway Correlates with Pathologic Complete Response to Doxorubicin-Based Neoadjuvant Chemotherapy in Human Breast Cancer. *Clinical Cancer Research*, 11(23), pp.8398-8402.

CANSA – The Cancer Association of South Africa. (2010). *National Cancer Registry*. [online] Available at: http://www.cansa.org.za/files/2015/10/NCR_Final_2010_tables1.pdf [Accessed 26 Dec. 2018].

CANSA – The Cancer Association of South Africa. (2018). *Position Statement on Breast Cancer*. [online] Available at: https://www.cansa.org.za/files/2018/10/Position-Statement-Breast-Cancer-October-2018.pdf [Accessed 7 Jan. 2019].

Carson, J., Hardee, J. & VanderVeen, B. (2016). The emerging role of skeletal muscle oxidative metabolism as a biological target and cellular regulator of cancer-induced muscle wasting. *Seminars in Cell & Developmental Biology*, 54, pp.53-67.

Carvalho, C., Santos, R., Cardoso, S., Correia, S., Oliveira, P., Santos, M. & Moreira, P. (2009). Doxorubicin: The Good, the Bad and the Ugly Effect. *Current Medicinal Chemistry*, 16(25), pp.3267-3285.

Ceelen, W. & Bracke, M. (2009). Peritoneal minimal residual disease in colorectal cancer: mechanisms, prevention, and treatment. *The Lancet Oncology*, 10(1), pp.72-79.

Chang, F., Lee, J., Navolanic, P., Steelman, L., Shelton, J., Blalock, W., Franklin, R. & McCubrey, J. (2003). Involvement of PI3K/Akt pathway in cell cycle progression, apoptosis and neoplastic transformation: a target for cancer chemotherapy. *Leukemia*, 17(3), pp.590-603.

Chao, Y., Shepard, C. & Wells, A. (2010). Breast carcinoma cells re-express E-cadherin during mesenchymal to epithelial reverting transition. *Molecular Cancer*, 9(1), p.179.

Chao, Y., Wu, Q., Acquafondata, M., Dhir, R. & Wells, A. (2012). Partial Mesenchymal to Epithelial Reverting Transition in Breast and Prostate Cancer Metastases. *Cancer Microenvironment*, 5(1), pp.19-28.

Chen, D., Lu, D., Lin, H. & Yeh, W. (2014). Mesenchymal Stem Cell-Induced Doxorubicin Resistance in Triple Negative Breast Cancer. *BioMed Research International*, 2014, pp.1-10.

Chen, W., Wang, H., Tang, Y., Liu, C., Li, H. & Li, W. (2010). Multidrug resistance in breast cancer cells during epithelial-mesenchymal transition is modulated by breast cancer resistant protein. *Chinese Journal of Cancer*, 29(2), pp.151-157.

Chen, Z., Yu, Y., Michalopoulos, G., Nelson, J. & Luo, J. (2014). The DNA Replication Licensing Factor Miniature Chromosome Maintenance 7 Is Essential for RNA Splicing of Epidermal Growth Factor Receptor, c-Met, and Platelet-derived Growth Factor Receptor. *Journal of Biological Chemistry*, 290(3), pp.1404-1411.

Cheruku, H., Mohamedali, A., Cantor, D., Tan, S., Nice, E. & Baker, M. (2015). Transforming growth factor-β, MAPK and Wnt signaling interactions in colorectal cancer. *EuPA Open Proteomics*, 8, pp.104-115.

Cheung-Ong, K., Giaever, G. & Nislow, C. (2013). DNA-Damaging Agents in Cancer Chemotherapy: Serendipity and Chemical Biology. *Chemistry & Biology*, 20(5), pp.648-659.

Christou, N., Perraud, A., Blondy, S., Jauberteau, M., Battu, S. & Mathonnet, M. (2017). E-cadherin: A potential biomarker of colorectal cancer prognosis. *Oncology Letters*, 13(6), pp.4571-4576.

Coates, A., Abraham, S., Kaye, S., Sowerbutts, T., Frewin, C., Fox, R. & Tattersall, M. (1983). On the receiving end—patient perception of the side-effects of cancer chemotherapy. *European Journal of Cancer and Clinical Oncology*, 19(2), pp.203-208.

Cortez, D., Glick, G. & Elledge, S. (2004). From The Cover: Minichromosome maintenance proteins are direct targets of the ATM and ATR checkpoint kinases. *Proceedings of the National Academy of Sciences*, 101(27), pp.10078-10083.

Croce, C. (2008). Oncogenes and Cancer. *New England Journal of Medicine*, 358(5), pp.502-511.

Davies, M., Robinson, M., Smith, E., Huntley, S., Prime, S. & Paterson, I. (2005). Induction of an epithelial to mesenchymal transition in human immortal and malignant keratinocytes by TGF-β1 involves MAPK, Smad and AP-1 signalling pathways. *Journal of Cellular Biochemistry*, 95(5), pp.918-931.

Davis, T. (2016). *The role of the AHNAK protein in breast cancer: Implications for tumour metastasis and chemoresistance*. Ph.D. Stellenbosch University.

Derynck, R., Akhurst, R. & Balmain, A. (2001). Erratum: TGF-β signaling in tumor suppression and cancer progression. *Nature Genetics*, 29(2), pp.117-129.

Dong, C., Wu, Y., Wang, Y., Wang, C., Kang, T., Rychahou, P., Chi, Y., Evers, B. & Zhou, B. (2012). Interaction with Suv39H1 is critical for Snail-mediated E-cadherin repression in breast cancer. *Oncogene*, 32(11), pp.1351-1362.

Duronio, R. & Xiong, Y. (2013). Signaling Pathways that Control Cell Proliferation. *Cold Spring Harbor Perspectives in Biology*, 5(3), pp.a008904-a008904.

Dworzak, F., Ferrari, P., Gavazzi, C., Maiorana, C. & Bozzetti, F. (1998). Effects of cachexia due to cancer on whole body and skeletal muscle protein turnover. *Cancer*, 82(1), pp.42-48.

Elmore, S. (2007). Apoptosis: A Review of Programmed Cell Death. *Toxicologic Pathology*, 35(4), pp.495-516.

Ewen, M., Sluss, H., Sherr, C., Matsushime, H., Kato, J. & Livingston, D. (1993). Functional interactions of the retinoblastoma protein with mammalian D-type cyclins. *Cell*, 73(3), pp.487-497.

Fabian, J., Daar, I. & Morrison, D. (1993). Critical tyrosine residues regulate the enzymatic and biological activity of Raf-1 kinase. *Molecular and Cellular Biology*, 13(11), pp.7170-7179.

Fang, J. & Richardson, B. (2005). The MAPK signalling pathways and colorectal cancer. *The Lancet Oncology*, 6(5), pp.322-327.

Fata, J., Chaudhary, V. & Khokha, R. (2001). Cellular Turnover in the Mammary Gland Is Correlated with Systemic Levels of Progesterone and Not 17β-Estradiol During the Estrous Cycle1. *Biology of Reproduction*, 65(3), pp.680-688.

Fei, L., Ma, Y., Zhang, M., Liu, X., Luo, Y., Wang, C., Zhang, H., Zhang, W. & Han, Y. (2017). RACK1 promotes lung cancer cell growth via an MCM7/RACK1/Akt signaling complex. *Oncotarget*, 8(25), pp.40501-40513.

Fei, L. & Xu, H. (2018). Role of MCM2–7 protein phosphorylation in human cancer cells. *Cell & Bioscience*, 8(1):43.

Foulkes, W., Smith, I. & Reis-Filho, J. (2010). Triple-Negative Breast Cancer. *New England Journal of Medicine*, 363(20), pp.1938-1948.

Fox, K., Brooks, J., Gandra, S., Markus, R. & Chiou, C. (2009). Estimation of Cachexia among Cancer Patients Based on Four Definitions. *Journal of Oncology*, 2009, pp.1-7.

Frogne, T., Jepsen, J., Larsen, S., Fog, C., Brockdorff, B. & Lykkesfeldt, A. (2005). Antiestrogen-resistant human breast cancer cells require activated Protein Kinase B/Akt for growth. *Endocrine-Related Cancer*, 12(3), pp.599-614.

Fry, C.S. & Rasmussen, B.B. (2011). Skeletal Muscle Protein Balance and Metabolism in the Elderly. *Current Aging Sciencee*, 4(3), pp.260-268.

Garnett, M. & Marais, R. (2004). Guilty as charged: B-Raf is a human oncogene. *Cancer Cell*, 6, pp.313-319.

Gilles, C., Polette, M., Mestdagt, M., Nawrocki-Raby, B., Ruggeri, P., Birembaut, P. & Foidart, J. (2003). Transactivation of vimentin by beta-catenin in human breast cancer cells. *Cancer Research*, 63(10), pp.2658-64.

Gilliam, L., Moylan, J., Patterson, E., Smith, J., Wilson, A., Rabbani, Z. & Reid, M. (2012). Doxorubicin acts via mitochondrial ROS to stimulate catabolism in C2C12 myotubes. *American Journal of Physiology-Cell Physiology*, 302(1), pp.C195-C202.

Gregor, M., Misch, E., Yang, L., Hummasti, S., Inouye, K., Lee, A., Bierie, B. & Hotamisligil, G. (2013). The Role of Adipocyte XBP1 in Metabolic Regulation during Lactation. *Cell Reports*, 3(5), pp.1430-1439.

Grosse-Wilde, A., Fouquier d'Hérouël, A., McIntosh, E., Ertaylan, G., Skupin, A., Kuestner, R., del Sol, A., Walters, K. & Huang, S. (2015). Stemness of the hybrid Epithelial/Mesenchymal State in Breast Cancer and Its Association with Poor Survival. *PLOS ONE*, 10(5), p.e0126522.

Guarino, M., Rubino, B. & Ballabio, g. (2007). The role of epithelial-mesenchymal transition in cancer pathology. *Pathology*, 39(3), pp.305-318.

Habets, P., Franco, D., Ruijter, J., Sargeant, A., Pereira, J. & Moorman, A. (1999). RNA Content Differs in Slow and Fast Muscle Fibers: Implications for Interpretation of Changes in Muscle Gene Expression. *Journal of Histochemistry & Cytochemistry*, 47(8), pp.995-1004.

Hahn, W. & Weinberg, R. (2002). Rules for Making Human Tumor Cells. *New England Journal of Medicine*, 347(20), pp.1593-1603.

Hanahan, D. & Weinberg, R. (2011). Hallmarks of Cancer: The Next Generation. *Cell*, 144(5), pp.646-674.

Harake, D., Franco, V., Henkel, J., Miller, T. & Lipshultz, S. (2012). Cardiotoxicity in childhood cancer survivors: strategies for prevention and management. *Future Cardiology*, 8(4), pp.647-670.

Hardee, J., Montalvo, R. & Carson, J. (2017). Linking Cancer Cachexia-Induced Anabolic Resistance to Skeletal Muscle Oxidative Metabolism. *Oxidative Medicine and Cellular Longevity*, 2017, pp.1-14.

Hemmings, B. & Restuccia, D. (2012). PI3K-PKB/Akt Pathway. *Cold Spring Harbor Perspectives in Biology*, 4(9), pp.a011189-a011189.

Hens, J. & Wysolmerski, J. (2005). Key stages of mammary gland development: Molecular mechanisms involved in the formation of the embryonic mammary gland. *Breast Cancer Research*, 7(5), pp.220-224.

Herceg, Z. & Wang, Z. (2001). Functions of poly(ADP-ribose) polymerase (PARP) in DNA repair, genomic integrity and cell death. *Mutation Research/Fundamental and Molecular Mechanisms of Mutagenesis*, 477(1-2), pp.97-110.

Heuberger, B., Fitzka, I., Wasner, G. & Kratochwil, K. (1982). Induction of androgen receptor formation by epithelium-mesenchyme interaction in embryonic mouse mammary gland. *Proceedings of the National Academy of Sciences*, 79(9), pp.2957-2961.

Hilmer, S., Cogger, V., Muller, M. & Le Couteur, D. (2004). The hepatic pharmacokinetics of doxorubicin and liposomal doxorubicin. *Drug Metabolism and Disposition*, 32(8), pp.794-799.

Hollestelle, A., Peeters, J., Smid, M., Timmermans, M., Verhoog, L., Westenend, P., Heine, A., Chan, A., Sieuwerts, A., Wiemer, E., Klijn, J., van der Spek, P., Foekens, J., Schutte, M., den Bakker, M. & Martens, J. (2013). Loss of E-cadherin is not

a necessity for epithelial to mesenchymal transition in human breast cancer. *Breast Cancer Research and Treatment*, 138(1), pp.47-57.

Horstman, A., Olde Damink, S., Schols, A. & van Loon, L. (2016). Is Cancer Cachexia Attributed to Impairments in Basal or Postprandial Muscle Protein Metabolism?. *Nutrients*, 8(8), p.499.

Housman, G., Byler, S., Heerboth, S., Lapinska, K., Longacre, M., Snyder, N. & Sarkar, S. (2014). Drug Resistance in Cancer: An Overview. *Cancers*, 6(3), pp.1769-1792.

Hovey, R. & Aimo, L. (2010). Diverse and Active Roles for Adipocytes During Mammary Gland Growth and Function. *Journal of Mammary Gland Biology and Neoplasia*, 15(3), pp.279-290.

Howard, B. & Lu, P. (2014). Stromal regulation of embryonic and postnatal mammary epithelial development and differentiation. *Seminars in Cell & Developmental Biology*, 25-26, pp.43-51.

Hoyle, P., Moye, P., Steelman, L., Blalock, W., Franklin, R., Pearce, M., Cherwinski, H., Bosch, E., McMahon, M. & McCubrey, J. (2000). Differential abilities of the Raf family of protein kinases to abrogate cytokine dependency and prevent apoptosis in murine hematopoietic cells by a MEK1-dependent mechanism. *Leukemia*, 14(4), pp.642-656.

Huber, M., Azoitei, N., Baumann, B., Grünert, S., Sommer, A., Pehamberger, H., Kraut, N., Beug, H. & Wirth, T. (2004). NF-κB is essential for epithelial-mesenchymal transition and metastasis in a model of breast cancer progression. *Journal of Clinical Investigation*, 114(4), pp.569-581.

Hudis, C. & Gianni, L. (2011). Triple-Negative Breast Cancer: An Unmet Medical Need. *The Oncologist*, 16(Supplement 1), pp.1-11.

Im, J., Keaton, M., Lee, K., Kumar, P., Park, J. & Dutta, A. (2014). ATR checkpoint kinase and CRL1 TRCP collaborate to degrade ASF1a and thus repress genes overlapping with clusters of stalled replication forks. *Genes & Development*, 28(8), pp.875-887.

Inman, J., Robertson, C., Mott, J. & Bissell, M. (2015). Mammary gland development: cell fate specification, stem cells and the microenvironment. *Development*, 142(6), pp.1028-1042.

Jackman, R. & Kandarian, S. (2004). The molecular basis of skeletal muscle atrophy. *American Journal of Physiology-Cell Physiology*, 287(4), pp.C834-C843.

Jeanes, A., Gottardi, C. & Yap, A. (2008). Cadherins and cancer: how does cadherin dysfunction promote tumor progression?. *Oncogene*, 27(55), pp.6920-6929.

Jolly, M., Ware, K., Gilja, S., Somarelli, J. and Levine, H. (2017). EMT and MET: necessary or permissive for metastasis?. *Molecular Oncology*, 11(7), pp.755-769.

Julien, S., Puig, I., Caretti, E., Bonaventure, J., Nelles, L., van Roy, F., Dargemont, C., de Herreros, A., Bellacosa, A. & Larue, L. (2007). Activation of NF-κB by Akt upregulates Snail expression and induces epithelium mesenchyme transition. *Oncogene*, 26(53), pp.7445-7456.

Jung, H., Kim, J., Kim, J., Kim, S., Yang, H., Lee, J., Lee, K., Kim, D., Kang, S., Kim, K., Kim, C. & Kim, J. (2015). Effect of muscle mass on toxicity and survival in patients with colon cancer undergoing adjuvant chemotherapy. *Supportive Care in Cancer*, 23(3), pp.687-694.

Justus, C., Leffler, N., Ruiz-Echevarria, M. & Yang, L. (2014). *In vitro* Cell Migration and Invasion Assays. *Journal of Visualized Experiments*, (88), pp.1-8.

Kalluri, R. & Neilson, E. (2003). Epithelial-mesenchymal transition and its implications for fibrosis. *Journal of Clinical Investigation*, 112(12), pp.1776-1784.

Kalluri, R. & Weinberg, R. (2009). The basics of epithelial-mesenchymal transition. *Journal of Clinical Investigation*, 119(6), pp.1420-1428.

Kerr, J., Wyllie, A. & Currie, A. (1972). Apoptosis: A Basic Biological Phenomenon with Wideranging Implications in Tissue Kinetics. *British Journal of Cancer*, 26(4), pp.239-257.

Kischkel, F., Hellbardt, S., Behrmann, I., Germer, M., Pawlita, M., Krammer, P. & Peter, M. (1995). Cytotoxicity-dependent APO-1 (Fas/CD95)-associated proteins form a death-inducing signaling complex (DISC) with the receptor. *The EMBO Journal*, 14(22), pp.5579-5588.

Klassen, O., Schmidt, M., Ulrich, C., Schneeweiss, A., Potthoff, K., Steindorf, K. & Wiskemann, J. (2016). Muscle strength in breast cancer patients receiving different treatment regimes. *Journal of Cachexia, Sarcopenia and Muscle*, 8(2), pp.305-316.

Kouros-Mehr, H. & Werb, Z. (2006). Candidate regulators of mammary branching morphogenesis identified by genome-wide transcript analysis. *Developmental Dynamics*, 235(12), pp.3404-3412.

Kruidering, M. & Evan, G. (2000). Caspase-8 in Apoptosis: The Beginning of "The End"?. *IUBMB Life*, 50(2), pp.85-90.

Kumari, S., Badana, A., G, M., G, S. & Malla, R. (2018). Reactive Oxygen Species: A Key Constituent in Cancer Survival. *Biomarker Insights*, 13, pp.117727191875539.

Kurokawa, M. & Kornbluth, S. (2009). Caspases and Kinases in a Death Grip. *Cell*, 138(5), pp.838-854.

Lambert, A., Pattabiraman, D. & Weinberg, R. (2017). Emerging Biological Principles of Metastasis. *Cell*, 168(4), pp.670-691.

Lambrechts, A., Van Troys, M. & Ampe, C. (2004). The actin cytoskeleton in normal and pathological cell motility. *The International Journal of Biochemistry & Cell Biology*, 36(10), pp.1890-1909.

Lee, H., Lin, E., Liu, L. & Smith, J. (2003). Gene expression profiling of tumor xenografts:In vivo analysis of organ-specific metastasis. *International Journal of Cancer*, 107(4), pp.528-534.

Lee, H., Park, Y., Lee, S., Cho, H., Kim, D., Lee, J., Kang, M., Seol, H., Shim, Y., Nam, D., Kim, H. & Joo, K. (2013). Alpha-Smooth Muscle Actin (ACTA2) Is Required for Metastatic Potential of Human Lung Adenocarcinoma. *Clinical Cancer Research*, 19(21), pp.5879-5889.

Leung, L. & Wang, T. (1999). Differential effects of chemotherapeutic agents on the Bcl-2/Bax apoptosis pathway in human breast cancer cell line MCF-7. *Breast Cancer Research and Treatment*, 55(1), pp.73-83.

Li, J., Deng, M., Wei, Q., Liu, T., Tong, X. & Ye, X. (2011). Phosphorylation of MCM3 Protein by Cyclin E/Cyclin-dependent Kinase 2 (Cdk2) Regulates Its Function in Cell Cycle. *Journal of Biological Chemistry*, 286(46), pp.39776-39785.

Li, Z., Yin, S., Zhang, L., Liu, W. & Chen, B. (2017). Prognostic value of reduced E-cadherin expression in breast cancer: a meta-analysis. *Oncotarget*, 8(10).

Liu, X. & Chu, K. (2014). E-Cadherin and Gastric Cancer: Cause, Consequence, and Applications. *BioMed Research International*, 2014, pp.1-9.

Lu, Z. & Xu, S. (2006). ERK1/2 MAP kinases in cell survival and apoptosis. *IUBMB Life (International Union of Biochemistry and Molecular Biology: Life)*, 58(11), pp.621-631.

Lühr, I., Friedl, A., Overath, T., Tholey, A., Kunze, T., Hilpert, F., Sebens, S., Arnold, N., Rösel, F., Oberg, H., Maass, N., Mundhenke, C., Jonat, W. & Bauer, M. (2012). Mammary fibroblasts regulate morphogenesis of normal and tumorigenic breast epithelial cells by mechanical and paracrine signals. *Cancer Letters*, 325(2), pp.175-188.

Lüpertz, R., Wätjen, W., Kahl, R. & Chovolou, Y. (2010). Dose- and time-dependent effects of doxorubicin on cytotoxicity, cell cycle and apoptotic cell death in human colon cancer cells. *Toxicology*, 271(3), pp.115-121.

Lyons, W. (1958). Hormonal synergism in mammary growth. *Proceedings of the Royal Society of London. Series B - Biological Sciences*, 149(936), pp.303-325.

Manning, B. & Toker, A. (2017). AKT/PKB Signaling: Navigating the Network. *Cell*, 169(3), pp.381-405.

Martin, S. & Green, D. (1995). Protease activation during apoptosis: Death by a thousand cuts?. *Cell*, 82(3), pp.349-352.

Mareel, M. & Constantino, S. (2011). Ecosystems of invasion and metastasis in mammary morphogenesis and cancer. *The International Journal of Developmental Biology*, 55(7-8-9), pp.671-684.

Masszi, A., Di Ciano, C., Sirokmány, G., Arthur, W., Rotstein, O., Wang, J., McCulloch, C., Rosivall, L., Mucsi, I. & Kapus, A. (2003). Central role for Rho in TGF-β1-induced α-smooth muscle actin expression during epithelial-mesenchymal transition. *American Journal of Physiology-Renal Physiology*, 284(5), pp.F911-F924.

McCubrey, J., Steelman, L., Chappell, W., Abrams, S., Wong, E., Chang, F., Lehmann, B., Terrian, D., Milella, M., Tafuri, A., Stivala, F., Libra, M., Basecke, J., Evangelisti, C., Martelli, A. & Franklin, R. (2007). Roles of the Raf/MEK/ERK pathway in cell growth, malignant transformation and drug resistance. *Biochimica et Biophysica Acta (BBA) - Molecular Cell Research*, 1773(8), pp.1263-1284.

McLean, J., Moylan, J. & Andrade, F. (2014). Mitochondria dysfunction in lung cancer-induced muscle wasting in C2C12 myotubes. *Frontiers in Physiology*, 5:503.

Melguizo, C., Cabeza, L., Prados, J., Ortiz, R., Caba, O., Rama, A., Delgado, A. & Arias, J. (2015). Enhanced antitumoral activity of doxorubicin against lung cancer cells using biodegradable poly(butylcyanoacrylate) nanoparticles. *Drug Design, Development and Therapy*, p.6433.

Min, K., Kwon, O., Smuder, A., Wiggs, M., Sollanek, K., Christou, D., Yoo, J., Hwang, M., Szeto, H., Kavazis, A. & Powers, S. (2015). Increased mitochondrial emission of reactive oxygen species and calpain activation are required for doxorubicin-induced cardiac and skeletal muscle myopathy. *The Journal of Physiology*, 593(8), pp.2017-2036.

Minotti, G., Menna, P., Salvatorelli, E., Cairo, G. & Gianni, L. (2004). Anthracyclines: Molecular Advances and Pharmacologic Developments in Antitumor Activity and Cardiotoxicity. *Pharmacological Reviews*, 56(2), pp.185-229.

Mitchell, M. (2018). *Metabolic reprograming and cancer resistance: an investigation into the metabolic control of cancer-associated fibroblasts on breast cancer cell survival and metastasis*. Ph.D. Stellenbosch University.

Monks, J., Smith-Steinhart, C., Kruk, E., Fadok, V. & Henson, P. (2008). Epithelial Cells Remove Apoptotic Epithelial Cells During Post-Lactation Involution of the Mouse Mammary Gland1. *Biology of Reproduction*, 78(4), pp.586-594.

Moritani, M. & Ishimi, Y. (2013). Inhibition of DNA binding of MCM2-7 complex by phosphorylation with cyclin-dependent kinases. *The Journal of Biochemistry*, 154(4), pp.363-372.

Morrison, D. (2012). MAP Kinase Pathways. *Cold Spring Harbor Perspectives in Biology*, 4(11), pp.a011254-a011254.

Nakano, H., Shindo, M., Sakon, S., Nishinaka, S., Mihara, M., Yagita, H. & Okumura, K. (1998). Differential regulation of I B kinase and by two upstream kinases, NF- B-inducing kinase and mitogen-activated protein kinase/ERK kinase kinase-1. *Proceedings of the National Academy of Sciences*, 95(7), pp.3537-3542.

National Cancer Institute. (2015). *What Is Cancer?*. [online] Available at: https://www.cancer.gov/about-cancer/understanding/what-is-cancer?redirect=true [Accessed 10 Sep. 2018].

Nelson, C., VanDuijn, M., Inman, J., Fletcher, D. & Bissell, M. (2006). Tissue Geometry Determines Sites of Mammary Branching Morphogenesis in Organotypic Cultures. *Science*, 314(5797), pp.298-300.

New Zealand Medicines and Medical Devices Safety Authority. (2014). *ADRIAMYCIN®*. [online] Available at: https://medsafe.govt.nz/Profs/datasheet/a/adriamycininj.pdf [Accessed 24 Dec. 2018].

Nicholson, K. & Anderson, N. (2002). The protein kinase B/Akt signalling pathway in human malignancy. *Cellular Signalling*, 14(5), pp.381-395.

Nieto, M. (2002). The snail superfamily of zinc-finger transcription factors. *Nature Reviews Molecular Cell Biology*, 3(3), pp.155-166.

Nishida, K., Yamaguchi, O. & Otsu, K. (2008). Crosstalk Between Autophagy and Apoptosis in Heart Disease. *Circulation Research*, 103(4), pp.343-351.

Ouyang, L., Shi, Z., Zhao, S., Wang, F., Zhou, T., Liu, B. & Bao, J. (2012). Programmed cell death pathways in cancer: a review of apoptosis, autophagy and programmed necrosis. *Cell Proliferation*, 45(6), pp.487-498.

Peinado, H., Olmeda, D. & Cano, A. (2007). Snail, Zeb and bHLH factors in tumour progression: an alliance against the epithelial phenotype?. *Nature Reviews Cancer*, 7(6), pp.415-428.

Peiris-Pagès, M., Martinez-Outschoorn, U., Pestell, R., Sotgia, F. & Lisanti, M. (2016). Cancer stem cell metabolism. *Breast Cancer Research*, 18(1).

Pouysségur, J., Volmat, V. & Lenormand, P. (2002). Fidelity and spatio-temporal control in MAP kinase (ERKs) signalling. *Biochemical Pharmacology*, 64(5-6), pp.755-763.

Reed, J. (1994). Bcl-2 and the regulation of programmed cell death. *The Journal of Cell Biology*, 124(1), pp.1-6.

Renehan, A., Booth, C. & Potten, C. (2001). What is apoptosis, and why is it important?. *British Medical Journal*, 322(7301), pp.1536-1538.

Renshaw, M., Ren, X. & Schwartz, M. (1997). Growth factor activation of MAP kinase requires cell adhesion. *The EMBO Journal*, 16(18), pp.5592-5599.

Riss, T., Moravec, R., Niles, A., Duellman, S., Benink, H., Worzella, T. & Minor, L. (2004). Cell Viability Assays. In: G. Sittampalam, N. Coussens and K. Brimacombe, ed., *Assay Guidance Manual*. [online] Eli Lilly & Company and the National Center for Advancing Translational Sciences. Available at: https://www.ncbi.nlm.nih.gov/books/NBK144065/ [Accessed 24 Aug. 2018].

Robinson, B., Sica, G., Liu, Y., Rohan, T., Gertler, F., Condeelis, J & Jones, J. (2009) Tumor microenvironment of metastasis in human breast carcinoma: A potential prognostic marker linked to hematogenous dissemination. Clinical Cancer Research 15, 2433–2441.

Rodriguez-Viciana, P., Marte, B., Warne, P. & Downward, J. (1996). Phosphatidylinositol 3' kinase: one of the effectors of Ras. *Philosophical Transactions of the Royal Society of London. Series B: Biological Sciences*, 351(1336), pp.225-232.

Russo, J., Tay, L. & Russo, I. (1982). Differentiation of the mammary gland and susceptibility to carcinogenesis. *Breast Cancer Research and Treatment*, 2(1), pp.5-73.

Sakakura, T., Nishizuka, Y. & Dawe, C. (1976). Mesenchyme-dependent morphogenesis and epithelium-specific cytodifferentiation in mouse mammary gland. *Science*, 194(4272), pp.1439-1441.

Sarnat, H. (1992). Vimentin and desmin in maturing skeletal muscle and developmental myopathies. *Neurology*, 42(8), pp.1616-1616.

Satelli, A. & Li, S. (2011). Vimentin in cancer and its potential as a molecular target for cancer therapy. *Cellular and Molecular Life Sciences*, 68(18), pp.3033-3046.

Sawada, K., Mitra, A., Radjabi, A., Bhaskar, V., Kistner, E., Tretiakova, M., Jagadeeswaran, S., Montag, A., Becker, A., Kenny, H., Peter, M., Ramakrishnan, V., Yamada, S. & Lengyel, E. (2008). Loss of E-Cadherin Promotes Ovarian Cancer Metastasis via 5-Integrin, which Is a Therapeutic Target. *Cancer Research*, 68(7), pp.2329-2339.

Scaffidi, C., Schmitz, I., Krammer, P. & Peter, M. (1999). The Role of c-FLIP in Modulation of CD95-induced Apoptosis. *Journal of Biological Chemistry*, 274(3), pp.1541-1548.

Schiaffino, S. & Reggiani, C. (2011). Fiber Types in Mammalian Skeletal Muscles. *Physiological Reviews*, 91(4), pp.1447-1531.

Schindelin, J., Arganda-Carreras, I., Frise, E., Kaynig, V., Longair, M., Pietzsch, T., Preibisch, S., Rueden, C., Saalfeld, S., Schmid, B., Tinevez, J., White, D., Hartenstein, V., Eliceiri, K., Tomancak, P. & Cardona, A. (2012). Fiji: an open-source platform for biological-image analysis. *Nature Methods*, 9(7), pp.676-682.

Shamas-Din, A., Brahmbhatt, H., Leber, B. & Andrews, D. (2011). BH3-only proteins: Orchestrators of apoptosis. *Biochimica et Biophysica Acta (BBA) - Molecular Cell Research*, 1813(4), pp.508-520.

Shaw, R. & Cantley, L. (2006). Ras, PI(3)K and mTOR signalling controls tumour cell growth. *Nature*, 441(7092), pp.424-430.

Shepherd, G. (2003). Hypersensitivity Reactions to Chemotherapeutic Drugs. *Clinical Reviews in Allergy & Immunology*, 24(3), pp.253-262.

Sherr, C. (1996). Cancer Cell Cycles. *Science*, 274(5293), pp.1672-1677.

Sherwood, L. (2013). *Introduction to Human Physiology*. 8th ed. International Edition: Y. Cossio.

Shi, Y., Moon, M., Dawood, S., McManus, B. & Liu, P. (2011). Mechanisms and management of doxorubicin cardiotoxicity. *Herz*, 36(4), pp.296-305.

Sishi, B., Loos, B., van Rooyen, J. & Engelbrecht, A. (2013). Autophagy upregulation promotes survival and attenuates doxorubicin-induced cardiotoxicity. *Biochemical Pharmacology*, 85(1), pp.124-134.

Shou, J., Massarweh, S., Osborne, C., Wakeling, A., Ali, S., Weiss, H. & Schiff, R. (2004). Mechanisms of Tamoxifen Resistance: Increased Estrogen Receptor-HER2/neu Cross-Talk in ER/HER2-Positive Breast Cancer. *JNCI Journal of the National Cancer Institute*, 96(12), pp.926-935.

Silberstein, G. & Daniel, C. (1982). Glycosaminoglycans in the basal lamina and extracellular matrix of the developing mouse mammary duct. *Developmental Biology*, 90(1), pp.215-222.

Singh, A. & Settleman, J. (2010). EMT, cancer stem cells and drug resistance: an emerging axis of evil in the war on cancer. *Oncogene*, 29(34), pp.4741-4751.

Sommers, C., Byers, S., Thompson, E., Torri, J. & Gelmann, E. (1994). Differentiation state and invasiveness of human breast cancer cell lines. *Breast Cancer Research and Treatment*, 31(2-3), pp.325-335.

Stead, B., Brandl, C., Sandre, M. & Davey, M. (2012). Mcm2 phosphorylation and the response to replicative stress. *BMC Genetics*, 13(1), p.36.

Sternlicht, M. (2006). Key stages in mammary gland development: The cues that regulate ductal branching morphogenesis. *Breast Cancer Research*, 8(1).201.

Steelman, L., Bertrand, F. & McCubrey, J. (2004). The complexity of PTEN: mutation, marker and potential target for therapeutic intervention. *Expert Opinion on Therapeutic Targets*, 8(6), pp.537-550.

Surov, A., Hainz, M., Holzhausen, H., Arnold, D., Katzer, M., Schmidt, J., Spielmann, R. & Behrmann, C. (2009). Skeletal muscle metastases: primary tumours, prevalence, and radiological features. *European Radiology*, 20(3), pp.649-658.

Tacar, O., Sriamornsak, P. & Dass, C. (2012). Doxorubicin: an update on anticancer molecular action, toxicity and novel drug delivery systems. *Journal of Pharmacy and Pharmacology*, 65(2), pp.157-170.

Taherian, A. & Mazoochi, T. (2012). Different Expression of Extracellular Signal-Regulated Kinases (ERK) 1/2 and Phospho-Erk Proteins in MBA-MB-231 and MCF-7 Cells after Chemotherapy with Doxorubicin or Docetaxel. *Iranian Journal of Basic Medical Sciences*, 15(1), pp.669-677.

Taylor, V., Wong, M., Brandts, C., Reilly, L., Dean, N., Cowsert, L., Moodie, S. & Stokoe, D. (2000). 5' Phospholipid Phosphatase SHIP-2 Causes Protein Kinase B Inactivation and Cell Cycle Arrest in Glioblastoma Cells. *Molecular and Cellular Biology*, 20(18), pp.6860-6871.

Thiery, J. (2002). Epithelial–mesenchymal transitions in tumour progression. *Nature Reviews Cancer*, 2(6), pp.442-454.

Tisdale, M. (2009). Mechanisms of Cancer Cachexia. *Physiological Reviews*, 89(2), pp.381-410.

Tozer, R., Tai, P., Falconer, W., Ducruet, T., Karabadjian, A., Bounous, G., Molson, J. & Dröge, W. (2008). Cysteine-Rich Protein Reverses Weight Loss in Lung Cancer Patients Receiving Chemotherapy or Radiotherapy. *Antioxidants & Redox Signaling*, 10(2), pp.395-402.

Tsuji, T., Ibaragi, S. & Hu, G. (2009). Epithelial-Mesenchymal Transition and Cell Cooperativity in Metastasis. *Cancer Research*, 69(18), pp.7135-7139.

Tubbs, A. & Nussenzweig, A. (2017). Endogenous DNA Damage as a Source of Genomic Instability in Cancer. *Cell*, 168(4), pp.644-656.

Tudzarova, S., Mulholland, P., Dey, A., Stoeber, K., Okorokov, A. & Williams, G. (2016). p53 controls CDC7 levels to reinforce G1 cell cycle arrest upon genotoxic stress. *Cell Cycle*, 15(21), pp.2958-2972.

Tzika, A., Fontes-Oliveira, C., Shestov, A., Constantinou, C., Psychogios, N., Righi, V., Mintzopoulos, D., Busquets, S., Lopez-Soriano, F., Milot, S., Lepine, F., Mindrinos, M., Rahme, L. & Argiles, J. (2013). Skeletal muscle mitochondrial uncoupling in a murine cancer cachexia model. *International Journal of Oncology*, 43(3), pp.886-894.

Umbas, R., Isaacs, W., Bringuier, P., Xue, Y., Debruyne, F. & Schalken, J. (1997). Relation between aberrant α-catenin expression and loss of E-cadherin function in prostate cancer. *International Journal of Cancer*, 74(4), pp.374-377.

VanHook, A. (2014). Proliferation or Differentiation Depends on ERK Localization. *Science Signaling*, 7(333), pp.ec187-ec187.

Velikova, G., Banks, R., Gearing, A., Hemingway, I., Forbes, M., Preston, S., Hall, N., Jones, M., Wyatt, J., Miller, K., Ward, U., Al-Maskatti, J., Singh, S., Finan, P., Ambrose, N., Primrose, J. & Selby, P. (1998). Serum concentrations of soluble adhesion molecules in patients with colorectal cancer. *British Journal of Cancer*, 77(11), pp.1857-1863.

Volkova, M. & Russell, R. (2011). Anthracycline Cardiotoxicity: Prevalence, Pathogenesis and Treatment. *Current Cardiology Reviews*, 7(4), pp.214-220.

Vuoriluoto, K., Haugen, H., Kiviluoto, S., Mpindi, J., Nevo, J., Gjerdrum, C., Tiron, C., Lorens, J. & Ivaska, J. (2010). Vimentin regulates EMT induction by Slug and oncogenic H-Ras and migration by governing Axl expression in breast cancer. *Oncogene*, 30(12), pp.1436-1448.

Wang, C., Mayo, M. & Baldwin, A. (1996). TNF- and Cancer Therapy-Induced Apoptosis: Potentiation by Inhibition of NF-kappa B. *Science*, 274(5288), pp.784-787.

Wang, Y., Shi, J., Chai, K., Ying, X. & Zhou, B. (2013). The Role of Snail in EMT and Tumorigenesis. *Current Cancer Drug Targets*, 13(9), pp.963-972.

Wang, Y., Wang, Y., Tay, Y. & Harris, D. (2000). Progressive adriamycin nephropathy in mice: Sequence of histologic and immunohistochemical events. *Kidney International*, 58(4), pp.1797-1804.

Wang, G., Wang, Y., Zhou, X. & Korth, M. (2001). Effects of doxorubicinol on excitation–contraction coupling in guinea pig ventricular myocytes. *European Journal of Pharmacology*, 423(2-3), pp.99-107.

Weinstein-Oppenheimer, C., Henriquez-Roldan, C., Davis, J., Navolanic, P., Saleh, O., Steelman, L., Franklin, R., Robinson, P., McMahon, M. & McCubrey, J. (2001). Role of the Raf signal transduction cascade in the in vitro resistance to the anticancer drug doxorubicin. *Clinical Cancer Research*, 7(9), pp.2898-2907.

Weir, G., Liwski, R. & Mansour, M. (2011). Immune Modulation by Chemotherapy or Immunotherapy to Enhance Cancer Vaccines. *Cancers*, 3(3), pp.3114-3142.

Williams, J. & Daniel, C. (1983). Mammary ductal elongation: Differentiation of myoepithelium and basal lamina during branching morphogenesis. *Developmental Biology*, 97(2), pp.274-290.

Wong, S., Fang, C., Chuah, L., Leong, C. & Ngai, S. (2018). E-cadherin: Its dysregulation in carcinogenesis and clinical implications. *Critical Reviews in Oncology/Hematology*, 121, pp.11-22.

Wu, X., Senechal, K., Neshat, M., Whang, Y. & Sawyers, C. (1998). The PTEN/MMAC1 tumor suppressor phosphatase functions as a negative regulator of the phosphoinositide 3-kinase/Akt pathway. *Proceedings of the National Academy of Sciences*, 95(26), pp.15587-15591.

Wu, Y., Zhang, X., Salmon, M., Lin, X. & Zehner, Z. (2007). TGFβ1 regulation of vimentin gene expression during differentiation of the C2C12 skeletal myogenic cell line requires Smads, AP-1 and Sp1 family members. *Biochimica et Biophysica Acta (BBA) - Molecular Cell Research*, 1773(3), pp.427-439.

Xiao, X., Grove, K. & Smith, M. (2004). Metabolic Adaptations in Skeletal Muscle during Lactation: Complementary Deoxyribonucleic Acid Microarray and Real-Time Polymerase Chain Reaction Analysis of Gene Expression. *Endocrinology*, 145(11), pp.5344-5354.

Yamaguchi, K., Shirakabe, K., Shibuya, H., Irie, K., Oishi, I., Ueno, N., Taniguchi, T., Nishida, E. & Matsumoto, K. (1995). Identification of a Member of the MAPKKK Family as a Potential Mediator of TGF-beta Signal Transduction. *Science*, 270(5244), pp.2008-2011.

Yang, E., Zha, J., Jockel, J., Boise, L., Thompson, C. & Korsmeyer, S. (1995). Bad, a heterodimeric partner for Bcl-xL and Bcl-2, displaces bax and promotes cell death. *Cell*, 80(2), pp.285-291.

Ye, H., Karim, A. & Loh, X. (2014). Current treatment options and drug delivery systems as potential therapeutic agents for ovarian cancer: A review. *Materials Science and Engineering: C*, 45, pp.609-619.

Yee, K., Weaver, V. & Hammer, D. (2008). Integrin-mediated signalling through the MAP-kinase pathway. *IET Systems Biology*, 2(1), pp.8-15.

Yeeles, J., Deegan, T., Janska, A., Early, A. & Diffley, J. (2015). Regulated eukaryotic DNA replication origin firing with purified proteins. *Nature*, 519(7544), pp.431-435.

Yu, M., Bardia, A., Wittner, B., Stott, S., Smas, M., Ting, D., Isakoff, S., Ciciliano, J., Wells, M., Shah, A., Concannon, K., Donaldson, M., Sequist, L., Brachtel, E., Sgroi, D., Baselga, J., Ramaswamy, S., Toner, M., Haber, D. & Maheswaran, S. (2013). Circulating Breast Tumor Cells Exhibit Dynamic Changes in Epithelial and Mesenchymal Composition. *Science*, 339(6119), pp.580-584.

Zeisberg, M. & Neilson, E. (2009). Biomarkers for epithelial-mesenchymal transitions. *Journal of Clinical Investigation*, 119(6), pp.1429-1437.

Zeisberg, M., Shah, A. & Kalluri, R. (2004). Bone Morphogenic Protein-7 Induces Mesenchymal to Epithelial Transition in Adult Renal Fibroblasts and Facilitates Regeneration of Injured Kidney. *Journal of Biological Chemistry*, 280(9), pp.8094-8100.

Zhang, J., Wang, X., Vikash, V., Ye, Q., Wu, D., Liu, Y. & Dong, W. (2016). ROS and ROS-Mediated Cellular Signaling. *Oxidative Medicine and Cellular Longevity*, pp.1-18.

Zhang, L., Zhou, F. & ten Dijke, P. (2013). Signaling interplay between transforming growth factor-β receptor and PI3K/AKT pathways in cancer. *Trends in Biochemical Sciences*, 38(12), pp.612-620.

Zheng, Z., Pavlidis, P., Chua, S., D'Agati, V. & Gharavi, A. (2006). An Ancestral Haplotype Defines Susceptibility to Doxorubicin Nephropathy in the Laboratory Mouse. *Journal of the American Society of Nephrology*, 17(7), pp.1796-1800.

Zhu, F., Zykova, T., Kang, B., Wang, Z., Ebeling, M., Abe, Y., Ma, W., Bode, A. & Dong, Z. (2007). Bidirectional Signals Transduced by TOPK-ERK Interaction Increase Tumorigenesis of HCT116 Colorectal Cancer Cells. *Gastroenterology*, 133(1), pp.219-231.

Appendix A – Supplementary Data

Caspase 3 expression in myotubes:

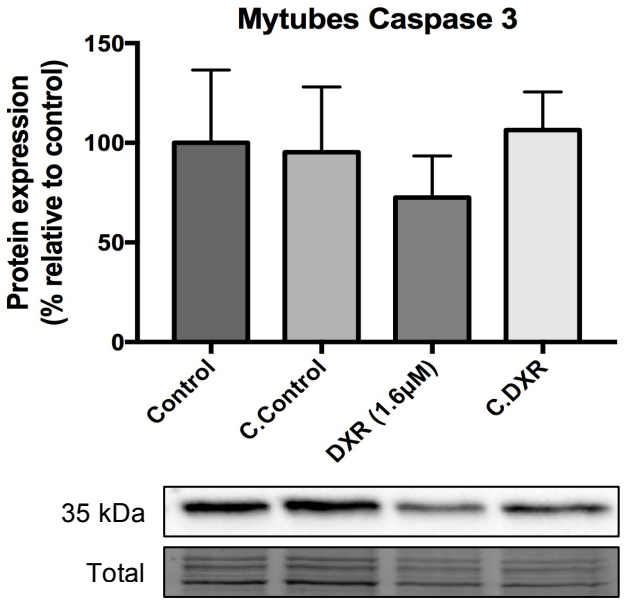

Figure A: Protein expression of Total Caspase 3 from western blot analysis after 24-hour treatment of myotubes. Myotubes were treated for 24-hours as Control, C.Control, DXR consisting of 1.6μM DXR, and C.DXR. Values expressed as percentage (%) of control with statistical representation as mean ±SEM with n = 3.

PARP expression in myotubes:

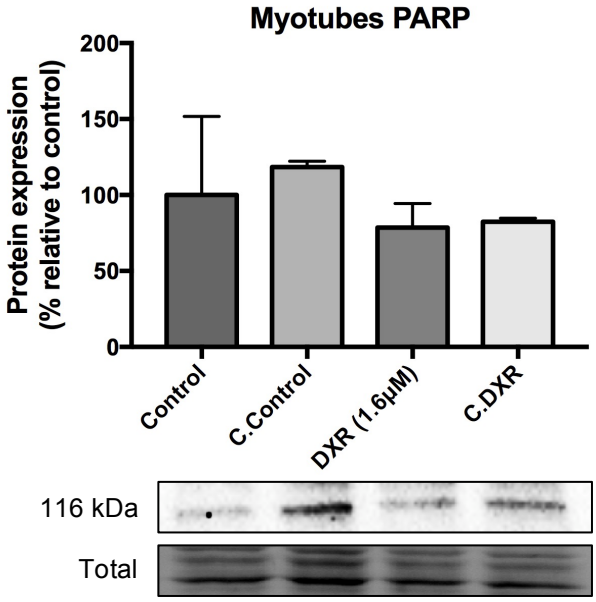

Figure B: Protein expression of Total PARP from western blot analysis after 24-hour treatment of myotubes. Myotubes were treated for 24-hours as Control, C.Control, DXR consisting of 1.6μM DXR, and C.DXR. Values expressed as percentage (%) of control with statistical representation as mean ±SEM with n = 3.

p62 expression in myotubes:

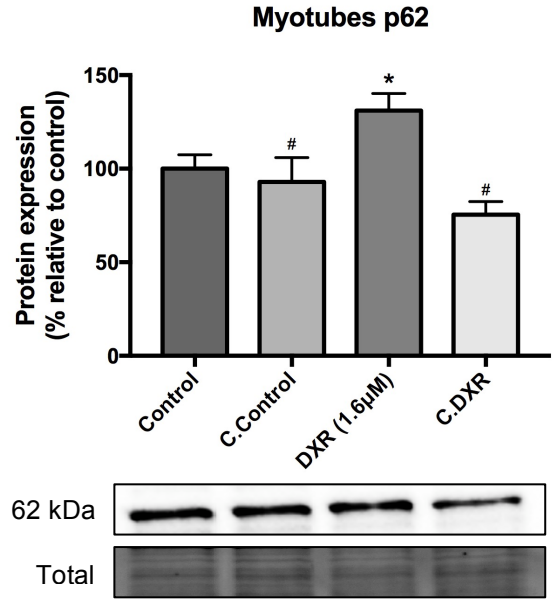

Figure C: Protein expression of p62 from western blot analysis after 24-hour treatment of myotubes. Myotubes were treated for 24-hours as Control, C.Control, DXR consisting of 1.6μM DXR, and C.DXR. Values expressed as percentage (%) of control with statistical representation as mean ±SEM with n = 3. *p<0.05 compared to Control, #p<0.05 compared to DXR.

LC3 expression in myotubes:

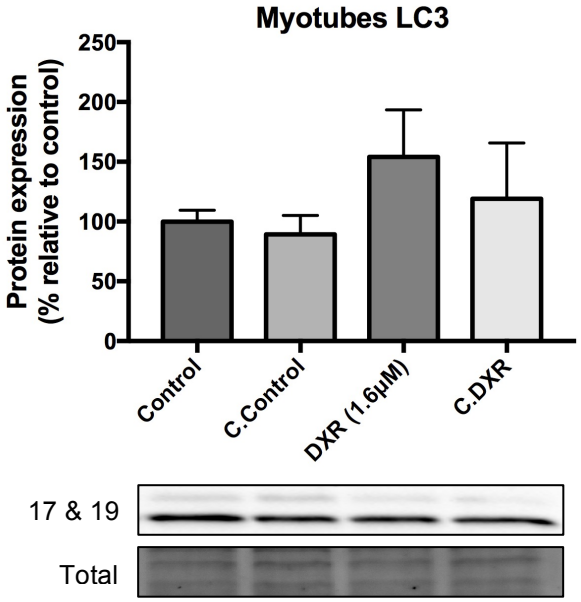

Figure D: Protein expression of LC3 from western blot analysis after 24-hour treatment of myotubes. Myotubes were treated for 24-hours as Control, C.Control, DXR consisting of 1.6μM DXR, and C.DXR. Values expressed as percentage (%) of control with statistical representation as mean ±SEM with n = 3.

Differentiation Media ratio's on E0771 cells:

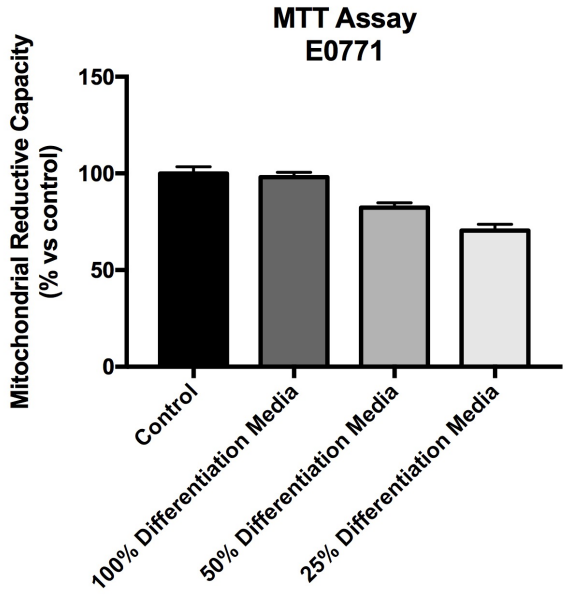

Figure E: MTT cell viability assay completed on E0771 cells with variety of concentrations of differentiation media. Control consists of 50% serum free media and 50% FBS containing media, 100% differentiation media consist of only differentiation media, 50% differentiation media consists of 50% serum free media and 50% differentiation media, and 25% differentiation media consists of 25% differentiation media, 25% FBS containing media and 50% serum free media.

α-Smooth Muscle Actin expression in myotubes:

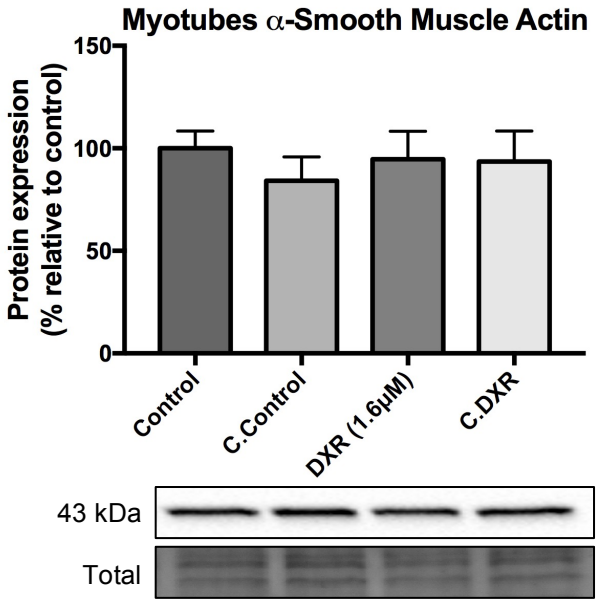

Figure F: Protein expression of α-Smooth Muscle Actin from western blot analysis after 24-hour treatment of myotubes. Myotubes were treated for 24-hours as Control, C.Control, DXR consisting of 1.6μM DXR, and C.DXR. Values expressed as percentage (%) of control with statistical representation as mean ±SEM with n = 3.

Vimentin expression in myotubes:

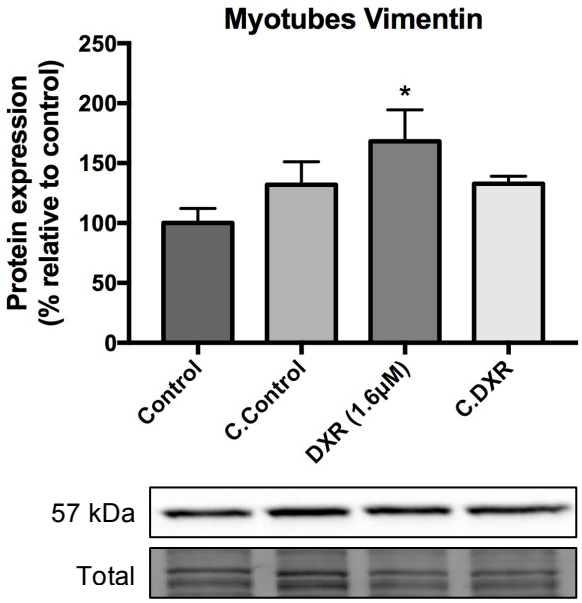

Figure G: Protein expression of Vimentin from western blot analysis after 24-hour treatment of myotubes. Myotubes were treated for 24-hours as Control, C.Control, DXR consisting of 1.6μM DXR, and C.DXR. Values expressed as percentage (%) of control with statistical representation as mean ±SEM with n = 3. *p<0.05 compared to Control.

Appendix B - Reagents

Table 1: Cell Culture Reagents

Reagent Name	Company Produced	Company Purchased	Cat #
Dulbecco's Modified Eagle's Medium	Gibco® by Life Technologies™	ThermoFisher Scientific®	#41965-062
Fetal Bovine Serum	Capricorn Scientific®	ThermoFisher Scientific®	#FBS-G1-12A
Penicillin-Streptomycin	Gibco® by Life Technologies™	ThermoFisher Scientific®	#15140-122
0.25% Trypsin-EDTA	Gibco® by Life Technologies™	ThermoFisher Scientific®	#25200072
Horse Serum	Lonza	BioWhittaker®	#14-403F
Doxorubicin	Lasec®	Lasec®	#FLAS25AC2050
MTT Powder	Sigma-Aldrich®	Sigma-Aldrich®	#M2003
Mitomycin C	Sigma-Aldrich®	Sigma-Aldrich®	#M4287
DMSO	Sigma-Aldrich®	Sigma-Aldrich®	#D2650
Cell tracker™ Green	Invitrogen™	ThermoFisher Scientific®	#C2925
Hoechst 33342	Sigma-Aldrich®	Sigma-Aldrich®	#B2261
Dako Fluorescent Mounting Media	Dako	Diagnostech®	#S302380
MitoSOX™	Invitrogen™	ThermoFisher Scientific®	#M36009

Table 2: General Reagents

Reagent Name	Company	Cat #
β-Mercaptoethanol	Sigma-Aldrich®	#M3148
APS	Sigma-Aldrich®	#A3678-25G
Bovine Serum Albumin (BSA)	Roche	#10735078001
Bromophenol Blue	Merck®	#SAAR1437500CB
Coomassie Brilliant Blue G	Sigma-Aldrich®	#27815-25G
Glycine	Merck®	#357002-1KG
EDTA	Sigma-Aldrich®	#EDS-100G
EGTA	Sigma-Aldrich®	#E-0396
Nonyl phenoxypolyethoxylethanol (NP-40)	Sigma-Aldrich®	#74385-1L
Phenylmethylsulfonyl Flouoride (PMSF)	Sigma-Aldrich®	#93482-50ml-F
Protease inhibitor Cocktail	Roche	#11893580001
Sodium chloride (NaCl)	Merck®	#1.06404
Sodium deoxycholate	Sigma-Aldrich®	#D6750-100G
Sodium dodecyl sulfate (SDS)	Sigma-Aldrich®	#L3771
Sodium fluoride (NaF)	Merck®	#193270
Sodium orthovanadate (Na_3VO_4)	Sigma-Aldrich®	#56508
TCE	Sigma-Aldrich®	#T54801
TEMED	Merck®	#1.10732.0100
Tris-base	Merck®	#648310
Triton-X	Sigma-Aldrich®	#X100
Tween-20	Sigma-Aldrich®	#P1379

Table 3: General Chemicals

Chemical Name	Company	Cat #
Ethanol	Protea Chemicals	#2207101022
Glycerol	Merck®	#SAAR2676520
Hydrochloric acid	Merck®	#SAAR3063040LP
Methanol	Merck®	#1.06009.2500
Phosphoric Acid	Merck®	#1.00573.2500
Propan-2-ol (Isopropanol)	Merck®	#SAAR5075040LC

Table 4: Protein Extraction & Western Blot Reagents

Reagent Name	Company	Cat #
Acrylamide (40%)	Merck®	#100640
Bio-Rad® Enhanced Chemiluminescence (ECL)	Bio-Rad®	#1705061
Bio-Rad® FastCast Gel Kit	Bio-Rad®	#1610185
Bio-Rad® RTA Midi PVDF Transfer Kit	Bio-Rad®	#1704273
BLUeye Prestained Protein Ladder	Biocom Biotech®	#PM007-0500

Table 5: Antibodies

Antibody Name	Company	Cat #
α-Smooth Muscle Actin	Abcam®	#ab7817
AKT	Cell Signalling Technology®	#9272
Anti-Mouse	Cell Signalling Technology®	#7076S
Anti-Rabbit	Cell Signalling Technology®	#7074S
Caspase 3 & Cleaved Caspase 3	Cell Signalling Technology®	#9662
E-cadherin	Cell Signalling Technology®	#14472
ERK 1 & ERK 2	Abcam®	#ab184699
MCM2	Abcam®	#ab108935
PARP & Cleaved PARP	Cell Signalling Technology®	#9532
Phosphorylated AKT (ser473)	Cell Signalling Technology®	#4060
Phosphorylated ERK 1 & ERK 2 (Thr202/Tyr204)	Cell Signalling Technology®	#4370
SNAIL	Cell Signalling Technology®	#3879
Vimentin	Cell Signalling Technology®	#5741

Appendix C – Reagent Protocols

1) Complete media

- 455mL DMEM
- 50mL FBS (10%)
- 5mL PenStrep (1%)

Store at 4°C

2) Differentiation media

- 455mL DMEM
- 5mL Horse serum (1%)
- 5mL PenStrep (1%)

Store at 4°C

3) Isoproponal/Triton-X solution (50:1):

Acidic Isoproponal

- 99mL Isoproponal
- 1mL concentrated HCl

Triton-X

- 0.1mL Triton-X
- 100mL dH_20

Isoproponal/Triton-X solution (50:1)

- 50mL 1% acidic Isoproponal
- 1mL 1% Triton-X

Store at RT

4) MTT solution (per well):

Light sensitive – keep MTT solution covered and switch off lights

- Dissolve MTT in PBS to 0.01g/mL
- Add remaining PBS (3 fold)
- Final ratio of 1:3 - [0.01g MTT/mL PBS] : [PBS]]

5) PBS

- 16.001g of NaCl
- 0.400g of KCl
- 2.882g of Na_2HPO_4
- 0.481g of KH_2PO_4
- Dissolve in 1.8L of dH_2O
- Adjust pH to 7.4
- Fill up till 2L
- Autoclaved PBS

Store at RT

6) 100mM EDTA:

- 1.4612g EDTA
- 50 mL dH_20
- Set to pH 8 to dissolve

Store at RT

7) 100mM EGTA:

- 1.90175g EGTA
- 50 mL dH_20
- Set to pH 8 to dissolve

Store at RT

8) 10% SDS:

- 50g SDS
- Make up to 500mL with dH_2O
- Heat slightly to dissolve

9) Modified RIPA Buffer (100mL):

To 50mL dH20

- 790mg Tris-base [± 65mM]
- 900mg NaCl [± 154mM]
- Stir until dissolved
- Adjust to pH 7.4
- 10mL of 10% NP-40 [1%]
- 10mL of 10% Na-deoxycholate [1%]
- Stir until solution is clear
- 5mL of 100mM EDTA [± 5mM]
- 5mL of 100mM EGTA [± 5mM]
- 1mL of 10% SDS [0.1%]
- Adjust to 100mL

Aliquot and store in fridge

Before use, add the following to 1 mL RIPA buffer:

- 42µl Protease Inhibitors Cocktail
- 5µl 200mM Na3VO4 [final 1mM]
- 5µl 200mM NaF [final 1mM]
- 5µl 200mM Phenylmethylsulfonyl Flouoride (PMSF) [final 1mM] (**Add last!** Very unstable in aqueous solutions)

10) Bradford Reagent (5X)

- Dissolve 500mg Coomassie Brilliant Blue G-250 in 250 mL 95% ethanol
- Add 500 mL Phosphoric acid and mix thoroughly
- Make up to 1L with dH_2O
- Filter and store @ 4°C

11) Bradford Working Solution

- Dilute stock in 1:4 ratio with dH_2O
- Filter using 2 filter papers at the same time, until solution is a light brown colour

Store at RT

12) Laemli's Sample Buffer (Stock Solution) (225mL)

- Dissolve 9.09g Tris in 100 mL dH20
- Add 6 mL 10% SDS, stir
- Set to pH 6.8 with HCl
- Make up to 150 mL dH_20
- In a glass beaker (not too small, approx. 400 mL) weigh off 60g glycerol
- Add 99.9 mL of the above solution to glycerol
- Add 26.4g SDS, dissolve thoroughly
- Add 0.225g Bromophenol Blue, dissolve thoroughly
- Make up to final volume of 225 mL with dH_20

Store at RT

13) Laemli's Sample Buffer (Working Solution) (1mL)

Prepare in fumehood

- 150ul β-mercaptoethanol
- 850ul sample buffer

Final concentrations when adding sample buffer to sample in ratio of 1:2

- 62.5mM Tris, pH 6.8
- 4% SDS
- 10% Glycerol
- 0.03% Bromophenol Blue
- 5% β-mercaptoethanol

Store at RT

14) 1.5M Tris-HCl pH8.8 (1L)

- 18.15g Tris
- 80mL dH_2O
- Adjust pH to 8.8 using HCl
- Make up to final volume of 1L

Store at RT

15) 0.5M Tris-HCl pH 6.8 (1L)

- 6g Tris
- 80mL dH_2O
- Adjust pH to 6.8 using HCl
- Make up to final volume of 1L

Store at RT

16) 10X TBS Buffer (2L)

- 48.4g Tris
- 160g NaCl
- Dissolve in 1.5L dH_20
- Set pH to 7.6 with HCl
- Adjust volume to 2L

Store at RT

17) 1X TBS-T Buffer (1L)

- 100 mL 10x TBS
- 900 mL dH_20
- 1 mL Tween

Store at RT

18) Glycine/Low PH Stripping Buffer (1L)

- 15g Glycine
- 10 mL 10% SDS
- 10 mL Tween-20
- 800 mL dH_20
- Adjust to pH 2.2 with HCl
- Adjust to final volume of 1L with dH_20

Store at RT. Throw away if solution becomes cloudy

19) Bio-Rad® 1X Transfer buffer

- 600 mL Ethanol
- 600 mL dH_20
- 300 mL 10X Transfer buffer

Store at RT

20) 10X Running Buffer

- 10g SDS
- 30.3g Tris
- 144.1g Glycine
- Dissolve in 800 mL of dH_2O
- Adjust volume to 1L

Store at RT

Appendix D – Protocols

Common volumes used for culturing

	T25	T75
Media	3 – 4 mL	8 – 10 mL
Trypsin	2 mL	4 mL
PBS	3 mL	9 mL

Thawing Cells Protocol:

Make sure everything is prepared and ready before thawing the vial and work quickly once thawed

1. Thaw cryovial in waterbath (37^{o}) – don't submerge above rim of lid
2. Add thawed cells to 15ml falcon containing 5ml media
3. Centrifuge at 1500rpm for 3min
4. Remove supernatant
5. Resuspend in volume of media being used to seed flask
6. Seed cell suspension in appropriate size flask
7. Refresh media either later on the same day or the following day

Trypsinising cells Protocol:

1. Remove media from flask
2. Add appropriate amount of trypsin and incubate in shaking incubator.
    - 3 minutes for E0771 cell line
    - 8 minutes for C2C12 cell line
3. Tilt the flask to collect all the trypsinised cells in the corner.
4. Remove and add to 15ml tube.
5. Rinse flask with volume of media equal to that of the trypsin to collect remaining cells and transfer to 15 mL or 50mL centrifuge tube.
6. Centrifuge at 1500rpm for 3min at 21^{o}C.
7. Carefully remove tube from centrifuge – check that pellet has formed
8. Decant majority of media-trypsin. Collect the remaining with a P1000 pipet being careful not to disturb the pellet
9. Resuspend in the appropriate amount of media
    - If splitting, take the appropriate number of cells and add to a new flask containing media.

Counting cells Protocol:

1. Clean cell counter and cover glass with ethanol
2. Following trypsinisation and centrifugation, resuspend pellet in an appropriate amount of media
    - Based on size of pellet – want to dilute enough to be able to count comfortably but not too dilute (if too dilute counting will be less accurate)
3. Make sure cell suspension is thoroughly mixed. Remove 30ul of cell suspension and add to both sides of cell counter
4. Check on microscope
5. Count three blocks on each side of counter. (Top left, top right and bottom right).
6. Calculations
    - Obtain average by adding totals from blocks together and dividing by six
    - Multiply by 10 000 to give number of cells per ml.

- Multiply by resuspended volume to give total number of cells.

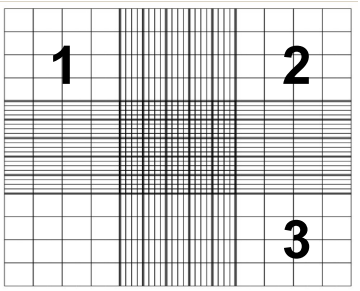

Seeding Cells Protocol:

1. Trypsinise cells, resuspend and count
2. Prepare master mix containing number of cells per ml and media
3. Add the appropriate amount of cell suspension master mix to each well
    - Make sure the cell suspension is thoroughly mixed before use
    - Use new tip for each well
    - Mix tube containing cells between each well with brief shake.
4. Mix plate to ensure cells are evenly distributed in wells – always check under microscope
5. Incubate

Freezing Cells Protocol:

1. Prepare cells by trypsinisation and resuspend in an appropriate volume of media
2. Count cells in suspension
3. If multiple vials are being frozen down, the multiplied volumes of each component can be prepared together in a falcon first and then aliquoted into the vials
4. After determining the total amount of cells in suspension, calculate the volumes required for each component of the freezing solution per vial
    - Must freeze down at least $1.5x10^6$ cells per vial
    - An appropriate amount of DMSO (5%) is added to make up to a final volume (1ml – 1.5ml, depending on size cryovial).
    - Excess volume made up of media
5. Add components to cryovials.
6. Incubate for 1-4hrs at -20°C
7. Incubation overnight at -80°C
8. Store in liquid nitrogen cell tanks

Differentiation of C2C12 Cells Protocol:

1. Seed the required amount of cells
2. After reaching 70% confluency, remove media and add appropriate amount of differentiation media to each well.
3. Incubate in growth conditions for 48 hours
4. Remove media and refresh with differentiation media
5. Incubate for growth conditions for 24 hours
6. Remove media and continue with treatment protocols

Treatment Protocol:

1. Mix treatments thoroughly using using Vortex-2 Gene®
2. Tilting plate to gather media to one area in well and remove media using pipette tip. Be careful not to disturb cells
3. Pre-wet tip and add appropriate volume of master mix to edge of well
4. Repeat for triplicate wells and use new tip for each well
5. Repeat for all treatment groups
6. Allow to incubate over 24 hours

MitoSOX™ Protocol:

1. Allow cell tracker dye vial to warm to room temperature
2. Dissolve 50 µg of product in 13 µL of DMSO (Stock = 5mM)
3. Dilute 6.5 µL of MitoSox stock with 65 µL Horse serum and 6 428.5 µL PBS (5µM)
4. Remove media and wash cells 1x with 400 µL warm PBS
5. Gently add 400 µL MitoSox working solution to each well
6. Incubate plate covered in foil under growth conditions for 15 minutes
7. Remove working solution and wash cells 1x with 400 µL warm PBS
8. Dilute 4 µL of Hoescht stock with 7 996 µL serum free media (5µM)
9. Add 400 µL Hoescht working stock to plate for 10 minutes
10. Wash cells 1x with 400 µL PBS
11. Fix cells in 4% paraformaldehyde for 10 minutes
12. Wash cells 1x with 400 µL PBS
13. Dry and mount with Dako fluorescent mounting media
14. Wrap plate in parafilm and store covered in foil in fridge
15. Image using Ex: 492 and Em: 517

Cell Tracker™ Protocol:

1. Allow cell tracker dye vial to warm to room temperature
2. Dissolve 50 µg of product in 10.76 µL of DMSO (Stock = 10mM)
3. Dilute 4 µL of cell tracker stock with 7 996 µL serum free media (5µM)
4. Warm cell tracker working solution at 37°C
5. Remove media and wash cells 1x with 500 µL warm PBS
6. Gently add 500 µL warm cell tracker working solution to each well
7. Incubate plate covered in foil under growth conditions for 30 minutes
8. Dilute 4 µL of Hoescht stock with 7 996 µL serum free media (5µM)
9. Add 500 µL Hoescht working stock to plate in final 10 minutes
10. Remove working solution
11. Wash cells 1x with 500 µL warm PBS
12. Fix cells in 4% paraformaldehyde for 5 minutes
13. Wash cells 1x with 500 µL PBS
14. Dry and mount with Dako fluorescent mounting media
15. Wrap plate in parafilm and store covered in foil in fridge
16. Image using Ex: 492 and Em: 517

Cell Viability Protocol:

1. Mix MTT solution thoroughly using using Vortex
2. Tilting plate to gather media to one area in well and remove media using 200µL pipette tip. Be careful not to disturb cells
3. Pre-wet tip and add 100µL of MTT solution to edge of well
4. Covered in foil and incubate for 1 hour at 37°C
5. Tilting plate to gather media to one area in well and remove MTT solution using 200µL pipette tip. Be careful not to disturb cells

6. Add 100µl Isoproponal/Triton-X to wells and to blank wells
7. Incubate for 5min on shaker
8. Read absorbance on plate reader at 595nm

Migration Scratch Assay Protocol:

1. Mitomycin C stock solution of of 0.4 mg/mL was prepared
2. Aliquots were made and stored at 4°C, shielded from light
    - Not to be stored for longer than a week as precipitation forms
3. Make three linear wounds in each well using a 200 µL pipette tip
4. Wash each well with warm PBS to remove cell debris
5. Add fresh growth media to each well
6. Capture initial (T0) images of each wound and record positions on microscope
7. Treat each well with appropriate treatment master mix
8. Add the appropriate amount (10 µg/mL) of Mitomycin C to each well
9. Cover plate in foil to protect from light and incubate at growth conditions
10. Repeat capturing of images at same positions of each wound at timepoints 6-hours (T1), 12-hours (T2) and 24-hours (T3)

Protein Extraction Protocol:

- **NB! – Work on ice!**

1. Retrieve cells
2. Remove media from cells with Pasteur pipette
3. Wash 2x with ice-cold PBS and Pasteur pipette
4. Add 80µL RIPA Buffer per well in 6-well plate or 150µL per T_{25} flask
5. Incubate for 2-5min, on ice
6. Using a cell scraper, scrape cells loose and collect in corner of flask
7. Clean scraper with EtOH between different flasks
8. Collect suspension from flask/plate and transfer to pre-cooled microtube
9. Sonicate for 5sec @ 5 amplitude
10. Incubate in fridge, on ice, until foam has settled (can also be stored at this point, -80°C)
11. Centrifuge for 2min @16.3g 4°C
12. Collect supernatant in new pre-cooled microtube
13. Store @ -80°C

Protein Determination Protocol:

1. If needed, thaw protein samples on ice
2. Thaw a 1mg/ml BSA stock solution
3. Prepare BSA working solution (200µg/ml) by diluting 100µl BSA with 400µl dH_2O (50ul BSA + 450ul dH_20 if using 2mg/ml BSA stock). Vortex
4. Prepare Bradford standards as follow (in duplicate):

Table 7: Volumes of components used to establish Bradford standards.

µg Protein	200µg/ml BSA	dH_2O	Bradford Reagent
0 (Blank)	0µl	100µl	900µl
2	10µl	90µl	900µl
4	20µl	80µl	900µl
8	40µl	60µl	900µl
12	60µl	40µl	900µl
16	80µl	20µl	900µl
20	100µl	0µl	900µl

5. Vortex protein samples
6. For each Bradford sample, add 5µl of protein sample to 95µl dH_20 and 900µl Bradford reagent. Prepare samples in duplicate.
7. Vortex Bradford samples and standards
8. Zero spectrophotometer with blank and set @ 595nm
9. Read absorbencies
10. Draw standard curve in Excel graph and plot values of sample to determine [protein sample]

Sample Preparation Protocol:

1. Prepare a working solution of Laemmli's sample buffer
2. Prepare samples by adding the appropriate amount of protein sample to sample buffer (as determined with Bradford Assay)
3. In order to give equal amounts of protein for loading = 20µg
4. Vortex samples
5. Store as ready-made samples @ -80°C

Proceeding with western blot

1. Thaw samples on ice
2. Punch a hole in the lid of each sample
3. Vortex samples and boil for 5min @ 95°C
4. Vortex samples before brief centrifugation (pulse) at 1.6 g
5. Samples now ready for loading

Stain Free SDS-Page Self Cast Gel Protocol:

1. Get clean pairs of spacer plates and short plates, Biorad casting frames (green), casting stands and the rubber gaskets that go in the bottom of the stand.
2. Place gaskets in the grooves at the base of the casting stands.
3. Clean the plates thoroughly with EtOH and place in the casting frames with the short plate facing to the front – secure with the clip on the casting stand.
4. Get 3 small beakers and label for H_2O, resolving gel (bottom) and stacking gel (top).
5. Make up the required resolving gel according to the recipe to make 4 gels.

Table 8: Volumes of components used for self-cast resolving gel.

Resolving Gel	
Gel constituent	**12% Gel**
dH_2O	8.5 ml
40% Acrylamide solution	6.0 ml
1.5M Tris-HCl, pH 8.8	5.0 ml
10% w/v sds	200 µl
10% w/v APS	200 µl
TCE	100 µl
TEMED (add last!)	8.0 µl

6. Add all the constituents with gentle swirling to mix, except the APS and TEMED.
7. Add the APS and swirl briefly to mix.
8. Add the TEMED, swirl briefly to mix.
9. Using plastic Pasteur pipette, quickly pour the gel mixture between the two plates (avoid air bubbles by pouring from the one corner) until the green line seen at back of plate from gasket.
10. Top with a layer of 100% EtOH to remove bubbles, leave smooth surfaces and prevents oxidation.
11. Allow gel to set (30 to 60 minutes). Prepare 1:10 dilutions of running buffer, TBS-T and transfer buffer.
12. When resolving gel is set, carefully pour off the EtOH and dab dry with blotting paper. Then prepare the stacking gel as follows (the amounts given are sufficient for 4 gels).

Table 9: Volumes of components used for self-cast stacking gel.

Stacking Gel	
Gel constituent	**4% Gel**
dH_2O	4.84 ml
0.5M Tris-HCl, pH 6.8	2.0 ml
40% Acrylamide solution	1.0 ml
10% w/v sds	80 µl
10% w/v APS	80 µl
TEMED (add last!)	8.0 µl

13. Add all the constituents with gentle swirling to mix, except the APS and TEMED.
14. Add the APS and swirl briefly to mix.
15. Add the TEMED, swirl briefly to mix
16. Using a plastic Pasteur pipette, quickly pour the gel mixture between the two plates until top of front plate.
17. Insert appropriate comb gently, pushing down and avoiding bubble formation (make sure comb corresponds to the gel thickness).
18. Allow to set for 30 minutes.
19. Retrieve the standard protein marker from the freezer and allow to equilibrate to room temperature.

Stain Free SDS-Page Fast Cast Gel Protocol:

Using Bio-Rad® TGX Stain-Free™ FastCast™ Acrylamide Kit, 12%.
Follow steps 1 – 4 of self cast gel protocol (Protocol f.3)

1. Make up the required resolving gel according to the recipe given by Bio-Rad® to make 4 gels.

Table 10: Volumes of components used for self-cast resolving gel.

Resolving Gel	
Gel constituent	**4% Gel**
Resolver A	12 mL
Resolver B	12 mL
TEMED	12 µL
10% APS	120 µL

1. Add all the constituents with gentle swirling to mix
2. Using plastic Pasteur pipette, quickly pour the gel mixture between the two plates (avoid air bubbles by pouring from the one corner) until the green line seen at back of plate from gasket.
3. Allow gel to set (30 to 60 minutes). Prepare 1:10 dilutions of running buffer, TBS-T and transfer buffer.
4. Prepare the stacking gel according to the recipe given by Bio-Rad® to make 4 gels.
    - Do not have to wait for resolver to set first before adding stacker

Table 11: Volumes of components used for self-cast stacking gel.

Stacking Gel	
Gel constituent	**4% Gel**
Stacker A	4 mL
Stacker B	4 mL
TEMED	8 µL
10% APS	40 µL

1. Add all the constituents with gentle swirling to mix
2. Using a plastic Pasteur pipette, quickly pour the gel mixture between the two plates until top of front plate.
3. Insert appropriate comb gently, pushing down and avoiding bubble formation (make sure comb corresponds to the gel thickness).
4. Allow to set for 1 hour.

SDS-PAGE Running Protocol:

1. Prepare BioRad Fast Cast Stain-Free gels or Self Cast according to instructions
    - Gels can be made beforehand and stored in the fridge in wetted paper towels and sealed in cling wrap
2. Thaw protein samples on ice
    - Prepared in 2:1 ratio of protein sample + Laemli's buffer
3. Punch hole in lid of microtube, mixed by vortexing briefly and boil for 5 min at 95°C
4. Spin samples down with quick pulse
5. Assemble the gasket
    - Assemble the gels onto the gasket with the comb facing inside
    - Fill the gasket with running buffer – check for leaks

- Carefully remove the combs and rinse out wells with P200 pipet (set to approx. 100 ul) and yellow tip

6. Load ladder (4 ul BLUeye)
7. Load samples
8. Place gasket into tank and fill with running buffer. Re-fill gasket if necessary
9. Attach lid (black on black, red on red) and plug into power pack
10. Run at 100 V for approx. 10 min (until sample has entered gel)
11. Increase to 150 V and run until blue dye front reaches the bottom of the gel (approx. 1 hr)
12. When finished, activate **immediately**
13. Activate stain-free properties of gel on ChemiDoc
    - Gel activation protocol, 2.5 min

Western Blot Transfer Protocol:

1. Prepare for transfer (few min beforehand)
    - Soak two pieces of Bio-Rad blotting paper in transfer buffer for 2 - 3 min
    - Activate piece of PVDF membrane in 100% methanol (10-15 sec) and then soak in transfer buffer for 2 min.
2. Assemble the transfer sandwich on the cassette base (anode) by placing one piece of blotting paper on the bottom, then the membrane, then gel, and finally, the second blotting paper on top. Use the blot roller to remove air from between the assembled layers.
3. Once the stacks are positioned in the cassette base, place the cassette lid on the base. The lid is reversible, but ensure that the electrical contacts fit closely into the slots in the base. Press the lid down firmly and turn the dial clockwise to engage the lid pins into the locking slots.
4. Load a second cassette if desired.
5. Slide the cassette (with the dial facing up) into the bay until it makes contact with the magnetic interlock and you hear a click. Cassettes can be inserted into the bays in any order, with or without power to the system.
6. Select the LIST button from the Home menu and the **MIXED MOLECULAR WEIGHT** transfer protocol from the Bio-Rad pre-programmed protocols or the user-defined protocol of choice.
7. To initiate the run, press the navigation button that corresponds to A:RUN for the cassette in the upper bay or B:RUN for the cassette in the lower bay.
8. After transfer, disassemble stack
    - Gel can be visualised to determine transfer efficiency if desired
9. Label membrane and rinse in 100% methanol
    - Labelling – only use soft pencil (black art pencil works well) and not markers or pens (causes smudges)
    - Place membrane only on ethanol cleaned surface (white tray from Chemidoc works well)
10. Air-dry membrane
    - Becomes white
    - Hold in fumehood for quicker drying
11. Re-hydrate membrane in 100% methanol
    - Until translucent, 10-15 sec
12. Wash membrane in TBS-T for 5 min
13. Image transfer on membrane on Chemidoc
    - Stain-free blot setting
    - If using for normalisation, make sure image is clean and not over-exposed

Western Blot Antibody Protocol:

1. Block membrane in 5% milk (prepared in TBS-T) for 1 hr with gentle shaking
    - Or 5% BSA (prepared in TBS-T) for when probing for phosphorylated proteins
2. Wash membrane 3x for 5 min in TBS-T

3. Incubate membrane on primary antibody at 4°C for 36-hours
    - Prepared in 50 ml centrifuge tube
    - Dilute antibody in TBS-T to desired concentration, normally 1:1000
    - Attach to rotators in walk-in fridge
4. Retrieve membranes
    - Stored primary antibody in fridge/freezer
5. Wash membrane 3x 5 min in TBS-T
6. Incubate membrane on secondary antibody for 1 hr at RT
    - Prepared in 50 ml centrifuge tube
    - Dilute antibody in TBS-T to desired concentration, normally 1:10 000
7. Wash membrane 3x 5 min in TBS-T
8. Develop
    - Prepare minimum amount of ECL needed in microtube in 1:1 ratio
    - Place membrane on Chemidoc and check position
    - Add ECL to the desired area and roll to ensure even spread. Roll away excess ECL

    a. Expose using desired settings

Science is a beautiful gift to humanity
We should not distort it
- A. P. J. Abdul Kalam